

N71-23258 NUS-679
NASA CR-117898

FINAL REPORT FOR UNMANNED
SPACECRAFT RTG SHIELD
OPTIMIZATION STUDY

For

Goddard Space Flight Center
Greenbelt, Maryland

NASA Contract Number: NAS5-11649

CASE FILE
COPY

J. J. Steyn
and
R. Huang

May 1970

NUS CORPORATION
4 Research Place
Rockville, Maryland 20850

NUS CORPORATION

**FINAL REPORT FOR UNMANNED
SPACECRAFT RTG SHIELD OPTIMIZATION STUDY**

For

**Goddard Space Flight Center
Greenbelt, Maryland**

NASA Contract Number: NAS5-11649

By

**J. J. Steyn
and
R. Huang**

May 1970

**NUS CORPORATION
4 Research Place
Rockville, Maryland 20850**

Approved: _____



**E. A. Saltarelli
Vice President and
Technical Director**

TABLE OF CONTENTS

	<u>Page</u>
1. INTRODUCTION	1
2. THEORETICAL DESCRIPTION	4
2.1 Introduction	4
2.2 Theoretical Discussion	5
3. CODE SØSC DESCRIPTION	18
3.1 Introduction	18
3.2 Code Logic	18
3.3 Code Operating Information	22
3.3.1 General	22
3.3.2 Code Constants	24
3.3.3 Card Input Details	25
3.3.4 Code Output	41
3.3.5 Discussion	47
4. DESIGN OF EXPERIMENT	50
5. SUMMARY AND CONCLUSIONS	54
REFERENCES	56
FIGURES	59
APPENDIX I INTERACTION PHYSICS REVIEW	70
II SUMMARY DESCRIPTION OF SUBPROGRAM NUGAM1	84
III CODE SØSC FORTRAN LISTING	93
IV CODE SØSC SAMPLE INPUT DATA LISTING	131
V CODE SØSC SAMPLE OUTPUT DATA LISTING	135
VI SUMMARY OF NUS-600 DETAIL EVALUATIONS	149

LIST OF FIGURES

<u>Figure No.</u>	<u>Title</u>	<u>Page</u>
1	Typical Unmanned Spacecraft	60
2	Schematic Drawing of Spacecraft Showing RTG Source, Shield and Detector Arrangement	61
3	Schematic Definition of Gamma Photon and Neutron Fluxes	62
4	Code SØSC Logic	63
5	Definition of Scattering Structure Coordinate Geometry	64
6	Code SØSC Routing Control Options	65
7	Energy Correspondence Bar Diagram	66
8	Source Term Fluxes at 687 cm From Tandem RTG's	67
9	Weight and Length of LiH + Pb Shield as a Function of LiH to LiH + Pb Length Ratio	68
10	Geometry for Proposed Experiment	69

SUMMARY

This contract final report discusses the development of analytic procedures and computer codes for the prediction of weight optimized radioisotope thermoelectric generator shields for unmanned spacecraft operating 'in vacuo'. An optimization code - - - SØSC, designed to determine shield optimum weights and dimensions with respect to specified criterion fast neutron plus gamma photon fluxes, is described. The code employs a combination of analytic, albedo and Monte Carlo techniques. A theoretical discussion and example predicted shield data are given as well as a proposed verifying experiment design.

1. INTRODUCTION

This final report, prepared for the National Aeronautics and Space Administration, GODDARD SPACE FLIGHT CENTER, by NUS CORPORATION, under Contract NAS5-11649, describes the analytic procedures and computer codes developed for prediction of weight optimized radiation shields for an unmanned spacecraft operating 'in vacuo'. The design of an experiment, to furnish data for comparison with and verification of predicted design, is also presented.

Analytic procedures and computer code logic have been combined to predict optimum weight shields for the protection of scientific experiments from the radiation fields of on-board radioisotope thermoelectric generators, during unmanned spacecraft missions. The optimum weight shield was determined as that exposing the science payload to a specified neutron plus gamma photon integral radiation number flux, when added to the spacecraft scattered radiation contribution. The angular-energy transport of radiation was obtained by an integrated combination of analytic, albedo and Monte Carlo techniques. This approach was considered as the most advantageous compromise for spacecraft engineering design purposes as opposed to the sole use of either a costly Monte Carlo calculation or a less accurate analytic approximation. The spacecraft assumed for the present study is presented schematically in Figure 1.

The work effort was specifically oriented to the radiation field at the energetic particle experiment package indicated in the spacecraft configuration of Figure 1, spacecraft general dimensions, deployment distances and materials were obtained from preliminary design drawings furnished by NASA-GSFC. The radioisotope thermoelectric generators (RTG's) were assumed to be plutonium-oxide fueled, viz. the SNAP-27.

A shield optimization study code --- SØSC was designed and developed to determine the shield material minimum thickness and weight required to limit the spacecraft mission experiment package to a specified radiation flux exposure, eg. ≤ 10 particles/cm²-sec. The incident criterion flux was taken as the sum of gamma photons and neutrons either transmitted by the shield or scattered by the spacecraft structure. Code SØSC predicts shield requirements for the case of gamma photons, according to a combination of analytic transmission theory, the Monte Carlo transport method, the albedo technique (backscattering theory) and the single scattering approximation method. It employs three component sub-codes for this determination, namely: XEST, NUGAM1 and ALB.

Although code SØSC is provisionally designed to evaluate fast neutron transport in a manner similar to that for gamma photons, photon transport was emphasized in this stage of the NASA program. The code is presently designed to evaluate neutron transport using relaxation theory methods. This course for the case of the SNAP-27 was based on the fact that the RTG total neutron emission rate in the axially perpendicular direction was reported as being 5.7×10^7 n/sec⁽¹⁾. This is in good agreement with, but less than an earlier NUS estimate of 1.0×10^8 n/sec reported in NUS-600⁽²⁾. Taking the gamma photon dose rate as one-tenth of the neutron dose rate and allowing for dose-to-flux conversion as well as spectral distribution gives an integrated RTG emitted photon source of $\sim 1.0 \times 10^9$ γ /sec, or approximately ten times that for neutrons. Data obtained late in the work program indicated a γ /n flux ratio of 1.8 and 18.0 for axial and radial emission, respectively. The 1.8 ratio indicates the neutron transport in the shield should be examined by a more exact method such as Monte Carlo.

Section 2 of this report presents the theory and logic on which code SØSC is based. Section 3 presents a description of the code and the necessary users input and output information. Section 4 presents a proposed design for a verifying laboratory experiment. Section 5 consists of a summary and conclusion with respect to the work reported. A brief review of the basic gamma photon and fast neutron physics required, is given in Appendix I while Appendix II recaps the basis of the Monte Carlo technique used.

2. THEORETICAL DESCRIPTION

2.1 Introduction

The radiation field emitted by an encapsulated plutonium oxide radioisotope thermoelectric generator (RTG) assembly consists primarily of an anisotropic polyenergetic distribution of gamma photons and fast neutrons. If RTG assemblies are boom mounted on a spacecraft, as depicted in Figure 1, then boom mounted science experiments packages may be exposed to excessive radiation fields. This radiation interference may be reduced by shielding the RTG's. If the spacecraft scattered radiation is not excessive then shadow shields may be used to reduce RTG radiation fluxes at the experiment to a criterion (acceptable) level. For a given shielding material the shield dimensions and thus weight, are optimized when the criterion flux is obtained. Further optimization may be obtained through judicious selection of materials and their deployment. In the event that the spacecraft scattered flux is excessive then additional RTG side shielding or geometrical redeployments must be considered.

In this report section the theoretical considerations of a method for determining the dimensionally and thus weight, optimized shield, consistent with the criterion flux condition, are presented. The discussion is restricted to the theory underlying the code developed for rapid predictions --- code SØSC; the code is described in Section 3.

The procedures developed use Monte Carlo technique, the albedo technique, single scatter approximation to best advantage to obtain an iterative solution of a basic transport relationship. Since code SØSC uses a modified version of the Monte Carlo code NUALGAM ⁽³⁾, the theory underlying the Monte Carlo code is reproduced in Appendix II, with revisions, from reference (3). This section then is concerned with the components and 'solution' of the basic transport expression. Although the discussion is general, the emphasis is given to

photon transport, as stated in Section 1. It is proposed that neutron transport be evaluated in an analogous fashion in the future. In this regard neutrons are considered in the review of the transport relationship.

2.2 Theoretical Discussion

For the purposes of this section the complex spacecraft configuration shown in Figure 1 is redrawn schematically in Figure 2. Only one RTG source is indicated and the mission experiment package is referred to as a detector. In addition, the spacecraft body is replaced by a simpler geometry and the boom-arms omitted.

The radiation number flux at a detector distant r_0 from a source $S (E_0)$, of neutrons or gamma photons E_0 , as in Figure 2, without a shadow shield, may be defined as

$$\phi_D (E_D) = \phi_\alpha (E_\alpha) + \phi_0 (E_0) \quad , \quad (1)$$

where

$$\phi_\alpha (E_\alpha) = \phi_{\alpha S} (E_{\alpha S}) + \phi_{\alpha R} (E_{\alpha R}) \quad ,$$

$\phi_{\alpha S} (E_{\alpha S})$ = the primary radiation number scattered to the detector by the area A composed of material j , distant r_1 and r_2 from the source and detector, respectively,

$$\begin{aligned} \phi_{\alpha R}(E_{\alpha R}) &= \text{the 'area A'-originating reaction product flux} \\ &\quad \text{reaching the detector,} \\ &= 0, \text{ for gamma photons as the primary radiation,} \\ &\quad \text{excepting photoneutron interactions } (\gamma, n), \\ \phi_0(E_0) &= \text{the uncollided primary radiation number reach-} \\ &\quad \text{ing the detector.} \end{aligned}$$

The energy arguments signify that the detected flux consists of radiation of primary energy E_0 , scattered energies $E_{\alpha S} (<E_0)$ and reaction product energies, E_R . The subscript α refers to the spacecraft structure as a secondary source, eg. scattering, i.e. to albedo fluxes.

The number flux reaching the detector with a shadow shield, composed of material i , as indicated in Figure 2, may be defined as

$$\phi_D(E_D) = \phi_{\alpha}(E_{\alpha}) + \phi_a(E_0; E_a), \quad (2)$$

where

$$\phi_a(E_0; E_a) = \text{the shield attenuated flux,}$$

$$= \phi_a(E_0) + \phi_a(E_a),$$

$$\begin{aligned} \phi_a(E_0) &= \text{the number flux transmitted by the shield} \\ &\quad \text{without interaction,} \end{aligned}$$

$$\phi_a (E_a) = \phi_{as} (E_{as}) + \phi_{ap} (E_{ap}) + \phi_{aR} (E_{aR}),$$

$\phi_{as} (E_{as})$ = the shield forward scattered radiation number flux reaching the detector,

$\phi_{ap}(E_{ap})$ = the gamma photon number flux resulting from pair production interactions in the shield,

= 0, for incident photon energies $E_0 \leq 1.02$ MeV,

= 0, for incident neutrons,

$\phi_{aR} (E_{aR})$ = the shield-originating reaction product number flux reaching the detector, e.g. gamma photons resulting from (n, γ) interactions,

= 0, generally, for gamma photons as the primary radiation, excepting such as photoneutron interactions, i.e. (γ, n) .

For fast neutrons as the primary incident radiation, the number flux terms $\phi_{aR} (E_{aR})$ and $\phi_{aR} (E_{aR})$ in Equation (1) and (2) refers to all product radiations, eg. neutrons, gamma photons, alphas, protons, depending on the reaction probabilities for each.

The number flux terms in Equations (1) and (2) may be estimated either from a combination of analytic relationships and published empirical data or from experiment, either numerical analogue, ie. Monte Carlo method or the conventional laboratory kind. The sole use of the Monte Carlo method is considered as being uneconomical and unjustified. A laboratory experiment is planned for the future by NASA-GSFC as part of the overall program. The present work is thus confined to number flux predictions obtained by analytic methods and by published empirical data and judicious use of Monte Carlo techniques.

Neglecting the reaction product number flux terms for the present, the detector incident number flux may be written as

$$\phi_D (E_D) = \phi_a (E_O) + \phi_a (E_a) + \phi_{\alpha s} (E_{\alpha s}) . \quad (3)$$

For a normally incident parallel radiation flux $\phi_O(E_O)$, the uncollided number flux transmitted through a shield of thickness L and reaching the detector, is obtained as

$$\phi_a (E_O) = \phi_O (E_O) e^{-\mu(E_O) \cdot L} , \quad (4)$$

where

$$\mu (E_O) = \text{the total linear attenuation coefficient of the shield material for radiation of energy } E_O; \text{ the notation } \Sigma \text{ is generally used for neutrons.}$$

The ratio of the shield total-to-uncollided transmitted flux is referred to as "build-up". The build-up factor may thus be defined as

$$B (E_O, L) = \frac{\phi_a (E_O) + \phi_a (E_a)}{\phi_a (E_O)} = \frac{\phi_a (E_O, E_a)}{\phi_a (E_O)} . \quad (5)$$

The total shield transmitted flux at the detector may be obtained from Equations (4) and (5) as

$$\phi_a (E_O; E_a) = B (E_O, L) \cdot \phi_O (E_O) \cdot e^{-\mu(E_O) \cdot L} , \quad (6)$$

if the build-up factor is known.

Although energy and dose build-up factors may be obtained for gamma photons^(4,5) and to a lesser degree for fast-neutrons they pertain in almost all cases to semi-infinite single-material-composition shields. For small finite shields, i.e. shadow shields, and number flux requirements as opposed to energy and dose, recourse

to either a laboratory experiment or a Monte Carlo study is a prerequisite. In the present work a Monte Carlo evaluation is underway for gamma photons and proposed for fast-neutrons.

For a spectrum of incident source particle energies the shield transmitted flux is obtained by integration as

$$\Phi_a(E_a) = \int_0^{\infty} \phi_a(E_o, E_a) dE_o \quad , \quad (7)$$

$$\approx \sum_{k=1}^q \phi_a(E_{ok}, E_a) \Delta E_k \quad (8)$$

For a stratified or homogenous shield composed of m materials, each of thickness l_i , Equation (8) may be rewritten

$$\Phi_a(E_a) \approx \sum_{k=1}^q \phi_o(E_{ok}) \prod_{i=1}^m B(E_o, l_i) e^{-\mu_i(E_{ok}) l_i} \quad , \quad (9)$$

$$= \sum_{k=1}^q \phi_o(E_{ok}) \cdot B(E_o)_m e^{-\mu_i(E_{ok}) \cdot l_i} \quad , \quad (10)$$

where

$B(E_o)_m$ = the build-up factor for the composite shield of m materials and incident radiation of energy E_o , and given geometry,

i = material identity index,

k = energy group index,

q = number of energy groups.

The uncollided number flux in the foregoing equations may be determined from a relationship of the kind

$$\phi_o(E_o) = \phi_o(E_o, r_o) = S(E_o) \cdot G(r_o) \quad , \quad (11)$$

where

$S(E_0)$ = source emission rate for radiation of energy E_0 ,

$G(r_0)$ = the geometry relationship for a source-to-detector distance r_0 .

For example, for an isotropically emitting point source and $r_0 \gg$ detector lateral extent, the geometry factor is

$$G(r_0) = (4\pi r_0^2)^{-1}. \quad (12)$$

Extended source and detector geometries may be evaluated according to the 'Point-Kernel Method',⁽⁴⁾

The number flux term, $\phi_{\alpha S}(E_{\alpha S})$ in Equation (3), resulting from primary gamma photons scattered by an area A , as in Figure 2, may be redefined as

$$\phi_{\alpha S}(E_{\alpha S}) = \int_A \phi_{\alpha S}(E_0, \theta, \theta_0, \varphi, r_1, r_2, t; i) dA, \quad (13)$$

where

dA = the differential scattering area,

θ_0 = the angle between the incident radiation direction and the outward normal of area dA ,

θ = the angle between the emergent (scattered) radiation direction and the outward normal of area dA ,

φ = the azimuth angle of scattering in the plane of area A ,

r_1 = the distance between the source and the area dA ,

r_2 = the distance between the area dA and the detector,

- t = the thickness of the scattering material at area dA, measured along the inward normal to dA,
- i = the identity index of the material of which dA is a part.

For a spectrum of source particle energies the energy integrated flux, $\Phi_{\alpha S}(E_{\alpha S})$, may be obtained by an integration similar to that of Equations (7) and (8), as

$$\Phi_{\alpha S}(E_{\alpha S}) = \int_0^{\infty} \phi_{\alpha S}(E_{\alpha S}) dE_0 \quad (14)$$

The flux term in the integrand of Equation (13) may be defined according to albedo theory as^(4,6)

$$\phi_{\alpha S}(E_{\alpha S}) = \phi_0(E_0, r_1) \cdot \frac{\cos \theta_0 \cdot dA \cdot \alpha(E_0, \theta_0, \theta, \varphi, t; i)}{r_2^2}, \quad (15)$$

where

$\alpha(E_0, \theta_0, \theta, \varphi, t; i)$ = the angular differential number current albedo with respect to the noted arguments (defined for Equation (13)),^(4,6)

$\phi_0(E_0, r_1)$ = number flux incident on area dA,
= $S(E_0) \cdot G(r_1)$, c.f. Equation (11).

The assumption underlying the use of the albedo technique for complex geometry analysis is that the scattered radiation particles emerge from the scattering medium surface at a point close to their point of entry. This assumption is generally justified⁽⁴⁾, eg. the separation distance between

entry and exit for one-half of all escaping gamma photons has been found to be less than one mean-free-path (for incident energy E_0). Photon scattering from very thin or laterally small structures of volume V , may be alternately predicted by the single-scattering approximation method⁽⁷⁾, from the relationship

$$\phi_{\text{oss}} = \int_V \phi_0(E_0, r_1) \cdot \frac{N_e \cdot \sigma_{\text{KN}}(E_0, \theta_s) dV}{r_2^2} \quad (16)$$

where

N_e = the scattering material electron density per cubic centimeter,

$\sigma_{\text{KN}}(E_0, \theta_s)$ = the Klein-Nishina angular-energy intensity distribution function⁽⁴⁾, for photons of energy E_0 and scattering angle θ_s ,

θ_s = the angle between the primary and scattered photon directions.

Equation (15) may be solved if values for the number albedo are known. The albedo may be determined by either a laboratory experiment or a Monte Carlo treatment. For gamma photons, recently developed modification of the moments method has been reported as a potential source of albedo data⁽⁸⁾. In the present work, experimental albedo data^(9,10), and empirical relationships in accord with both experimental and Monte Carlo results^(4,6,11,12), were used for gamma photons. A similar approach is proposed for the case of fast-neutrons.

Since weight is the product of volume and density, the weight optimization of an axially symmetric shadow shield of specified composition may be considered as an optimization of shield thickness, L_{min} , such that

$\phi_D(E_D)_{\gamma, n} \leq C$, where C is a specified criterion, eg. 10 particles/cm²-sec. The optimum, or minimum weight of a right-cylindrical shield of radius R_S , may be obtained as

$$W_{\min} = \pi R_S^2 L_{\min} \cdot \rho \quad , \quad (17)$$

$$= \pi R_S^2 \sum_{i=1}^m \ell_{i\min} \cdot \rho_i \quad , \quad (18)$$

where

ρ_i = the density of shield material i ,

ρ = the weighted density of the shield,

= the shield material actual density if $m = 1$.

The total number flux reaching the detector for the case of a polyenergetic source, is obtained from Equation (2) doubly integrated over primary and secondary energies, as

$$\begin{aligned} \Phi_D = \int_{E_D} \Phi_D(E_D)_{\gamma, n} dE_D &= \int_{E_O, E_\alpha} \phi_\alpha(E_\alpha)_{\gamma, n} dE_O dE_\alpha + \int_{E_O, E_a} \phi_a(E_O; E_a)_\gamma dE_O dE_\alpha + \\ &+ \int_{E_O, E_a} \phi_a(E_O; E_a)_n dE_O dE_\alpha \quad , \end{aligned} \quad (19)$$

where the subscripts γ and n denote gamma photons and fast neutrons. The use of the albedo and build-up factor concepts is tantamount to an integration over E_α and E_a , respectively.

Equation (19) may be further redefined as

$$F = \int_{E_O, E_a} \phi_a(E_O; E_a)_\gamma dE_O dE_a + \int_{E_O, E_a} \phi_a(E_O; E_a)_n dE_O dE_a \quad , \quad (20)$$

where

$$F = \int_{E_D} \phi_D(E_D)_{\gamma, n} dE_D - \int_{E_0, E_\alpha} \phi_\alpha(E_\alpha)_{\gamma, n} dE_0 dE_\alpha, \quad (21)$$

$$= C - \int_{E_0, E_\alpha} \phi_\alpha(E_\alpha)_{\gamma, n} dE_0 dE_\alpha. \quad (22)$$

The flux terms in Equation (20) may be obtained from Equations (10) and (13) and L_{min} obtained by an iterative solution. For example, for a single material shield exposed to a monoenergetic source of neutrons and photons, Equation (20) reduces to

$$F = \phi_0(E_0)_\gamma B(E_0)_\gamma e^{-\mu(E_0)_\gamma L} + \phi_0(E_0)_n B(E_0)_n e^{-\mu(E_0)_n L} \quad (23)$$

The foregoing theoretical discussion has presumed a knowledge of gamma photon and fast neutron interaction phenomena. Such phenomena and the relevant interaction physics are summarily reviewed in the Appendix I. In addition, a familiarity with the solution of radiation transport problems by means of the Monte Carlo method is presumed; the reader is referred to the references in this regard^(13,14).

The second term in the right-side of Equation (20) is defined by Equation (2). It includes the shield originating neutron-reaction product flux $\phi_{aR}(E_{aR})$, as yet not discussed in any detail. Although the flux $\phi_{aR}(E_{aR})$ reaching the detector, may be predicted by means of either a laboratory experiment or a Monte Carlo code evaluation, it may be estimated for the case of reaction product gamma photons such as result from fast neutron inelastic scatters or absorptions in an axially symmetric shadow shield, as

$$\phi_{aR}(E_{aR}) = \int_0^L g \cdot G(r_\ell) \cdot \sum_\gamma(E_0) \cdot \phi_0(E_0)_n \cdot (1 - e^{-\lambda\tau}) \cdot e^{-\sum_{Tot}(E_0)\ell} \cdot e^{-\mu(E_{aR})(L-\ell)} d\ell, \quad (24)$$

where

g = the cross-section area of the axially symmetric shadow shield,

- $= \pi R_S^2$, for a cylindrical shield,
- l = the distance from the shield face at the source to the differential volume $g.dl$ (see Figure 3),
- $G(r_\ell)$ = the geometry factor for distance r_ℓ , c.f. Equation (11),
- r_ℓ = the distance from the differential volume $g.dl$ to the detector (see Figure 3),
- $\Sigma_\gamma(E_0)$ = the linear attenuation coefficient of the shield material for fast-neutrons of energy E_0 , for production of gamma photons,
- $\Sigma_{Tot}(E_0)$ = the total linear attenuation coefficient of the shield material for fast-neutrons of energy E_0 ,
- $\phi_0(E_0)_n$ = the shield normally and parallel incident flux of fast neutrons of energy E_0 ,
- $= \phi_0(E_0, (r_0 - r_\ell))_n$, c.f. Equation (11),
- $\mu(E_{aR})$ = the total linear attenuation coefficient of the shield material for reaction product gamma photons of energy E_{aR} ,
- λ = the radioactive decay constant of the reaction-produced or compound nucleus,
- τ = the duration of exposure to the neutron flux.

For inelastic scattering the decay constant in Equation (24) is relatively large and thus

$$1 - e^{-\lambda\tau} \approx 1.0 . \quad (25)$$

This is also true for activation where the product $\lambda \cdot \tau$ is large .

Considering again the primary radiation emitted by the sources , a modified form of Equation (24) , where g, l, r_l and the exponent $\mu(E_{\alpha R})(L-l)$ are replaced by dA, t, r_2 and $\mu(E_{\alpha R}) \cdot t$ respectively , may be defined as

$$\phi_{\alpha R}(E_{\alpha R}) = \int_0^t dA \cdot G(r_2) \cdot \Sigma \gamma(E_0) \cdot \phi_0(E_0, r_1) \cdot (1 - e^{-\lambda\tau}) e^{-\Sigma_{Tot}(E_0)t} \cdot e^{-\mu(E_{\alpha R})t} dt, (26)$$

to estimate the spacecraft structure reaction product 'albedo', α_R for prediction of fluxes, $\phi_{\alpha R}(E_{\alpha R})$; α_R is analogous to α of Equation (15) for $(\theta_0, \theta, \phi) = (0, 0, 0)$. This albedo, valid for normal incidence and emergence, may be used as in Equation (29) of Section 3.2, to estimate the angular differential albedo. Primary and secondary energy integrations of Equations (24) and (26) are as defined for Equation (20).

The shadow shield as a secondary source of both photons and neutrons , ie. scattered and reaction product radiation, has been discussed. Scattering to the detector may be accounted for either by the use of the build-up factor concept or a Monte Carlo analysis and reaction product radiation intensity may be predicted by the use of Equation (24) or a Monte Carlo analysis .

In addition to being a second order source , the shield may also be considered a third order source , ie. primary radiation interacting in the shield may produce secondary radiation which in turn may interact with the spacecraft structure to yield a third order flux at the detector .

The detected flux resulting from such interactions in the spacecraft structure may be predicted in accord with either Equations (15), (16) or (26) and

discussions thereto, providing the shield-originating flux $\phi_0(E_{aR}, r_{1s} \text{ shield}) = \phi_0(E_{aR}, r_{1s})$, is known and substituted for $\phi_0(E_0, r_1)$. The night-cylindrical shield originating flux in the axially perpendicular direction, may be estimated as

$$\phi_0(E_{aR}, r_{1s}) = \int_0^L f(R_s, r_{1s}, E_{aR}) \cdot \Sigma_\gamma(E_0) \cdot \phi_0(E_0) n(1 - e^{-\lambda\tau}) \cdot e^{-\Sigma_{Tot}(E_0)\ell} d\ell, \quad (27)$$

where the function $f(R_s, r_{1s}, E_{aR})$, valid for $\ell \ll r_{1s}$, takes the shield self-absorption into account. This function is defined for the cylinder as

$$f(R_s, r_{1s}, E_{aR}) = \frac{g}{2\pi} \int_0^\beta d\beta \int_{y_1}^{y_2} \frac{e^{-\mu(E_{aR})(y-y_1)}}{y} dy, \quad (28)$$

where

$$\begin{aligned} y_1 &= r_{1s} \cos \beta - R_s \cos \psi, \\ y_2 &= r_{1s} \cos \beta + R_s \cos \psi, \\ \psi &= \pi - \sin^{-1} \left(\frac{r_{1s} \sin \beta}{R_s} \right), \\ y &= \text{integration variable; a distance,} \\ \beta &= \text{integration variable, an angle,} \\ \beta_1 &= \text{the limit, } \sin^{-1} (R_s / r_{1s}) \\ r_{1s} &= \text{the shield-to-spacecraft 'area dA' distance;} \\ &\quad \text{analogous to } r_1 \text{ (see Figure 3).} \end{aligned}$$

For reasons of clarity the fluxes discussed in this report section are schematically summarized in Figure 3.

3. CODE SØSC DESCRIPTION

3.1 Introduction

This report section describes the general logic, user information and preliminary results obtained using code SØSC, a spacecraft shield optimizing study code, a code written in the FORTRAN-IV language for the IBM-360/91 digital computer. Code SØSC consists of three distinct component code complexes: XEST, NUGAM1 and ALB. Code XEST predicts approximate shield dimensions based on analytic methods. Code NUGAM1 predicts shield build-up factors for final shield dimensions, by the Monte Carlo method. Code ALB determines flux intensities resulting from scattering by the spacecraft structure, based on the albedo technique and/or the single scatter approximation.

The code may be optionally run to evaluate spacecraft scattering only or instead to optimize the shadow shield, neglecting spacecraft scattering. Thus if the scatter contribution is already known then it may be input instead of calculated and the shield optimization carried out.

Code SØSC logic is presented in Section 3.2. Code SØSC consists of a main controlling program --- MAIN, a shield thickness prediction program --- XEST, a complex geometry scatter flux program --- ALB, and a Monte Carlo buildup factor calculating program --- NUGAM1. Development work on these programs focussed on gamma photon transport as noted in Section 1 of this report. Neutron transport was coded according to 'removal' theory^(4, 15).

3.2 Code Logic

MAIN executes input and final output operation. Details of the input-output are given in Section 3.3.3. The main programs call ALB to determine F for Equation (20). It calls XEST to estimate an approximate thickness value, L_{min_e} , for Equation (20). The Monte Carlo code, NUGAM1, is called to

determine buildup factors corresponding to the estimated value of L_{min_e} . Using the thus determined values of F and the buildup factors, the code solves Equation (18) for the optimum thickness L_{min} , by iteration. It will optionally recall NUGAM1 to determine the deviation of the buildup factors for L_{min} from those for L_{min_e} . If this deviation exceeds a tolerance value the code will reiterate. Iteration may be arrested at any loop number specified by the user. Code SØSC logic is summarized in Figure 4.

Code ALB determines the angular-energy integrated flux scattered to the detector by the spacecraft complex structural components illuminated by primary source radiation. Code ALB consists of an albedo package and a generalized geometry package. In its present form the albedo package is only coded for gamma photons because of the lack of fast neutron differential number albedo data. It is proposed to generate fast neutron data according to the Monte Carlo technique, in the future.

The albedo routines in code ALB determine the scattered energy integrated flux $\phi_{\alpha S}(E_{\alpha S})$ defined by Equation (13). The main calling program carries out the integration over primary source energies. The gamma photon number current albedos defined by Equation (15) were obtained from the relationship

$$\alpha(E_o, \theta_o, \theta, \varphi, t; i) = \alpha(E_o, 0, 0, 0, \infty; i) \cdot f(\theta_o) \cdot \cos\theta \cdot g(t), \quad (29)$$

$$= \alpha(E_o; i) \cdot f(\theta_o) \cdot \cos\theta \cdot g(t), \quad (30)$$

where

$\alpha(E_o; i)$ = the angular differential number current albedo for gamma photons perpendicularly incident ($\theta_o=0$) and emergent ($\theta=0$) from scattering material i , ie. $180^\circ (= \theta_s)$ backscatter,

$g(t)$ = a function to account for reduced backscattering from a material of finite thickness t ,

$f(\theta_o)$ = a function to account for the albedo behaviour with change in θ_o .

From reference (16), the azimuthal dependence may be defined in terms of θ , θ_0 and the total scattering angle θ_s , as

$$\varphi = \cos^{-1} \left[\frac{\cos\theta_s + \cos\theta_0 \cos\theta}{\sin\theta \sin\theta_0} \right]$$

where

θ_s = the angle between the incident and emergent photon vectors, i. e., the scattering angle.

The present version of code ALB assumes^(9,10,12)

$$f(\theta_0) = \cos\theta_0, \quad (31)$$

and⁽¹¹⁾

$$g(t) = \alpha(E_0, t; i) / \alpha(E_0; i), \quad (32)$$

$$= 1 - e^{-ct}, \quad (33)$$

where c is a constant such that $g(t) = 0.99$, for $t = 2\lambda(E_0)_i$; $\lambda(E_0)$ is the mean-free-path in material i for photons of energy E_0 . Code ALB uses scattering angle θ_s to eliminate the albedo dependence on azimuth φ , in accord with the method of reference (16).

Experimentally measured values for the perpendicular differential number current albedo $\alpha(E_0; i)$, obtained from references (9,10), were encoded. For fast neutrons, Monte Carlo data from reference (12) was used for preliminary evaluations.

The code ALB geometry routines require that the spacecraft structure be defined in terms of the spatial coordinates of simple geometrical shapes, e.g. cylinders, tubes, boxes, slabs, etc. These shapes allow the flat-sided cylindrical spacecraft body, boom-arms, antennae,

science platforms, etc. to be accounted for. Coordinates are specified with respect to a reference Cartesian coordinate frame as shown in Figure 5. The Cartesian frame may be located arbitrarily but the spacecraft vertical axis is suggested for the Z-axis of the frame. From an engineering standpoint, coordinates may be readily obtained from preliminary or final design drawings. The code determines whether the radiation illuminated surfaces are visible to the detector. It subdivides cylindrical regions radially into planar strips for albedo determinations. The dimensions of the strips are determined as a function of the specific cylinder radius with respect to distance from source and detector. The lateral extent of all plane areas is subdivided into dimensions which are small relative to distance from source and detector. Cylindrical scattering may be optionally carried out according to either the albedo or single scatter methods. Booms are evaluated using the single scatter technique. Wall thickness must be specified for all volume geometries; solids may be specified by taking the wall thickness equal to the radius for a cylinder or the half-breadth in the case of a box.

Code XEST determines the value of L_{\min} satisfying equation (20) and thus obtains W_{\min} of equation (17), or the li_{\min} of equation (18). Although specifically designed for the purpose of shadow shield optimization it is coded for larger shields. Code XEST solves equation (20) by the technique of iteration. For the first iteration the code assumes a build-up factor of unity to determine $L_{\min_e}^{(1)}$. For the second iteration a Monte Carlo build-up factor based on $L_{\min_e}^{(1)}$ and calculated by NUGAM1 is used to iterate $L_{\min_e}^{(2)}$. Iteration is arrested when

$$\left| \left(L_{\min_e}^{(h)} - L_{\min_e}^{(h-1)} \right) / L_{\min_e}^{(h)} \right| \leq \epsilon, \quad (34)$$

where

ϵ = preassigned tolerance,

h = iteration number.

3.3 CODE OPERATING INFORMATION

3.3.1 General

Code SØSC is written in FORTRAN-IV for the NASA-GSFC IBM-360/91 digital computer. It may be run on any IBM-360 with sufficient core size, ie. the present version requires bytes, (4 bytes/word). There are no Sense Switch or special tape requirements. Input formats are standard FORTRAN-IV, as given in any IBM or CDC Fortran manual; the code has been designed with a view to ease of translation for use on other than IBM computers. Input/output tapes are presently coded as LI and LØ equal to 5 and 6, respectively, at the beginning of MAIN. A code listing is given in Appendix III.

Section 3.3.2 defines the constants appearing in the various subroutines throughout the code. Input card details, order, formats, restrictions and location are given in Section 3.3.3. Card numbers are encircled and defined in the order in which they are read by the code. A sample input listing is presented in Appendix IV. Code output is reviewed in Section 3.3.4. Section 3.3.5 is a discussion of the results obtained with code SØSC. Appendix V is a sample output listing. It corresponds to the sample input of Appendix IV. Debug type output may be obtained by input of card ③. The user is cautioned with respect to profusion of output under this option - - - a trial using sample data is recommended first. The code SØSC input data card deck consists of twenty-two (22) types of cards, referred to as Card ①, Card ②, etc. If the type requires more than a single card the reference is made to Card Set ○.

Code NUGAM1 determines the angular energy transport of gamma photons in a finite cylindrical shield. It was derived from an existing Monte Carlo source self-absorption code --- NUALGAM, developed for NASA-GSFC by NUS Corporation, and described in NUS-536⁽³⁾. This code follows photon transport and considers pair-production, Compton scattering and photo-electric interaction phenomena. A description of this code is given in Appendix II. In code NUGAM1, the shield may be composed of a single material of simple or complex composition or stratifications i.e. "discs", of simple or complex composition, including vacuum. The code is presently designed for either an axial point or plane parallel source but may be readily adapted to other distributions. Similarly, the code may be readily modified to allow the study of annular-cylindrical shields, rectangular slabs, etc.

The source spectral distribution may consist of a large number of photon energy groups. In order to reduce costly Monte Carlo evaluation at each energy the code may be restricted to user selected energy groups in the energy domain. Intermediate energy evaluations over the source spectrum are obtained by quadratic interpolation.

Code NUGAM1 may be used to determine angular differential forward build-up for gamma photons. Preliminary studies with this code, which may be either called by code SØSC or used as a separate code, have revealed that the forward buildup factor for the shadow shields is less than that to be expected for a large (semi-infinite) shield, in agreement with qualitative argument.

3.3.2 Code Constants

The constant 0.51097 is required for energy conversion from MeV to the unit of electron rest mass. This value appears in subroutines DCØMP, GENSIG, ØUTPUT, SINGSC SPECTM, and XEST.

The constants PYE, RADAP and CMPI are coded in MAIN and communicated by CØMMØN/CØNST/ and CØMMØN/CØRDS/. They are defined as PYE = $\pi = 3.14159$, RADAP = factor for conversion of angles from degrees to radians, CMIP = factor for conversion from cm to inch.

The Avogadro number, 0.6023×10^{24} , is used in subroutines GENSIG and NENSIG.

The constant value 0.28183×10^{-12} cm used in subroutine CIGMA is the classical electron radius, r_0 .

The constant value 0.49895×10^{-24} used in subroutine SIGMA is equal to $2\pi r_0^2$.

The experimental albedo data used in subroutine ALBEDØ are given in reference (9). The number albedos DAØN, the corresponding energies EE and the atomic number MN of the scattering medium are coded in the DATA statements in ALBEDØ.

The value 0.69314718 in subroutine INDEX is the natural logarithm of 2. Gamma photon and fast neutron cross-sections input data may be taken directly from the references (17, 18, 19, 20, 21, 22).

3.3.3 Card Input Details

<u>NAME</u>	<u>COLUMN</u>	<u>FORMAT</u>	<u>DESCRIPTION, PURPOSE OR USE</u>
<u>Card ①</u> (single card to define the problem case path; 1814; MAIN)			
(NPATH (I), 18)	1-4, 5-8, etc.	14	Execution path options (see Figure 6 for specific integer values)
<u>Card ①-1</u> (single card; 6F10.4; MAIN)			
XS	1-10	F10.4	Cartesian coordinates (x, y, z) of the source geometric center (inches)*.
YS	11-20	F10.4	
ZS	21-30	F10.4	
XD	31-40	F10.4	Cartesian coordinates (x, y, z) of the point detector eg. science package (inches)*.
YD	41-50	F10.4	
ZD	51-60	F10.4	
RADIUS	61-66	F6.3	Radius of shield (inches).
DIST	67-72	F6.3	Source to shield distance (inches).

*The reference Cartesian frame (and its origin) are located by the user as described in Section 3.2.

Card ② (single card; 3I 5, F10.5; MAIN)

NE	1-5	I5	Number of gamma source spectrum energy increment midpoints (≤ 20).
NG	6-10	I5	Input card option signal: =0, gamma source only, ie. input card sets ③ and ④. =1, neutron source only, ie. input card sets ⑤ and 6. =2, gamma and neutron source, ie. input cards sets ③ through ⑥.

<u>NAME</u>	<u>COLUMN</u>	<u>FORMAT</u>	<u>DESCRIPTION, PURPOSE OR USE</u>
NNE	11-15	I5	Number of fast neutron source spectrum energy increment mid-points (≤ 20).
INE	16-20	I5	Number of equal energy intervals in escape spectrum from in the range 0 to EE(NE) (≤ 25).
NØPT	21-25	I5	Option for intermediate output =0, no intermediate output, $\neq 0$ intermediate output and NGAMA set equal to 100.
NRAND	26-30	I5	Initial random number (must be odd number and different for each job submitted)
NØES	31-35	I5	Number of indices (and history multipliers) in card set (2) -1 and -2; \leq INE.
ALLOWF	36-42	F7.4	Total number flux allowed at the detector, $(\gamma + n)/\text{cm}^2\text{-sec}$.
ECT	43-49	F7.4	Low energy cut-off (MeV).
ARREST	50-56	F7.4	The iteration arresting criterion, ϵ , as in Equation (34) and Figure 4; a fraction.
TANDEM	57-63	F7.4	The number of tandem sources, ie. final data is multiplied by TANDEM, eg. = 2 for configuration of Figure 1.
FRG	64-70	F7.4	Gamma photon source axial-to-radial emission ratio; axial is in source-to-detector direction.

<u>NAME</u>	<u>COLUMN</u>	<u>FORMAT</u>	<u>DESCRIPTION, PURPOSE OR USE</u>
FRN	71-77	F7.4	Fast neutron source axial-to-radial emission ratio.
<u>Card Set 2 -1</u> (single card input only if NE > 4; 20I4; MAIN)			
LE(1)	1-4	I4	Index of source spectrum first selected energy midpoint at which a buildup factor is to be determined by code NUGAM1; intermediate index values will be code interpolated (first energy is lowest energy).
LE(2)	5-8	I4	Ditto For second selected energy midpoint
LE(NOES)		I4	Ditto for NOES selected energy midpoint
<u>Card Set 2 -2</u> (single card; 20F4.0; MAIN)			
HGAMA (1)	1-4	F4.0	Multiplier for obtaining the number of Monte Carlo histories (in thousands) to be generated at the selected energy index LE(1); eg. HGAMA(1) = 3.0 generates 300 3000 histories.
NGAMA (2)	5-8	F4.0	Ditto for LE(2)
HGAMA (NOES)		F4.0	Ditto for LE(NOES)

<u>NAME</u>	<u>COLUMN</u>	<u>FORMAT</u>	<u>DESCRIPTION, PURPOSE OR USE</u>
<u>Card Set ③</u> ((NE/12) + 1 cards*; 12F6.2; MAIN)			
EE(1)	1-6	F6.2	Gamma photon source spectrum energy at first (lowest energy) increment mid-point (MeV).
EE(2)	1-6	F6.2	Ditto for second energy
EE(12)	7-12	F6.2	Ditto for twelfth energy
EE(NE)	-	F6.2	Ditto for NE energy

*NE/12 = 0 if NE < 12; = 1 if 12 ≤ NE < 24; etc. This integer meaning applies throughout Section 3.3.

<u>Card Set ④</u> ((NE/7) + 1 cards; 7F10.3; MAIN)			
SS(1)	1-10	F10.3	Gamma photon source isotropic emission rate corresponding to energy EE(1); (photons/second).
SS(2)	11-20	F10.3	Ditto for EE(2)
SS(7)	61-70	F10.3	Ditto for EE(7)
SS(NE)	-	F10.3	Ditto for EE(NE)

<u>NAME</u>	<u>COLUMN</u>	<u>FORMAT</u>	<u>DESCRIPTION, PURPOSE OR USE</u>
-------------	---------------	---------------	------------------------------------

Card Set 5 ((NNE/7) + 1 cards; 7F10.3; MAIN)

EN(1)	1-10	F10.3	Fast neutron source spectrum energy at first (lowest energy) increment mid-point (MeV).
EN(2)	11-20	F10.3	Ditto for second energy
.			
EN(7)	61-70	F10.3	Ditto for seventh energy
.			
EN(NNE)	-	F10.3	Ditto for EN(NNE)

Card Set 6 ((NNE/7) + 1 cards; 7F10.3; MAIN)

SN(1)	1-10	F10.3	Fast neutron source isotropic emission rate corresponding to energy EN(1) (n/second).
SN(2)	11-20	F10.3	Ditto for EN(2)
SN(7)	61-70	F10.3	Ditto for EN(7)
.			
SN(NNE)	-	F10.3	Ditto for EN(NNE)

Card 7 (single card; 12; ALB)

NORF	1-2	I2	Number of spacecraft scattering structural members in the problem model, ie defines the number of times card sets 8 through 15 are to be repeated; card sets
------	-----	----	--

<u>NAME</u>	<u>COLUMN</u>	<u>FORMAT</u>	<u>DESCRIPTION, PURPOSE OR USE</u>
			⑪ through ⑬ not input the M value repeated (structural material unchanged).
<u>Card ⑧</u> (single card; A22; ALB)			
STRUCT	1-8	"A8"	Alphanumeric name of spacecraft scattering member geometry, eg. BOOM, CYLINDER, etc.
POINT	9-16	"A8"	Alphanumeric name of spacecraft scattering member identifier or label, e.g. M-F.
RMAT	17-22	"A6"	Alphanumeric name of spacecraft scattering member material, eg. IRON, LEAD, etc.
<u>Card ⑨</u> (single card; I1, I4, 2I5, 3F10.5; ALB)			
NNNN	1	I1	The number of spacecraft scattering member material elements, eg. = 2 for Al_2O_3 . (assumed =1 if input omitted)
M	2-5	I4	Atomic number of spacecraft scattering material.
IP	6-10	I5	Number of Cartesian coordinate points required to describe spacecraft scattering member, eg. = 2 for cylinder. (see Figure 5).
IK	11-15	I5	Spacecraft scattering member geometry identifier: = 0 , plane = 1 , boom arm or cylinder = 2 , rectangular box structure

<u>NAME</u>	<u>COLUMN</u>	<u>FORMAT</u>	<u>DESCRIPTION, PURPOSE OR USE</u>
T2	16-25	F10.5	Spacecraft scattering member thickness for plane or outer radius for cylinder or boom (inches).
T1	26-35	F10.5	Spacecraft scattering member inner radius for cylinder or boom; not required for plane (inches).
Tb	36-45	F10.5	Photon scattering method option: $\neq 0$, albedo method $= 0$, single scattering method if IK = 0 or 1 .
NT	46-50	I5	Single to signify the direction of the outward normal for plane (see Figure 5) $= + 1$, if origin (0,0,0) of Cartesian frame is within material defined by surface $= - 1$, if origin outside (and thus "viewing") the plane $= 0$ or blank , if IK = 0 (i.e. not a plane).

Card Set 10 ((IP/3) + 1 cards; 9F8.5; ALB)

X(1)	1-8	F8.5	} Cartesian coordinates (x,y,z,) of first point required to describe location of spacecraft scattering member (inches)*. (See IP of Card Set <u>9</u> and Figure 5).
Y(1)	9-16	F8.5	
Z(1)	17-24	F8.5	
.	.	.	

*The order of input of the coordinates must be clockwise "viewing" each surfact from "outside" the volume; the input order for surfaces may be arbitrary.

<u>NAME</u>	<u>COLUMN</u>	<u>FORMAT</u>	<u>DESCRIPTION, PURPOSE OR USE</u>
X(IP)	-	F8.5	Cartesian coordinates (x, y, z) of IP th coordinate point required to describe location of space-craft scattering member (inches). (see IP of Card Set (9) and Figure 5).
Y(IP)	-	F8.5	
Z(IP)	-	F8.5	

Card (11) (single card; 3I5; GENSIG) (See Figure 7)

NINT	1-5	I5	Gamma photon cross-section table parameter; 2^{NINT} energy intervals/group.
ILØW	6-10	I5	Cross-section table parameter; $2^{ILØW}$ is lowest energy bound of table (m_0c^2 units).
IHIGH	11-15	I5	Cross-section table parameter; 2^{IHIGH} is highest energy bound of table (m_0c^2 units).

Card (12) (single card; 15, 3F10.5; GENSIG)

ME	1-5	I5	The number of energies for which cross-section data to be input.
DENSTY	11-20	F10.5	The density of the medium element for which cross-section data to be input (gm/cc).
ATØMNØ	21-30	F10.5	The atomic number of the medium element for which cross-section data to be input.
ANDAW	31-40	F10.5	The atomic weight of the medium element for which cross-section data to be input.

<u>NAME</u>	<u>COLUMN</u>	<u>FORMAT</u>	<u>DESCRIPTION, PURPOSE OR USE</u>
Card Type 13 ((ME/3) + 1 cards; 9E8.3; GENSIG)			
E(1)	1-8	E8.3	First (lowest) energy for input of cross-section data (MeV).
SIGPE(1)	9-16	E8.3	Photoelectric cross-section for energy E(1), (barns/atom).
SIGPP(1)	17-24	E8.3	Pair-production cross-section for energy E(1), (barns/atom).
E(2)	25-32	E8.3	Similar to E(1)
SIGPE(2)	33-40	E8.3	Similar to SIGPE(1)
SIGPP(2)	41-48	E8.3	Similar to SIGPP(1)
E(3)	49-56	E8.3	Similar to E(1)
SIGPE(3)	57-64	E8.3	Similar to SIGPE(1)
SIGPP(3)	65-72	E8.3	Similar to SIGPP(1)
E(4)	1-8	E8.3	Similar to E(1)
.			
.			
E(ME)	-	E8.3	Highest energy for input of cross-section data (MeV).
SIGPE(ME)	-	E8.3	Photoelectric cross-section for energy E(ME) (barn/atom).
SIGPP(ME)	-	E8.3	Pair-production cross-section for energy E(ME) (barn/atom).

<u>NAME</u>	<u>COLUMN</u>	<u>FORMAT</u>	<u>DESCRIPTION, PURPOSE OR USE</u>
-------------	---------------	---------------	------------------------------------

Card (14) and Card Set (15) are not input in the present code version. They will be input in a future version for neutron scattering calculations. Although they are not input (and the code does not expect them) they are detailed.

Card (14) (single card; I2, 3F10.5; NENSIG)

NN	1-2	I2	Number of energies for which fast neutron cross-sections are input.
DENSTY	3-12	F10.5	Density as in Card (12).
ATØMNØ	13-22	F10.5	Atomic number as in Card (12).
ANDAN	23-32	F10.5	Atomic weight as in Card (12).

Card Set (15) ((NN/3) + 1 cards; 9F7.2; NENSIG)

ENN(1)	1-7	F7.2	First (lowest) energy for input of fast neutron cross-section (MeV).
XSN(1)	8-14	F7.2	Fast neutron total cross-section for energy ENN(1) (barn/atom).
XAN(1)	15-21	F7.2	Fast neutron scattering cross-section for energy ENN(1) (barn/atom).
.			
.			
.			
XAN(3)	57-63	F7.2	Fast neutron scattering cross-section for energy ENN(3) (barn/atom).
.			
.			
.			
.			

<u>NAME</u>	<u>COLUMN</u>	<u>FORMAT</u>	<u>DESCRIPTION, PURPOSE OR USE</u>
ENN(NN)	-	F7.2	Highest fast neutron scattering cross-section for energy ENN(NN) (barn/atom).
XSN(NN)	-	F7.2	Fast neutron total cross-section for energy ENN(NN) (barn/atom).
XAN(NN)	-	F7.2	Fast neutron scattering cross-section for energy ENN(NN) (barn/atom).
Card 16 (single card; 'A80'; MAIN)			
TITLE	1-80	'A80'	Alphanumeric description of shield for user identity.
Card 17 (single card; I5; MAIN)			
NØM	1-5	I5	Number of shield material layers, i.e. >1 for a laminar shield (≤9).
Card 18 (single card; 9(F5.2,I2); MAIN)			
RA(1)	1-5	F5.2	Shield layer thickness fraction with respect to shield total thickness; for first (1 at source end of shield) layer.
NELE(1)	6-7	I2	Number of elements in first shield layer.
.			
.			
.			
RA(NØM)	57-61	F5.2	Shield layer thickness fraction with respect to shield total thickness; for last (NØM) shield layer.
NELE(NØM)	62-63	I2	Number of elements in shield layer NØM.

<u>NAME</u>	<u>COLUMN</u>	<u>FORMAT</u>	<u>DESCRIPTION, PURPOSE OR USE</u>
-------------	---------------	---------------	------------------------------------

Card Set (19) $\left[\left(\left(\sum_{I=1}^{NOM} NELE(I) \right) / 7 \right) + 1; 7(F4.0, F6.4); MAIN \right]$

ZZ(1,1)			Atomic number of first shield layer, first elemental component.
DENSY(1,1)			Density in first shield layer of material ZZ(1,1) elemental component.
.			
.			
ZZ(NOM, NELE(NOM))			Density in NOM shield layer of material ZZ(NOM, NELE(NOM)) elemental component.

Card Set (20) (GENSIG)

Consists of Card Set (11) repeated once to define energy variables for the shield.

Card Set (21) (NENSIG)

Consists of Card (12) and Card Set (13) to define shield photon cross-sections, repeated for each shield element and each layer, i.e., Cards (12) and (13), input as a pair, N times, where

$$N = \sum_{I=1}^{NOM} NELE(I)$$

Card Set (22) (NENSIG)

Similar to Card (14) and Card Set (15) to define shield fast neutron cross-sections, repeated for each shield and each layer, i.e., Cards (14) and (15), both input, N times, where

$$N = \sum_{I=1}^{NOM} NELE(I)$$

The remainder of this section consists of comments and additional explanation of the input just described. Only those items which it is felt require special treatment will be discussed.

NPATH (I): The option values input on Card (1) route the code as shown in Figure 6. New values must be input for each shield case being studied. At present only the first seven (7) options are used by the code; the remainder NPATH (8) to NPATH (18) are spare for future use.

XS, YS, ZS, XD, YD, ZD, RADIUS, DIST:

The first six items input on Card (1) -1 define the geometric center of the source on tandem source pair and the point detector. The input values are relative to the location of the Cartesian axes and origin chosen by the user. All coordinates unput are similarly referenced. The items RADIUS and DIST correspond to R_s and r_{OS} defined in Figures 2 and 3, respectively.

INE, NORP, NRAND, ALLOWF, ECT, ARREST, FRG, FRN: The shield escape distribution is catergorized into an energy spectrum of INE groups. NOPT allows the user to obtain a profusion of code intermediate output, if $\neq 0$, however only 100 Monte Carlo histories are traced in this event. Repeated use of the same input value of NRAND will result in identical results, hence the instruction that arbitrary but differing values be input for a sequence of runs and run sets. The NASA-GSFC IBM-360 random number generating code requires that NRAND be an odd number. ALLOWF is equivalent to the specified criterion flux, C , defined preceeding Equation (17). $C = 10.0$ in the present report examples. Monte Carlo histories are terminated for photons whose energy is degraded below ECT. ECT should be input such that it is $\geq 2^{ILOW}$ (see Figure 7). In the present work examples ECT was taken as 0.1 MeV. Monte Carlo computer time is

generally increased by decreasing ECT. Buildup factor iteration, as in Figure 4 is arrested according to an input value of the fraction, ARREST, which corresponds to ϵ in Figure 4 and Equation (34). Taking Figure 8 as an example the axial-to-radial emission, ratios FRG and FRN are obtained as 0.0833 and 0.804, respectively.

NE, LE(I), NØES, HGAMA(I): if the source spectrum contains a large number of energy groups, e.g. NE = 18, the Monte Carlo evaluation is carried out at the user selected group indices (LI(I), I = 1, NØES) and intermediate values quadratically interpolated, e.g. evaluation may be requested at LE(I) = 1, 5, 7, 9, 15 and 18 where NØES + 6 (the number of indices). Since transport intensity is a function of energy for a given material, the number of Monte Carlo histories per energy index may be varied through an input of HGAMA(I), e.g. for the above HGAMA(I) might be = 5, 4, 3, 2, 2, and 1 which corresponds to 5000, 4000, 2000 and 1000 histories.

NØRF, M: card sets ⑧ through ⑮ are input NØRF times after input of card ⑦ (NØRF). Since card sets ⑪, ⑫ and ⑬ are cross sections for scattering items defined by cards ⑧, ⑨ and ⑩ and thus may be the same for many sequentially input items, their ⑪ - ⑬ input is emitted for repeating value of M. For example, if three aluminum and two iron structural members defined by five repeats of cards ⑧, ⑨ and ⑩ then in turn, M = 13, 13, 13, 26, 26, and ⑪ through ⑬ input twice (for the underlined M).

X(I), Y(I), Z(I), IP, IK, T2, T1, TB, NT: References to Figure 5 is recommended. The coordinates of the corners of each geometry defining the scatter structure model are specified by X(I), Y(I), and Z(I). For a triangular or quadrilateral plane area, the number of corners IP = 3 and 4, respectively. IP = 24 for a box structure; 4 corners/face for six faces. For a box or quadrilateral plane the angles

subtended by the sides are arbitrary. For a cylinder (or boom tube) only the coordinates of the axial ends are specified, and thus $IP = 2$; the inner and outer radii are specified per $T1$ and $T2$ respectively. $T2$ specifies wall thickness for a plane or box. Since a cylinder and a plane may be optionally analyzed by either the albedo or single scatter technique, the decision is specified through the value of TB . In order to define the "exterior" side of planar media the direction of the outward normal is specified (+) or (-) per $NT = \pm 1$. The user must determine whether the origin (0,0,0) is "inside or outside" of the planar medium. If the origin is inside the medium then $NT=+1$, else $= -1$. It is pointed out that the code automatically subdivides cylinders radially and axially into elemental areas which are small relative to the distance from either source or detector; this is necessary to maintain validity of inverse square relationships. The shapes allowed by the code may be combined to generate other geometries, e.g. a cone may be represented as isosceles plane area triangles in contact on each side.

$NINT$, $IL\emptyset W$, $IHIGH$: the cross-section table generated by subroutine GENSIG consists of $(IHIGH - IL\emptyset W)$ energy groups, each containing 2^{NINT} sub-intervals. The total number of subintervals, over all groups, is equal to $1 + (IHIGH - IL\emptyset W) 2^{NINT}$. The energy width of each sub-interval within any given group is the same and equal to $2^{N-1} (2^{IL\emptyset W} / 2^{NINT})$, where N is the group interval number, beginning at $N = 1$, the lowest group. The energy bounds of group 1 are $2^{IL\emptyset W}$ and $2^{IL\emptyset W + 1}$. The energy bounds of group N are $2^{IHIGH-1}$ and 2^{IHIGH} . The energy unit pertinent to this entire explanatory comment is m_0c^2 ($= .51097$ MeV). An illustration of this comment is given in Figure 7. The relationship of the cross-sections generated with respect to ECT are also indicated. It should be noted that $ECT \geq 2^{IL\emptyset W}$.

NELE, DENSTY, ATØMNØ, ANDAW: where the source medium consists of only a single element, e.g. Fe, the earlier descriptions are considered adequate. Where the source consists of such as a compound then further clarification is now given:

Card types (12) and (13) (or (14) and (15)) for spacecraft (read as 19 through 22 for shield) must be repeated for each element in the compound, e.g. for Sm_2O_3 , input data for Sm and for O. Continuing with Sm_2O_3 as the example, NELE = 2, to indicate two elements (Sm and O); ATØMNØ, ANDAW are input as 62.0, 150.35 and 8.0, 16.0, respectively. Only the input values of DENSTY need reflect the number of atoms of Sm and O in Sm_2O_3 . DENSTY is determined as

$$\begin{aligned} \text{DENSTY} \Bigg|_{\text{Sm}} &= \frac{2 * \text{ANDAW}/\text{Sm}}{\text{ANDAW}/\text{Sm}_2\text{O}_3} * \text{DENSTY}/\text{Sm}_2\text{O}_3 \\ &= \frac{2 * 150.35}{348.7} * 1.51 = 1.302 \end{aligned}$$

and

$$\text{DENSTY}/\text{O} = \frac{3 * 16}{348.7} * 1.51 = 0.208$$

ME, SIGPE, SIGPP, E: the cross-section data required for input on card type (13) may be obtained from the references (17-21). The number of value-sets input from energy E (1) to E (ME), need only encompass the energy range 2^{LOW} to 2^{HIGH} , with spacing as per the references. The code generates its own cross-section table using logarithmic interpolation. A table of E, SIGPE, SIGPP is given in Appendix VI of reference (3).

RA(I), NELE(I): the shield may be defined as having laminar layers (R(I), I=1, NØM) and each lamination may have NELE(I) elemental components. RA(I) is a fractional length, e.g. if the shield length = L and RA(1), RA(2) and RA(3) are = 0.1, 0.2 and 0.7, then the lamination lengths, in the source to detector direction are lengths 0.1L, 0.2L and 0.7L. The code determines the optimum value of L. Each lamination I, may have elemental composition NELE(I) e.g. NELE(1), NELE(2) and NELE(3) = 2, 1 and 1, for a three layer LiH + Fe + Pb shield.

3.3.4 Code Output

Throughout the discussion in this section, reference to the Sample Code Output listing of Appendix V is necessary and understood. Output which is adequately defined by headings is either not discussed or mentioned only briefly. Output pages are referred to by means of the encircled letters A, B, C, etc.

Ⓐ This page consists of the input gamma spectrum and/or neutron spectrum data and the flux at the detector for each energy interval.

Ⓑ This page consists of the albedo and single scatter information for each input scattering item (e.g. spacecraft structural member or component).

The total (integrated) scattered flux at detector is also given.

Ⓒ This page consists of shield information: source energy groups, shield material composition, buildup factors, direct and attenuated fluxes as well as the estimated thickness and weight. Initial output of this page for each shield is for buildup factors of unity.

Ⓓ The values on this page are as input according to Section 3.3.3, with a number of exceptions, namely:

1. ESCAPE SPECTRUM ENERGIES (MC**2) — photons escaping from the source cylinder are terminally categorized within these energy bounds.
2. ESCAPE SPECTRUM ANGLES (RADIANS) — photons escaping from the source cylinder are terminally categorized within solid angles defined by the escape angles. Zero angle is defined along the + Z-axis in the direction "source to detector".

Ⓔ These page(s) consist of the terminal results of unscattered photon escapes categorized as a function of source energy. The source photon energies are identified obviously for each table, as are the escape angles and solid angles (both in radians). The other columns are identified as follows:

1. NUMBER — the number of photons escaping between angle A_i and A_{i+1} , ie. in the noted solid angle; based on 4π space.
2. NUMBER/STER — the number of photons escaping between angle A_i and A_{i+1} , per steradian.

3. FRACT/STER — the number of photons escaping between angle A_i and A_{i+1} , per steradian per total number of source photon histories initiated.
4. PAIR PHOTOONS — the number of pair photons escaping between angle A_i and A_{i+1} .
5. UNSCATTERED ESCAPES — the total number of source photons escaping without a single collision, ie. the sum of item 1 above is given at the bottom of each table.
6. NUMBER AV/STER — the average number of escaping photons per steradian, ie. the sum of item 1 divided by 4π .
7. PAIR PHOTON ESCAPES — the total number of unscattered pair photons escapes, ie. the sum of item 4.
8. NO PP IN FWD CONE — the total number of unscattered pair photon escape in the forward 10 degree cone. Note: in this discussion 'forward' 10 degree cone excludes shield side escapes ie. forward face escapes only.

(F) These page(s) consist of the terminal results of scattered photon escapes categorized according to escape energy interval tables. The escape interval energies, angles and solid angles are identified obviously. The remaining columns are analogous to E above, except for the following:

1. SCATTERED ESCAPES — the total number of source photons escaping after one or more scatterings is given at the bottom of each table, analogous to C4, above.
2. P. E. ABSORPTIONS — the total number of source photons "lost" to photoelectric absorption.
3. NO .IN FWD CONE/STER — the scattered photon escapes in the the forward 10 degree cone; number per steradian.

Ⓒ The output on this page consists largely of summarization of the data in E and F above. Initial and Cut-off energies are in MeV units. The TOTAL NO. OF COLLISIONS does not refer to a terminal classification and is thus only of either statistical or incidental interest. The termination table consists of the following:

1. ENERGY — the number of histories terminated through scatter reducing the photon energy below the input cut-off energy (ECT) threshold. Such terminations are considered as absorptions.
2. WEIGHT — the number of histories terminated through the weight being reduced to less than the termination threshold value (coded as 10^{-5}). Such terminations are regarded as absorptions.
3. ESCAPE — the number of histories terminated through TOTAL UNSCATTERED ESCAPE plus TOTAL SCATTERED ESCAPE, ie. the sum of items 5 and 6 listed below.
- 3A. TOTAL ESCAPING FRACTION — escaping fraction per history, ie. item 3 divided by the total number of histories.
4. ABSORBED (1. + 2. + 7.) — the number of histories terminated through ENERGY plus WEIGHT plus PHOTOELECTRIC ABSORPTION, ie., the sum of items 1, 2 and 7.
5. TOTAL UNSCATTERED ESCAPES — this is item E4 repeated.
- 5A. TOTAL UNSCATTERED FRACTION — item G5 per history.

6. TOTAL SCATTER ESCAPES — the number of scattered escaping photons summed over all escape energies.
- 6A. TOTAL SCATTERED ESCAPE FRACTION — item G6 per history.
7. PHOTOELECTRIC ABSORPTION — the number of photoelectrically absorbed photons summed over all energies.
8. PAIR PRODUCTION PHOTONS — the total number of 0.51 annihilation photons originating in pair production interactions.
9. TOTAL ESCAPES IN FWD 10 - DEG CONE — total escapes through forward 10 degree cone and summed over all energies.
10. TOTAL IN FWD CONE/STER — item G9 per steradian.
11. TERMINATION PAIR PHOTONS—this termination table categorizes the fate of the shield pair produced photons.
12. TALLY CHECK—this item should equate to the total number of photon histories.

Page sets D, E, F and G are output for each input index LE(I) and iteration, i.e. NØES times for each iteration, e.g. if 3 iterations then D, E, F and G are output 3* NØES times. At the end of each iteration i.e. every NØES set of D, E, f and G, page C is repeated. The last page C output is the final result for each shield problem and is thus noted. The final results on page C consist the gamma photon and fast neutron source spectra as well as the corresponding iterated buildup factors and detectable attenuated fluxes. The note of change of flux as a function of shield length is tabulated for four shield lengths in the "length-vicinity" of the criterion flux. The first length value: the table is the predicted

optimum obtained by quadratic interpolation remaining three values .
The optimum shield length L , weighted density ρ and total weight, W ,
are given. The total structural scattered and shield attenuated fluxes
calculated by the code are also output, as are the same values corrected
for the number of spacecraft symmetric sources or source tandems, eg.
in the example in Appendices IV and V, TANDEM = 2.0, corresponding
to the two Fondem sets shown in Figure 1. Thus although the code
calculated scattered and attenuated fluxes of 0.608 and by TANDEM = 2
to equate to ALLOWF = 10.0 when summed, ie. the values become 1.216
and 8.784 particles/cm² second .

3.3.5. Discussion

Sample results obtained with the SØSC code are reviewed in this report section. They assume the typical unmanned spacecraft as in Figure 1. The dimensions of this craft were obtained either directly or by scaling NASA-GSFC preliminary design drawings.

The sample calculations assumed four (4) SNAP-27 RTG's, each five (5) years aged and of 1575 thermal watt capacity. The RTG's were taken as being in tandem pairs as in Figure 1. The science experiment package was located 6.87 meters from the RTG's. The unshielded direct and energy integrated number fluxes at the experiment package were taken as $25.2 \gamma/\text{cm}^2\text{-sec}$ and $13.5 \text{ neutrons}/\text{cm}^2\text{-sec}$ per tandem pair of RTG's; these values were obtained from NASA source data. Fluxes in the axially perpendicular direction (radial) were taken as 12.0 and 1.25 times those in the axial direction. The fluxes assumed at a distance of 6.87 meters from RTG tandem pair are shown in Figure 8.

The spacecraft structure scattered flux at the science package was predicted by the code as being $1.22 \text{ particles}/\text{cm}^2\text{-sec}$, for the four RTG's. The Code SØSC predictions for 8.04 cm diameter optimum weight shields, per RTG tandem pair and the noted materials, were:

LiH	Al	Fe	Pb	
1651	1932	2451	2617	grams
(3.64	4.26	5.40	5.75	lbs)

A two lamination shield of total length 10.56 cm, made up of 1.056 cm Pb (nearest source) and 9.504 cm Al requires a shield weighing 1900 gm. This is 32 gm less than an Al shield and 3.4 cm shorter in length. A laminar shield of Pb and LiH, in the same length fractions, 0.1 and 0.9, reduced

the optimum weight to 1580 gm for a length of 16.59 cm compared with 39.5 cm for a LiH shield. A reversal of the shield material order from 0.1 Pb + 0.9 LiH to 0.9 LiH + 0.1 Pb, in the direction: source to detector, led to a weight reduction from 1580 to 1550 gms. Although two laminations of the same materials (e.g. Pb-Al-Pb-Al) generally did not.

Figure 9 shows the weight of a LiH + Pb shield as a function of the ratio of LiH length to total shield length. The optimum weight shield is seen to be given for a ratio of 0.92 (i.e. 0.92 LiH + 0.08 Pb). The optimum is obtained for a slope of zero. The dashed curve in Figure 8 indicates the change in total length of the LiH + Pb shield. At a length ratio of 0.92 the total length is < 50% of the 'all' LiH shield; at a weight ratio of 0.83 (weight \approx 1600 gm) the total length is reduced by a factor of \sim 3. Thus this curve, obtained by running code SØSC, allows a best compromise between optimum weight and shield length to be chosen; this may be important in a spaceflight mission launching where volume is a prime consideration.

When only gamma photons were considered high atomic numbered material gave the most favorable results. For the sample case, ignoring neutrons i.e. photons only, tungsten and tin shields weights were predicted as 1567 and 1903 gm.

The sample problem output given in Appendix V indicates, on page type C, the range of the buildup factors for the case of the 0.9 LiH + 0.1 Pb shield. They can be seen to range from 1.0 to 1.08, as compared with 1.0 to 1.15 for 0.1 Pb + 0.9 LiH; for Pb only, the factor ranged from 1.0 to 1.33. The build-up factor behaviour in the shadow shield is quite different from the expected for a semi-infinite or bulk, shield. Photons and even neutrons, have a high probability of escaping after one or more scatters. This coupled with the low

probability of being scattered to the distant detector accounts for the values being only some 10 or 20% above unity. Only radiation escaping through the shield face closest to the detector were considered as possible contributors to the buildup factor

From the sample problems run and reported herein and as substantiated by earlier determinations reported in NUS-600⁽²⁾, the assumed spacecraft-payload design yields an energy and particle integrated flux at the payload which is ~ 10% scatter and ~ 90% shield attenuated. This supports the approximated approach to the scatter problem which is designed into Code SØSC.

Code SØSC determinations of the scattered flux at the science experiment, i.e. at the detector, although based on albedo and single-scatter techniques which are, of course, approximate, allow the inclusion of all structural detail. The direct and complete Monte Carlo approach to the scatter problem would be prohibitively complex and costly and would still only provide a good approximation. The Monte Carlo approximation may be inferred from the fact that even in simple geometries Monte Carlo predictions frequently deviate 10% to 50% from good experimental data.

Calculations reported in NUS-600⁽²⁾ indicated relatively good agreement between single scatter and albedo predictions for geometries where material was either relatively thin or where such as tube members were being considered. Sample evaluations from NUS-600 are reproduced in Appendix VI of this present report.

4. DESIGN OF EXPERIMENT

The design of an experiment to verify the predictions of code SØSC, is outlined in this report section. The experiment is required to verify both the spacecraft scattered and shield transmitted radiation fluxes as well as the optimum shield weight and configuration. Although the experiment must necessarily be carried out in a terrestrial laboratory and thus be influenced by such as air and laboratory structural material interactions as opposed to the ideal in-vacuo environment of deep space, these effects can generally be corrected for.

Referring to Figure 3, the experiment must provide data to substantiate predictions of flux: $\phi_{\alpha}(E_{\alpha}) + \phi_a(E_o; E_a)$ as well as give optimum shield length, L. The experiment should be carried out for both gamma photons and neutrons. In order to carry out the experiment for an actual spacecraft with PuO₂ fuelled RTG sources, the spacecraft, RTG's and a suitable detection system are required to be located in a suitable laboratory. Assuming the availability of these items the experiment becomes very straight forward. Such an experiment requires an efficient detector for fast neutrons in the presence of a relatively high gamma photon field, e.g. a liquid organic scintillator such as NE-213 or -218* which allow pulse shape discrimination for detected photon rejection to be accomplished. The gamma photons will be most efficiently detected by a thallium-activated sodium-iodide scintillation detector. The detection capabilities and necessary subsequent analysis for both of these detector types with respect to the proposed experiment, have been adequately described in NUS-486⁽³²⁾.

In the likely event that an actual spacecraft is unavailable for an experiment, a mock-up may be fabricated using "everyday" materials of composition, dimension and mass closely similar to that of a spacecraft. Again laboratory neutron and gamma sources may be judiciously substituted for an actual RTG assembly.

* NE-213 and NE-218 are organic liquid scintillators manufactured by: Nuclear Enterprises, Inc., San Carlos, California.

However, accepting the fact that a mock-up experiment will verify code SØSC data, leads to the obvious idea of simplifying the mock-up. For example, the use of a small number of typical structural component mock-ups will suffice for comparison of experimental data with code predictions for the same configuration. Shield transmission may be studied experimentally by the use of axially located and adjacent thin discs in various quantities and material combinations. This approach to the experiment allows its economical implementation in a conventional laboratory. It requires the availability of the necessary detectors and an associated multichannel pulse-height analyzer as well as neutron and gamma photon sources of known emission strength.

Figure 10 (a) shows a source, detector, shield and scatterer located in the geometry of a proposed experiment. Although the distances r_0 , r_1 and r_2 should be chosen such as to model the experiment after the actual spacecraft configuration, dependence on source strength and detection statistics will generally dictate their actual dimensions. For example, since shield attenuation factors will generally be studied in the range 0.2 to 0.02 a source strength, $S_0 \sim 1.0 \text{ mC}$, is desirable to yield a statistically good detector count rate for $r_0 = 1$ meter; inverse-square law considerations allow strength to be determined for other values of r_0 . Removal of the shield will yield detector count rates larger in accord with the noted attenuation factors. The flux scattered to the detector by the spacecraft mock-up member, of area A, will be less than that along path r_0 , in the ratio $r_0^2 / (r_1^2 + r_2^2)$ for geometrical reasons, assuming total reflection at A. Since reflection will be far from total, being instead expressed by the differential albedo (see Section 3.2.) and since the actual value of the area A is also a factor, it will be necessary to use a source strength, $S_\alpha \gg S_0$, for this experiment phase. Actual source strengths S_0 and S_α may be varied to some extent by choice of counting duration.

Referring to Figure 10 (a), and assuming sources S_0 and S_α , the experiment may be carried out as follows:

I using source S_α , detect radiation transmitted by a shield of length L and scattering from an area A. Increasing L incrementally the detector will eventually detect only radiation scattered by area A. In this manner $\phi_\alpha(E_\alpha)$ is experimentally obtained after background subtraction and spectral unfolding analysis. The choice of shield material for this phase is not critical since only elimination of direct radiation is a requirement. Background is determined by repeating the experimental counting for the "infinitely thick" shield with the scattering area A removed. It is recommended that the area A be located away from laboratory structure throughout the experiment. The methods noted here are very similar to those successfully employed in the research of reference (10) excepting that radiation beam collimation will be as indicated in Figure 10 (a).

II using a source S_0 which is identical to S_α in all respects except emission strength, scattered flux may be taken as $= (S_0/S_\alpha) \cdot \phi_\alpha(E_\alpha)$, for the shield phase of the experiment; this assumes the presence of area A. Since area A is not necessary for this phase of the experiment, the geometry of Figure 10 (b) is proposed. In Figure 10 (b), the detector is shielded from radiation other than that transmitted by the shield. The detector response function is obtained by counting source radiation with the shield removed; this takes detector shielding and collimation effects into account. For a given shield composition and length the transmitted radiation flux $\phi_a(E_0; E_a)$ is obtained. If code SØSC is run for S_0 , r_0 and this flux as the criterion flux and ALB is omitted then comparison of the computed shield with the experiment shield may be carried out. Laminated shield verifications may be studied in the same manner.

Although the above experiment description calls for reduction of radiation counts to particle fluxes , approximate results may be obtained without reduction if the researcher is cognizant of detector response as a function of energy.

5. SUMMARY AND CONCLUSIONS

Analytic procedures and computer codes have been developed for the prediction of weight optimized radioisotope thermoelectric generator shields to protect science experiments for unmanned spacecraft operating in deep space. The analytic procedures, presented in Section 2.2, consist of iteratively solving the basic transport relationship after first determining the spacecraft scattered flux component. The transport relationship is solved through the use of the Monte Carlo technique and analytic approximation. The scattered flux is obtained through the use of albedo, single scatter and analytic techniques.

A FORTRAN IV IBM-360/91 digital computer code package --- SØSC was designed and developed to carry out the prediction of optimum shield weights and dimensions. This code uses all of the developed procedures to best advantage. In addition to its designed application of shield design for protection of science experiments it may be used to either design shadow shields or to map radiation scattering for general application.

In addition to the technique and code development, an experiment to evaluate predicted data has been presented. This experiment, outlined in section 4, is proposed for future effort. The anticipated spectrometry data to be obtained from the experiment may be readily analyzed with the aid of the spectral analysis codes CUPED⁽³³⁾, CUNED⁽³⁴⁾ and SØSC developed by NUS for NASA-Goddard Space Flight Center.

It is proposed that a future work program consider the incorporation into code SØSC, of a Monte Carlo neutron transport routine. It is also proposed that code SØSC be modified to take neutron scattering from the spacecraft structure into account. Consideration should also be given to the production of secondary radiation in the shield as a result of neutron interactions, e.g. activation gamma photons. It is proposed that gamma photon transport results - - - albedos, single scattering and buildup factors - - - obtained in the work scope being

developed by NUS for NASA-GSFC under contract NAS5-11781, be incorporated into SØSC to the extent necessary and appropriate.

It is concluded that code SØSC and its encoded techniques provide a useful addition to the field of spacecraft radiation transport. The code makes a valuable engineering tool available for both preliminary and final craft engineering design.

REFERENCES

1. ANDERSON, M. E., and NEFF, R. A., "Neutron Emission Rates and Energy Spectra of Two Pu²³⁸ Power Sources", Nuclear Applications and Technology, 7, 62-65 (1969).
2. STEYN, J. J., and HUANG, R., "Mid-Term Report for Unmanned Spacecraft RTG Shield Optimization Study", NUS-600 (1969).
3. STEYN, J. J. and STRAHL, J. T., "NUALGAM - A Monte Carlo Code to Predict the Angular Energy Escape of Gamma Photons from Cylindrical Sources", NUS-536 (1969).
4. JAEGER, R. G., Editor-in-Chief, "Engineering Compendium on Radiation Shielding", Vol. I: Shielding Fundamentals and Methods, Springer-Verlag, New York, Inc. (1968).
5. TRUBEY, D. K., "A Survey of Empirical Functions Used to Fit Gamma Ray Build-up Factors", ORNL-RSIC-10 (1966).
6. SELPH, W. E., "Neutron and Gamma-Ray Albedos", ORNL-RSIC-21 (1968).
7. ROCKWELL III, THEODORE, Editor, "Reactor Shielding Design Manual", TID-7004, p. 317 (1956).
8. SMITH, C. V. and SCOFIELD, N.E., "The Moments Method Used to Determine the Energy Albedo of Gamma Rays from Cesium-137 Impinging on Aluminum and Iron Barriers", USNRDL-TR-67-120, U. S. Naval Radiological Defense Laboratory, (September 1967).
9. STEYN, J. J., "Backscatter of Normally Incident Gamma Photons From Semi-Infinite Media of Varying Atomic Number", Ph. D. Thesis, Univ. of Toronto (1965).
10. STEYN, J. J. and ANDREWS, D. G., "Experimental Differential Number, Energy and Exposure Albedos for Semi-Infinite Media, for Normally Incident Gamma Photons", Nucl. Sci. Eng., 27, 318 (1967).
11. BULATOV, B. P. and GARUSOV, E. A., "Co⁶⁰ and Au¹⁹⁸ Gamma Ray Albedos of Various Materials", J. Nucl. Energy, Part A: Reactor Science, 11, 159 (1960).

12. FRENCH, R. L. and WELLS, M. B., "An Angle-Dependent Albedo for Fast-Neutron-Reflection Calculations", Nucl. Sci. Eng., 19, 441-448 (1964).
13. CASHWELL, E. D., and EVERETT, C. J., "Monte Carlo Method For Random Walk Problems", Pergamon Press (1959).
14. SHREIDER, YU A. (Editor), "The Monte Carlo Method", Pergamon Press (1966).
15. AVERY, A. F., et al., "Methods of Calculation for Use in the Design of Shields for Power Reactors", AERE-R-3216 (1960).
16. SHOEMAKER, N. F. and HUDDLESTON, C. M., "Economy of Experiment in Dose Albedo", Nucl. Sci. Eng., 18, 113-115 (1964).
17. WHITE-GRODSTEIN, G., "X-Ray Attenuation Coefficients from 10 keV to 100 MeV", NBS Circular 583 (1957).
18. MCGINNIES, R. T., "X-Ray Attenuation Coefficients from 10 keV to 100 MeV", Supplement to NBS Circular 583 (1959).
19. HUBBELL, J. H. and BERGER, M. J., "Photon Attenuation and Energy Absorption Coefficients Tabulations and Discussion", NBS report 8681 (1966).
20. STORM, E., GILBERT, E., and ISRAEL, H., "Gamma Ray Absorption Coefficients For Elements 1 to 100 Derived from Theoretical Values of NBS", LASL-2237 (1959).
21. HUBBELL, J. H., "Photon Cross Sections, Attenuation Coefficients, and Energy Absorption Coefficients From 10 keV to 100 GeV", NSRDS-NBS 29, (1969).
22. GOLDBERG, M. D., et al., "Neutron Cross Sections", BNL-325, Second Edition, Supplement Number 2.
23. EVANS, R. D., "The Atomic Nucleus", McGraw-Hill Book Co., Inc., (1955).
24. FANO, U., SPENCER, L. V., and BERGER, M. J., "Handbuch der Physik", XXXVII/2, 660, (1959).

25. HEITLER, W., "The Quantum Theory of Radiation", Third Edition, Oxford University Press, (1960).
26. COMPTON, A. H., and ALLISON, S. K., "X-Rays in Theory and Experiment", D. Van Nostrand Co., Second Edition, (1963).
27. FANO, U., Nucleonics, "Gamma-Ray Attenuation", 11, 8-12, 9, & 55-61, (1953).
28. SEGRE, E., "Nuclei & Particles", Benjamin Publishing Company, (1964).
29. BLATT, J. M., and WEISSKOPF, V. F., "Theoretical Nuclear Physics", John Wiley & Sons, (1958).
30. _____, "Random Number Subprogram ---RAN", IBM Systems Reference Library, File 7040/7090-20, Form C20-1604-3, page 61 (December 1965).
31. Kahn, H., "Applications of Monte Carlo", AECU-3259 (1954).

FIGURES

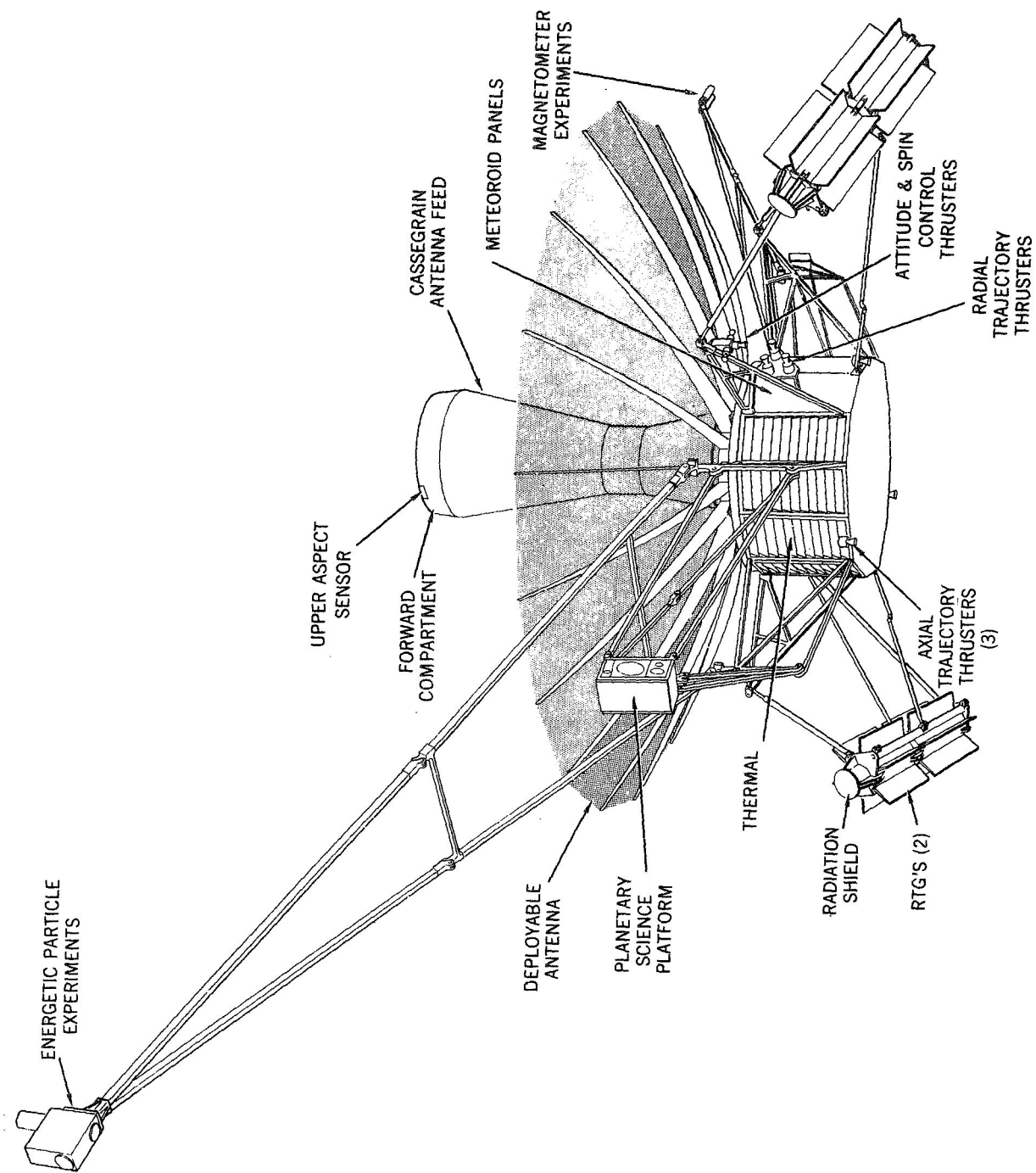


FIGURE 1
TYPICAL UNMANNED SPACECRAFT

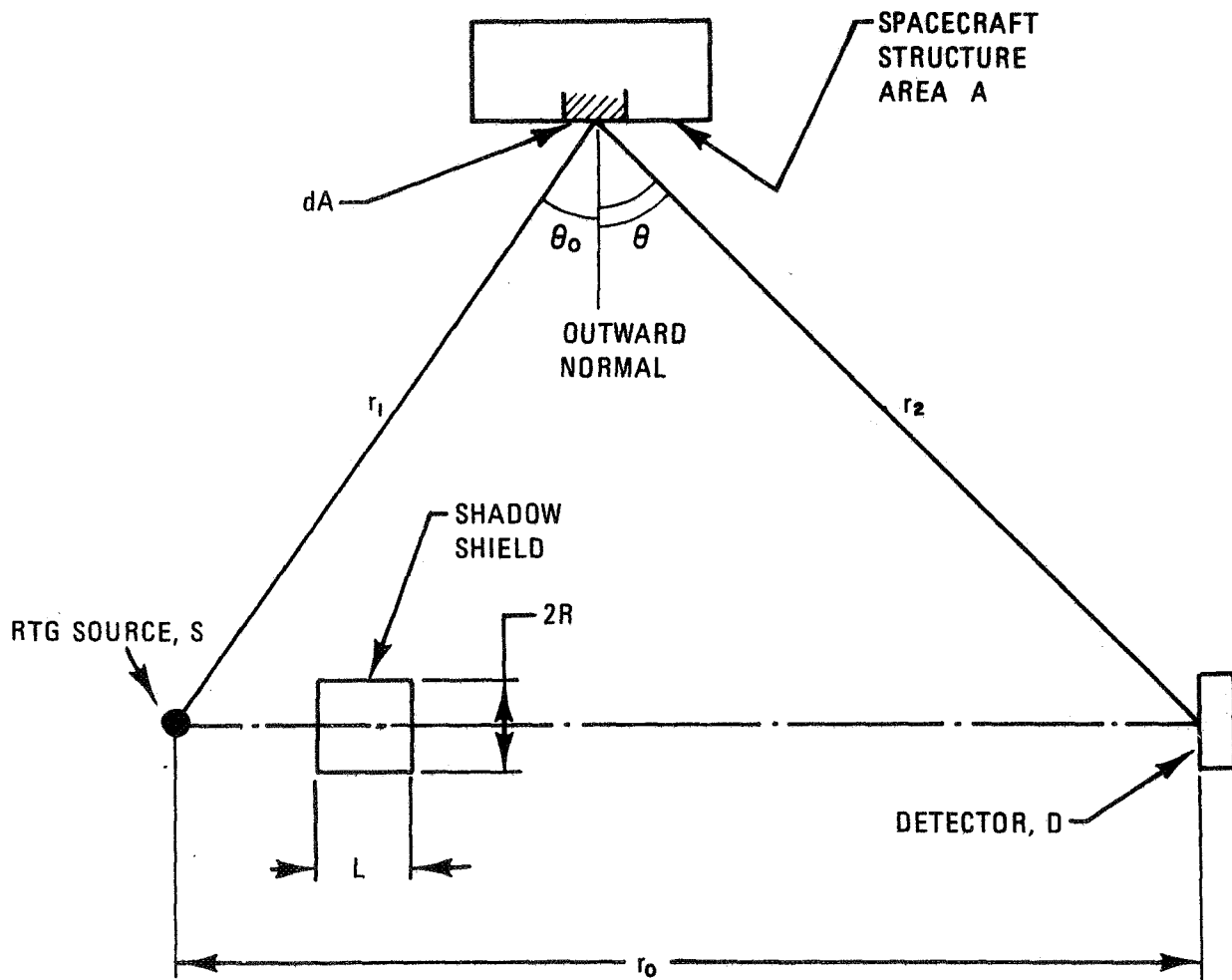
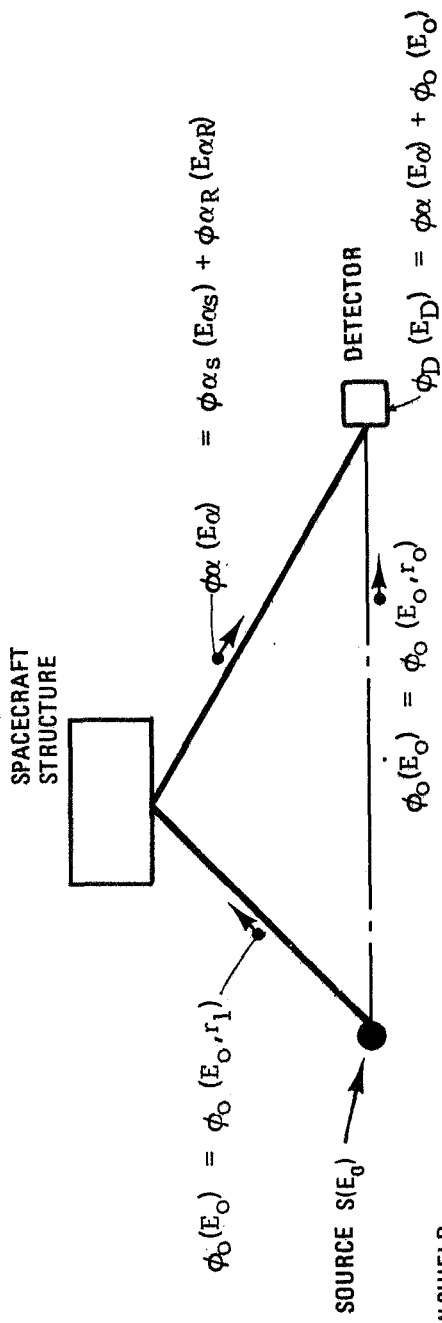


FIGURE 2
 SCHEMATIC DRAWING OF SPACECRAFT SHOWING
 RTG SOURCE, SHIELD AND DETECTOR ARRANGEMENT



a) NO SHADOW SHIELD

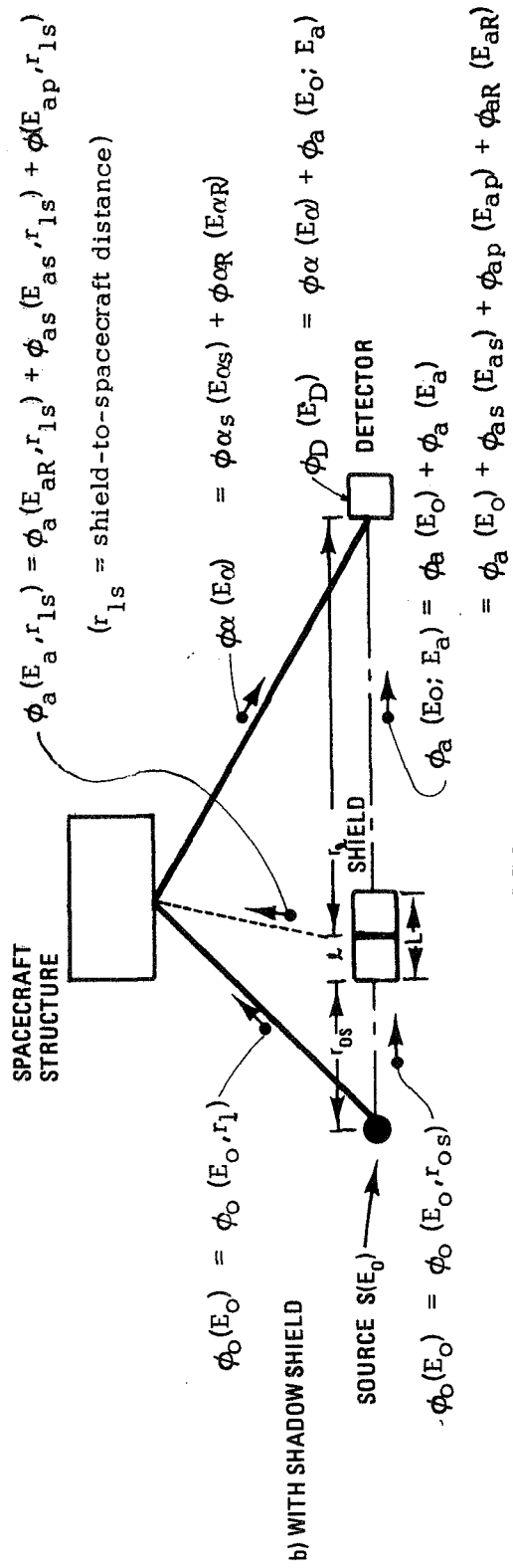


FIGURE 3

SCHEMATIC DEFINITION OF GAMMA PHOTON AND NEUTRON FLUXES

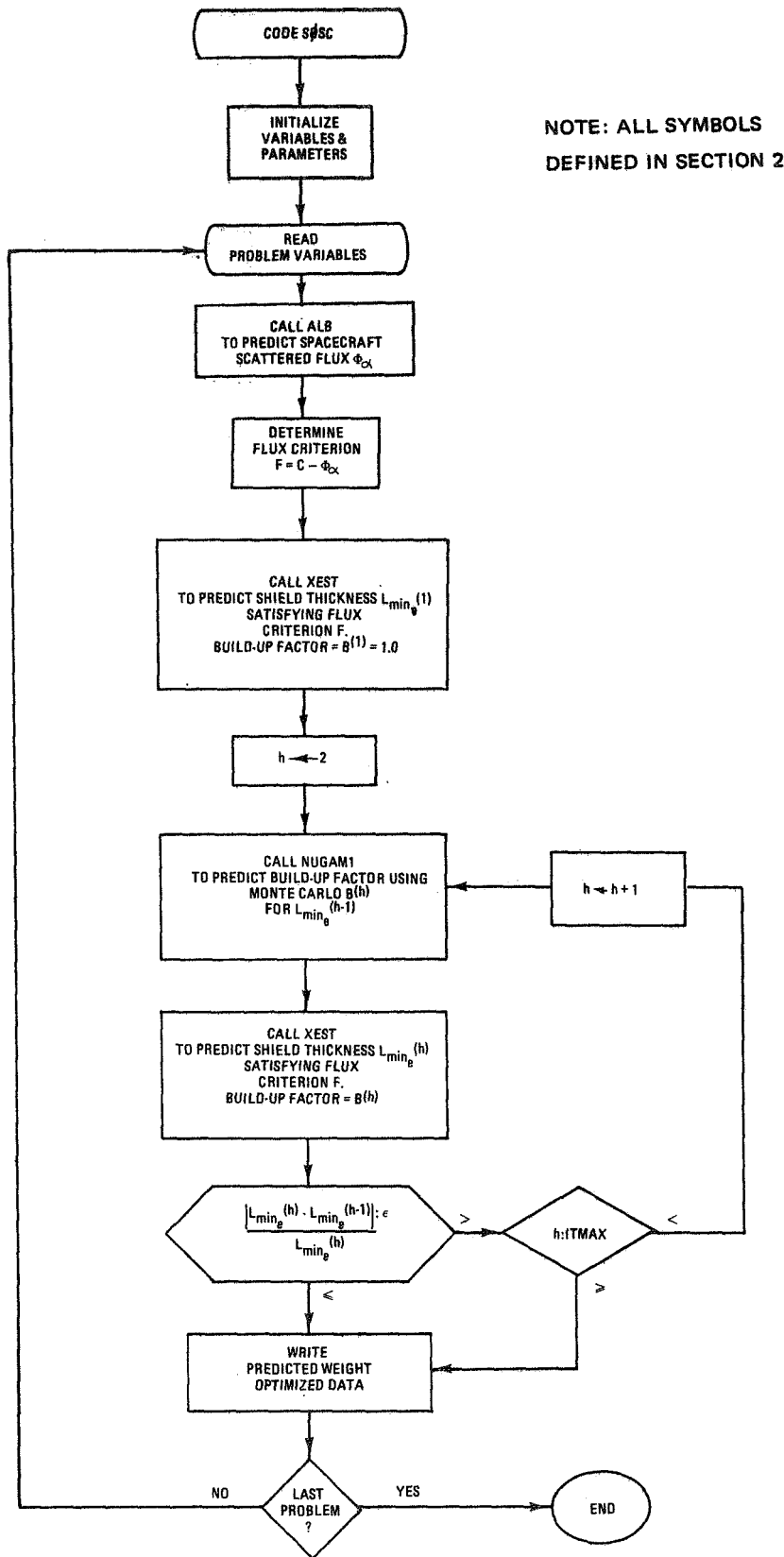
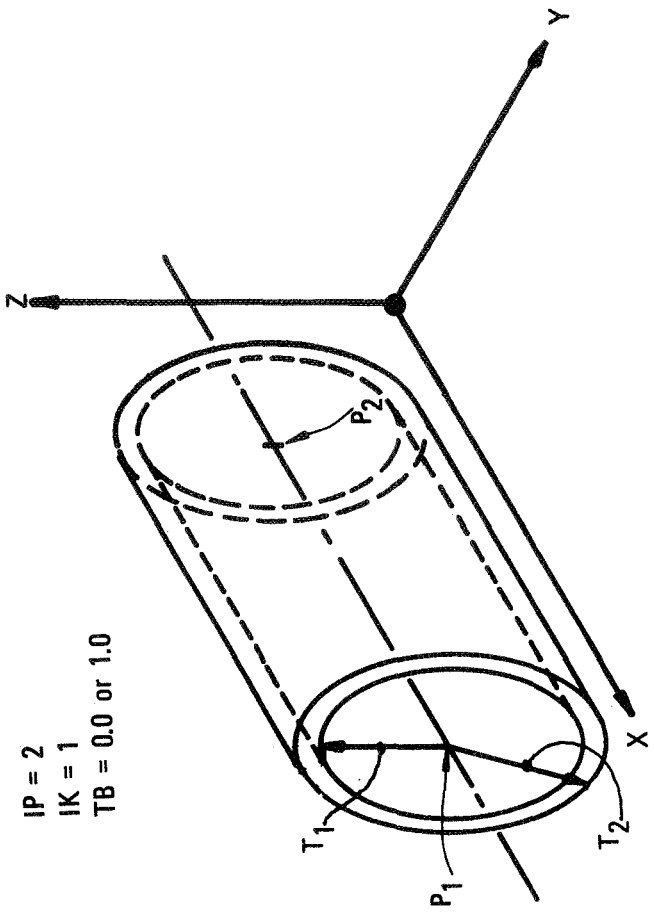
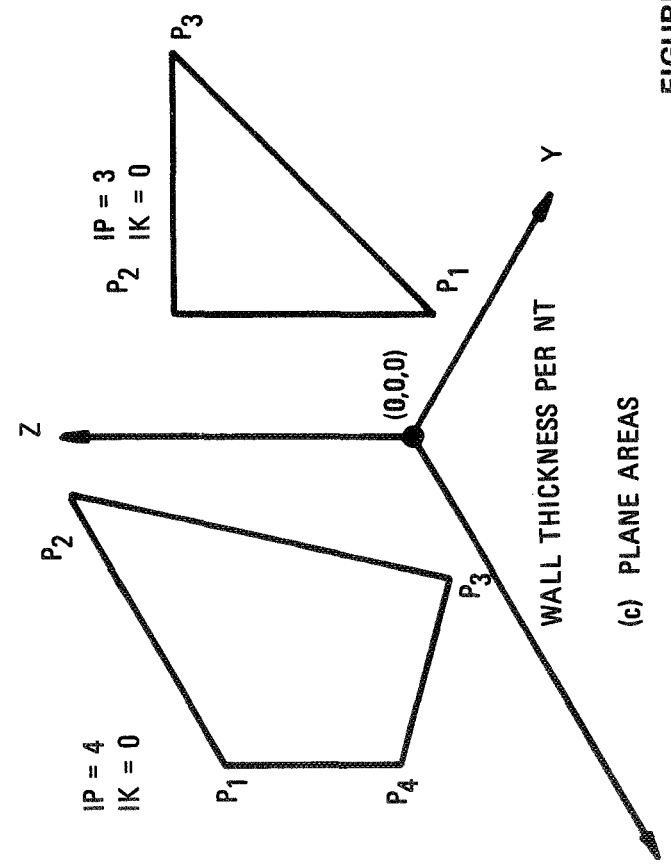


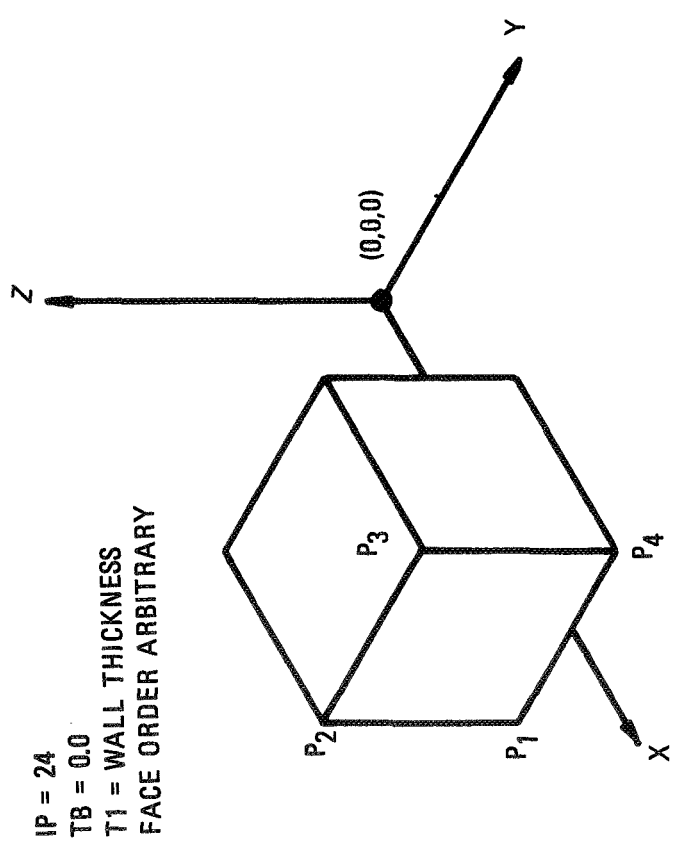
FIGURE 4
CODE SOSC LOGIC



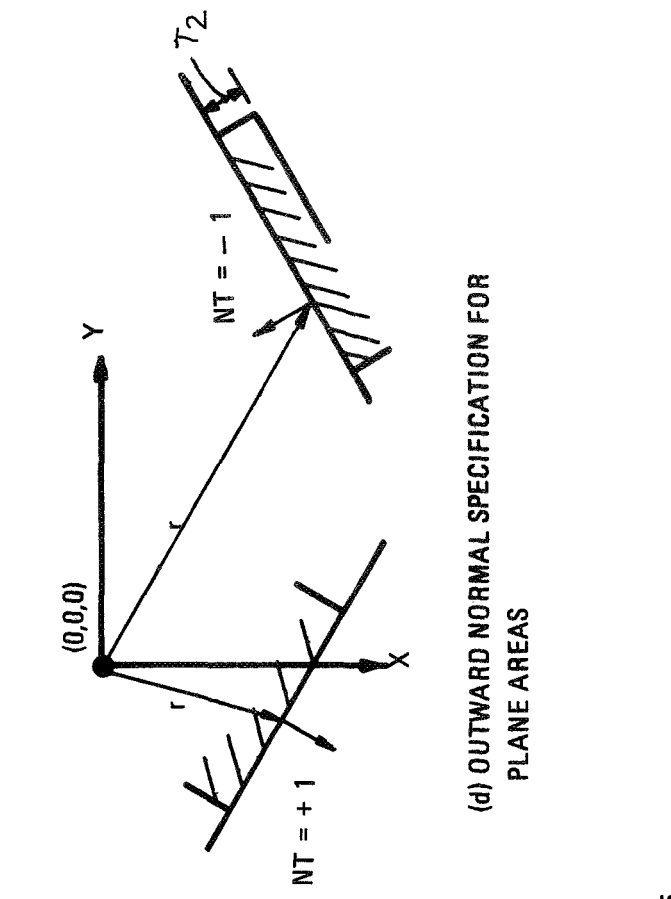
(a) BOX (6-SIDED POLYHEDRON)



(b) CYLINDER OR TUBE



(c) PLANE AREAS



(d) OUTWARD NORMAL SPECIFICATION FOR PLANE AREAS

FIGURE 5

DEFINITION OF SCATTERING STRUCTURE COORDINATE GEOMETRY

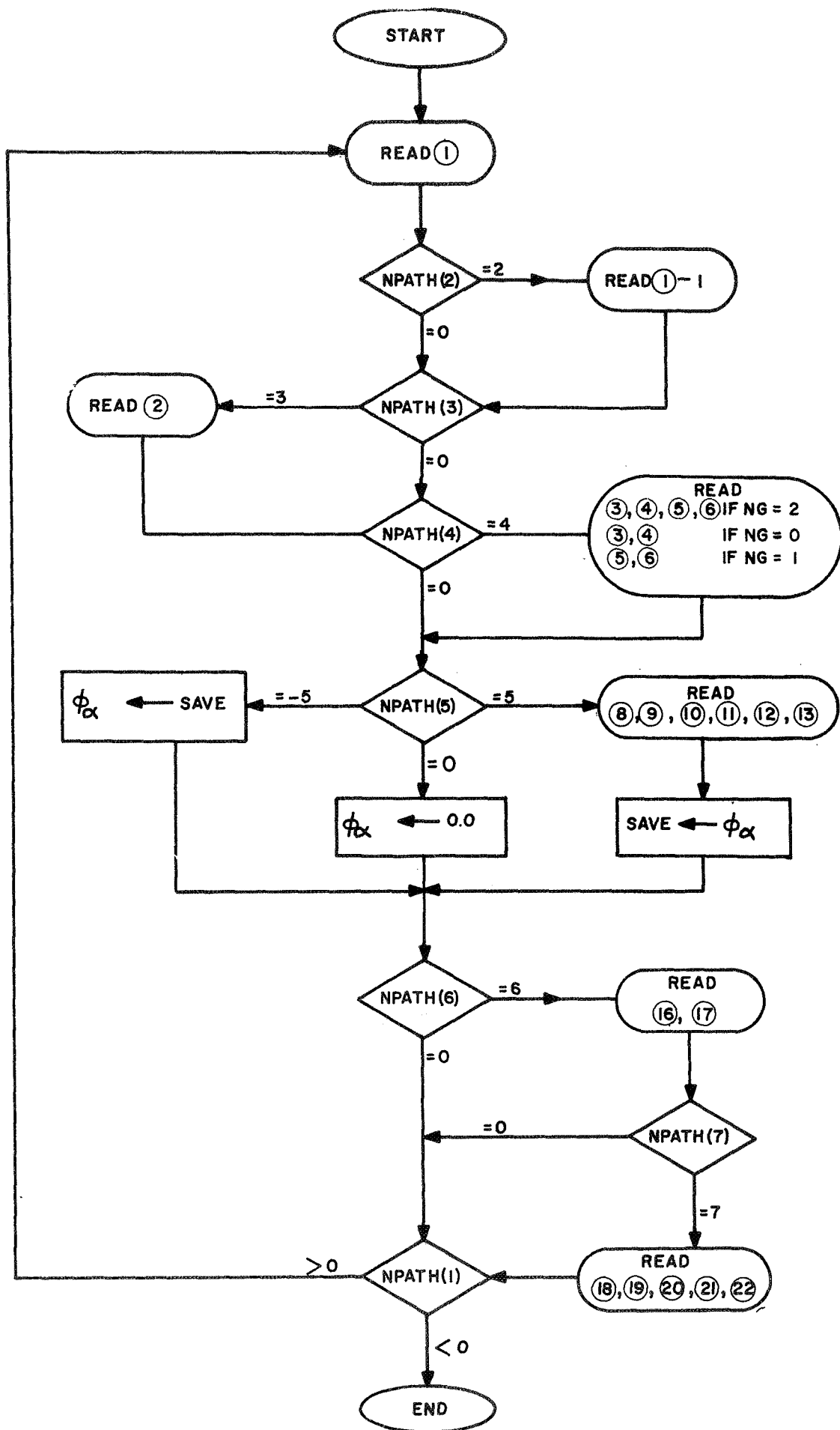


FIGURE 6

CODE SØSC ROUTING CONTROL OPTIONS

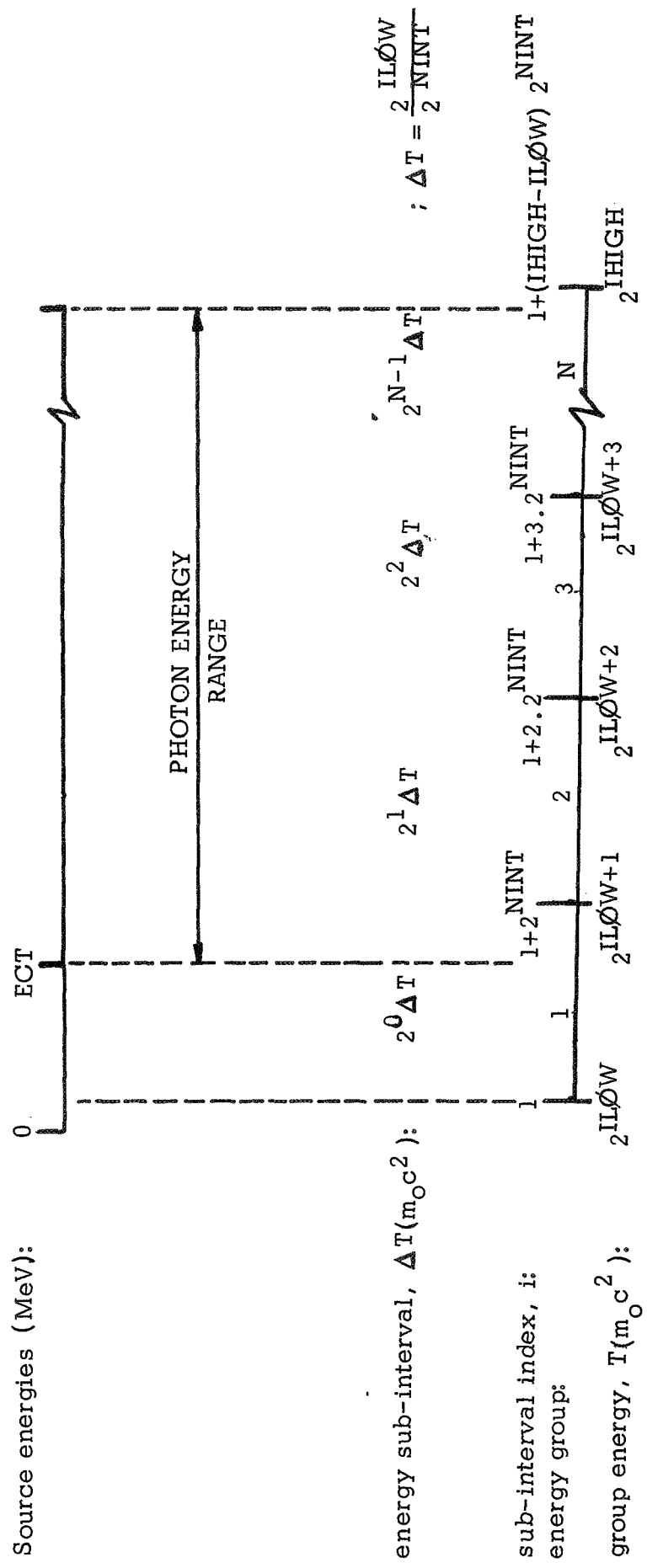


FIGURE 7
Energy Correspondence Bar Diagram

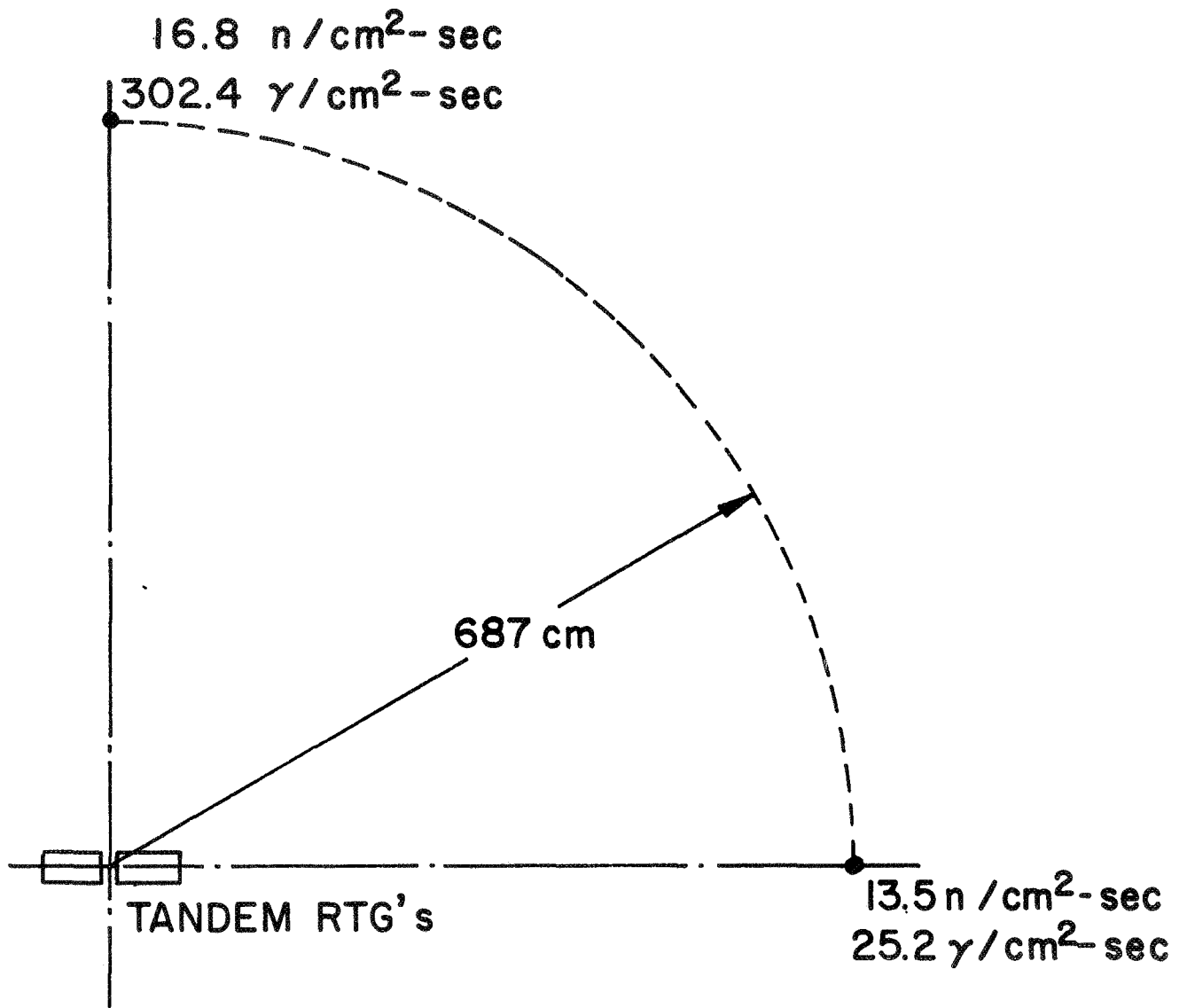


FIGURE 8

SOURCE TERM FLUXES AT 687 cm
FROM TANDEM RTG's

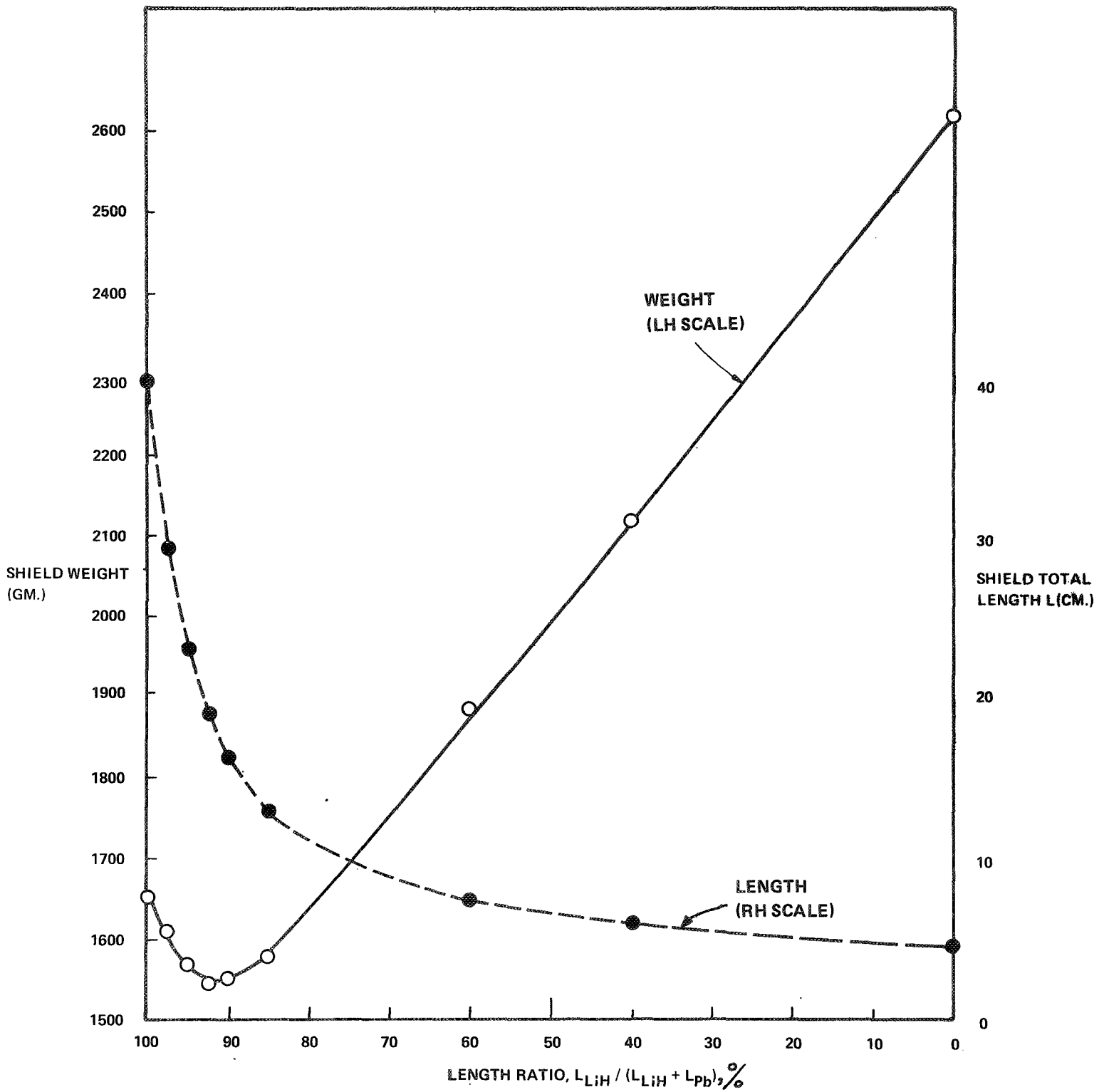
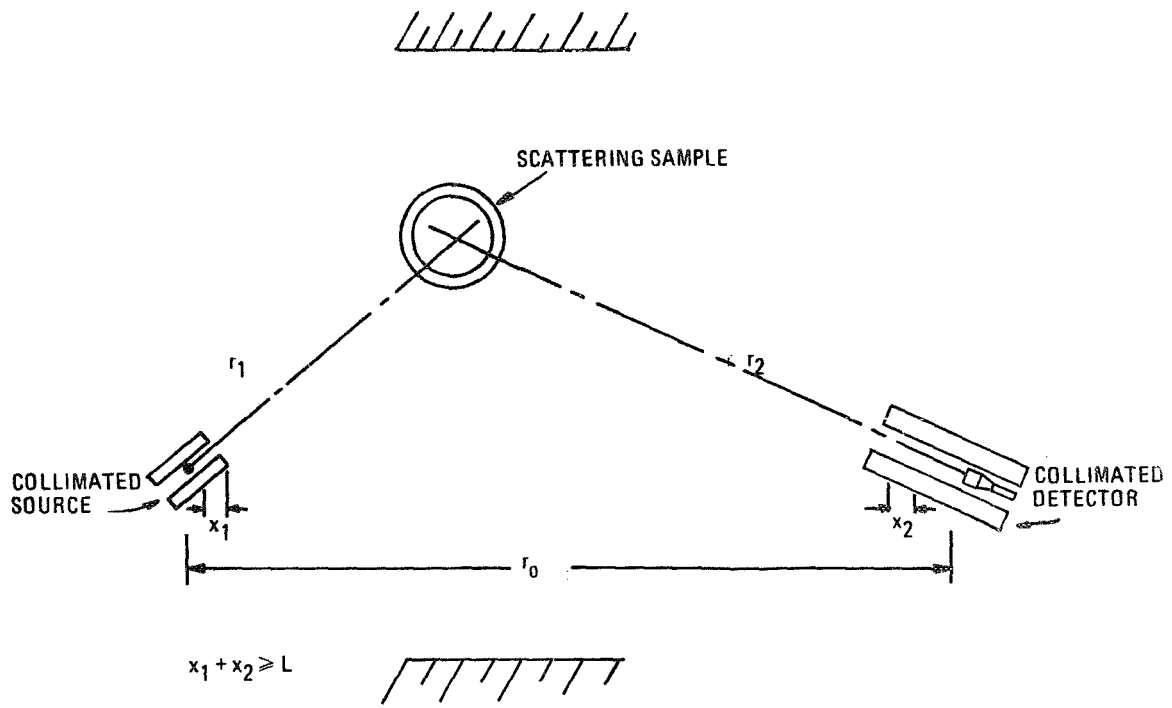
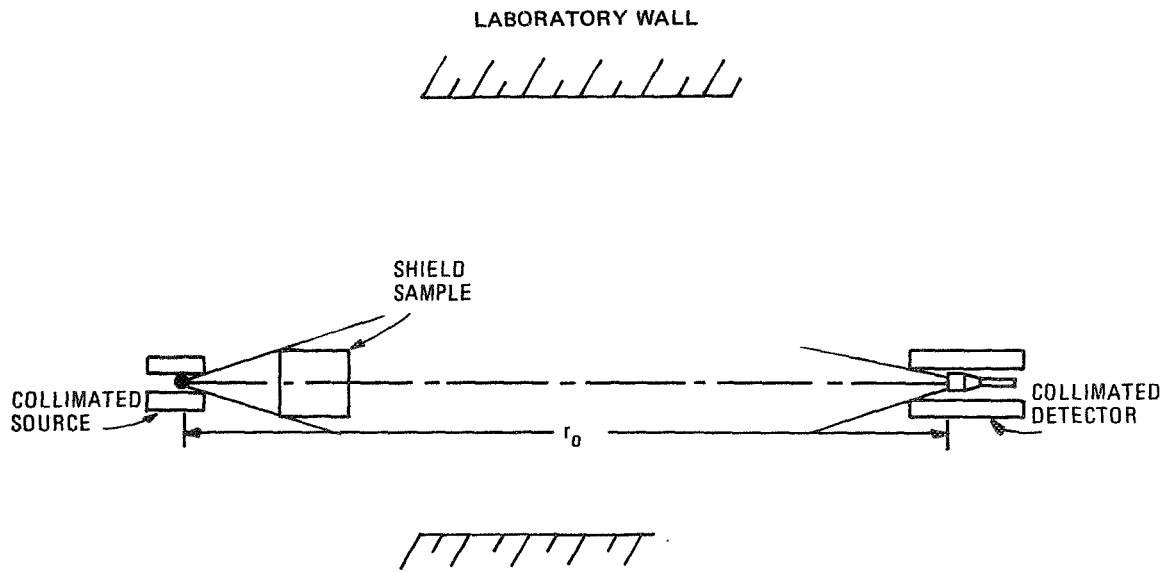


FIGURE 9

WEIGHT AND LENGTH OF LiH + Pb SHIELD
AS A FUNCTION OF LiH TO LiH + Pb LENGTH RATIO



(a)



(b)

FIGURE 10

GEOMETRY FOR PROPOSED EXPERIMENT

APPENDIX I
INTERACTION PHYSICS REVIEW

APPENDIX I

INTERACTION PHYSICS REVIEW

I GAMMA PHOTON INTERACTION PHENOMENA

In their passage through a medium, photons interact with the electrons and nuclei of atoms in their path. These phenomena form the basis both for their detection and for the deposition of their energy. A discussion of the kind and effect of these interactions as they pertain to the present work is given in this report section (23-27).

There are four kinds of basic gamma photon interaction processes (27), of which only two are relevant in the present work, namely:

- a) interaction with atomic electrons,
- b) interaction with the electric field surrounding nuclei or electrons.

The effect of (a) may be either scattering or absorption; the latter is the Photoelectric Effect. The scattering may be either one of the two types:

1. Compton inelastic scattering (incoherent), or
2. Rayleigh elastic scattering (coherent).

The effect of (b) is the disappearance of the photon and the creation of an electron-pair; this phenomenon is referred to as the Pair Production Effect.

A brief discussion of these four microscopic phenomena, and their macroscopic attenuating effect on a beam of photons, follows under the headings:

- A) Photoelectric Effect
- B) Compton Scattering
- C) Rayleigh Scattering
- D) Pair Production
- E) Attenuation

A. Photoelectric Effect

At relatively low photon energies the most probable effect of an interaction is absorption of the incident photon by an electron of the traversed medium followed by ejection of that electron and emission of either characteristic X-rays or "Auger electrons" as explained below. This phenomenon, called the Photoelectric Effect, results in the complete disappearance of the incident photon.

In order that total absorption may take place, and momentum be conserved, the interacting electron must be initially bound, in which case the residual atom recoils. The most tightly-bound electron, with respect to the incident photon energy, has the greatest probability of absorbing the photon. The interaction cross-section is a maximum when the photon energy E_γ is just equal to the electron binding energy; it decreases gradually as E_γ increases, and decreases sharply as E_γ decreases. The most tightly-bound electron in an atom is in the K-shell; it accounts for in excess of 80% of the photoelectric absorptions, with the L-shell accounting for most of the remainder. The energy of the ejected electron, or photoelectron as it is usually called, is given by:

$$E_e = h\nu_o - E_{eb}, \text{ (MeV)} \quad (1)$$

where

$$h\nu_o = \text{incident photon energy (MeV).}$$

$$E_{eb} = \text{electron binding energy (MeV).}$$

The energy E_{eb} is carried away from the atom by radiation emitted as the inner shell vacancy is filled by an outer shell electron, such radiation is referred to as Characteristic X-rays. If the X-rays interact with an outer shell electron as they leave the atom, they will be absorbed and the absorbing electron emitted instead -- an Auger electron. The nuclear decay processes of internal conversion and electron capture may also

lead to the emission of characteristic X-rays; so also will the absorption of beta particles.

The photoelectric effect does not lend itself easily to explicit theoretical calculation. Determinations of its cross-sections are usually based on a combination of empirical treatments which vary according to the energy range under consideration. It is the practice of most researchers to make use of tabulations for σ_{PE} , the photoelectric cross-section.

B. Compton Scattering Effect

As the wavelength of gamma photons decrease and their photon energy increases, their behaviour tends towards that of a particle and their identity with a wave diminishes. The region of this transition corresponds to the Compton scattering "threshold." This threshold, not sharply-defined, is entered upon gradually as $h\nu_0 \rightarrow m_0 c^2$, (= 0.51 MeV), where m_0 equals the rest mass of the electron. Viewed as solid bodies, the photon and the electron have comparable "masses." As the Compton effect becomes significant, the photoelectric effect significance diminishes.

Compton scattering may be considered as an inelastic collision between an incident photon and a "free" electron of the medium; the collision is analogous to that of billiard ball mechanics. The electron may be thought of as free to recoil on the basis of $h\nu_0 \gg E_{eb}$, as a result of which the incident photon may transfer a portion of its momentum and energy. The consequence of the collision is a scattered photon of energy $h\nu_1$, travelling in a new direction and at an angle θ with the original photon direction, and a recoiling electron of energy E_e making an angle ψ with the incident photon direction. $\theta_{max} = 180^\circ$; $\psi_{max} = 90^\circ$.

The angular and energy relationships of these statements may be expressed as:

$$E_{\gamma_1} = \frac{E_{\gamma_0}}{1 + \frac{E_{\gamma_0}}{m_0 c^2} (1 - \cos \theta)}, \text{ MeV.} \quad (2)$$

$$E_e = E_{\gamma_0} - E_{\gamma_1} \quad (3)$$

$$E_{\gamma} = h\nu, \text{ MeV.} \quad (4)$$

$$\cot \psi = (1 + \alpha'_0) \tan \frac{\theta}{2} \quad (5)$$

where

E_{γ_0} = incident photon energy, MeV.

E_{γ_1} = scattered photon energy, MeV.

θ = angle between incident and scattered photon directions.

ψ = angle between incident photon and recoil electron directions.

For convenience in the remainder of this section the following conventional short form is used:

$$\alpha'_0 = \frac{E_{\gamma_0}}{m_0 c^2}, \quad \alpha'_1 = \frac{E_{\gamma_1}}{m_0 c^2} \quad (6)$$

The differential "collision" cross-section for the scattering of photons into a given solid angle $d\Omega$ at a particular angle θ is given by the Klein-Nishina formula, as

$$d\sigma = \frac{r_e^2}{2} d\Omega \left\{ \frac{(1 + \cos^2 \theta)}{[1 + \alpha'_0 (1 - \cos \theta)]^2} \right\} \times \left\{ 1 + \frac{\alpha'^2_0 (1 - \cos \theta)^2}{(1 + \cos^2 \theta) [1 + \alpha'_0 (1 - \cos \theta)]} \right\} \quad (7)$$

where

$$\begin{aligned} d\sigma &= \text{differential cross-section, cm}^2/\text{electron} \\ d\Omega &= 2\pi \sin \theta d\theta, \text{ the differential solid angle} \\ r_e &= \text{"classical electron radius, } \frac{e^2}{m_0 c^2} \\ &= 2.818 \times 10^{-13} \text{ cm.} \end{aligned}$$

Equation (7) assumes the incident photons to be unpolarized. It indicates that for large α'_0 , scattering is predominantly in the forward cone. As $\alpha'_0 \rightarrow 0$, and $\cos \theta \rightarrow 1$, we see

$$d\sigma \rightarrow \frac{r_e^2}{2} (1 + \cos^2 \theta) d\Omega \quad (8)$$

From Equation (2) equation (7) may be rewritten in terms of energy

$$\frac{d\sigma}{d\alpha'_1} = \frac{\pi r_e^2}{\alpha'^2_0} \left\{ \frac{2}{\alpha'_0} - \frac{2}{\alpha'_1} + \frac{1}{\alpha'^2_0} + \frac{1}{\alpha'^2_1} - \frac{2}{\alpha'_0 \alpha'_1} + \frac{\alpha'_0}{\alpha'_1} + \frac{\alpha'_1}{\alpha'_0} \right\} \quad (9)$$

for

$$\alpha'_0 \geq \alpha'_1 \geq \frac{\alpha'_0}{(1 + 2\alpha'_0)}$$

The integration of Equation (9) over all scattered energies yields the total Compton scattering cross-section per electron, σ_{cs} , :

$$\sigma_{cs} = 2\pi r_e^2 \left\{ \frac{1 + \alpha'_o}{\alpha'_o{}^3} \left[\frac{2\alpha'_o(1 + \alpha'_o)}{1 + 2\alpha'_o} - \ln(1 + 2\alpha'_o) \right] + \frac{\ln(1 + 2\alpha'_o)}{2\alpha'_o} - \frac{1 + 3\alpha'_o}{(1 + 2\alpha'_o)^2} \right\} \quad (10)$$

The total Compton scattering cross-section per atom is given by $Z \cdot \sigma_{cs}$, where Z is atomic number.

C. Rayleigh Scattering Effect

In Compton scattering the atomic electrons are assumed to be unbound. This assumption is only valid at photon energies which are large with respect to the electron binding energy. A low energy photon may be elastically scattered by a tightly bound atomic electron, with the atom as a whole absorbing the recoil momentum. A bound electron has a "mass" which is equivalent to that of its atom. The energy transferred to the atom is small, and so the scattered photon proceeds with a relatively unaltered energy and only a slightly altered direction. This effect is known as the Rayleigh or small-angle scattering effect.

Since all the electrons in a given atom behave similarly, Rayleigh scattering is coherent. Because all the atoms of a given solid may be packed regularly, the effect may extend to the electrons of different atoms. When the scattering angle, $\theta_R \approx 0$, the scattering will be in phase, i.e. constructive interference. As θ_R increases the tendency

is towards destructive interference and so the scattered photons will be found concentrated mainly in a narrow forward cone, and to a lesser extent in other discrete directions. This may be realized from consideration of the photon wavelength, and the atomic radius, analogous to Bragg reflection. This behaviour differs from Compton scattering, where the independence of the electrons precludes the likelihood of interference.

The transition from Rayleigh scattering to Compton scattering is smooth with increasing energy, E_{γ_0} . The Rayleigh scattered photon does not have a unique energy as a function of scattering angle, having instead an energy distribution peaked at a value close to that given by Equation (2).

D. Pair Production Effect

At photon energies of approximately 1.0 MeV the predominant interaction phenomenon is Compton scattering. As E_{γ_0} is increased considerably above this energy the photon may interact with the electric field surrounding either a nucleus or an electron. The photon will be absorbed and replaced by a pair of electrons, a positron and a negative electron. This effect is called Pair Production.

The cross-section for pair production in the field of an orbital electron is negligible until $E_{\gamma_0} \geq 4 m_0 c^2$, (= 2.04 MeV). Nuclear pair production, however, has a cross-section which begins at the photon threshold energy $2 m_0 c^2$, (= 1.02 MeV), and increases rapidly thereafter.

The electron pair share and carry away the energy in excess of that required for their creation, as kinetic energy; this may be expressed as

$$(E_{e^-} + E_{e^+}) = E_{\gamma_0} - 2m_0c^2 \quad (11)$$

The free positron is quickly annihilated by a negative electron after its kinetic energy has been dissipated. The annihilation yields a randomly oriented pair of back-to-back photons, each with an energy of m_0c^2 .

The electron pair are distributed mainly in the forward direction with the average angle of "deflection" being expressed by m_0c^2/E_e .

For $2m_0c^2 < E_{\gamma_0} < 4m_0c^2$, $\sigma_{pp} \propto Z^2$.

E. Attenuation

The passage of a beam of photons through a medium is characterized by their interactions with the atoms of that medium. This leads to a reduction in the number of uncollided primary photons at a depth. The reduction is referred to as the attenuation of the incident photon number.

The discussion on interactions has shown that the total microscopic energy dependent cross-section for a particular interaction process occurring, is given by either σ_{PE} , $Z\sigma_{CS}$, σ_{RS} or σ_{PP} . The total cross-section $\sigma_{TOT}(E_{\gamma_0})$, for "some" process occurring, is then given by the sum of the partial cross-sections as

$$\sigma_{TOT}(E_{\gamma_0}) = \sigma_{TOT} = \sigma_{PE} + Z\sigma_{CS} + \sigma_{RS} + \sigma_{PP}, \text{ (cm}^2\text{/atom)} \quad (12)$$

from which a total macroscopic cross-section per cm of path may be defined as

$$\mu_{TOT}(E_{\gamma_0}) = \mu_{TOT} = N\sigma_{TOT}, \text{ (cm}^{-1}\text{)} \quad (13)$$

and similarly

$$\mu_{PE} = N\sigma_{PE} ; \mu_{CS} = NZ\sigma_{CS} ; \mu_{RS} = N\sigma_{RS} ; \mu_{PF} = N\sigma_{PF} \quad (14)$$

where

$$N = \frac{\rho \times A_v}{M} ; \quad (\text{atoms present/cc}) \quad (15)$$

assuming one type of atom only.

ρ = density of medium, (gm/cc).

A_v = Avogadro number, (atoms/mole); 6.023×10^{-23}

M = atomic or molecular weight.

The inverse of Equation (13) is defined as the mean free path, l_{TOT} , for a photon prior to interaction, i.e.

$$l_{TOT} = \frac{1}{\mu_{TOT}} , \quad (\text{cm}) \quad (16)$$

Similarly l_{RE} , l_{CS} , l_{RS} , and l_{PF} may be defined from Equation (14). The total macroscopic cross-section is generally referred to as the total linear attenuation coefficient.

The number of normally incident photons per cm^2 -sec in a parallel beam which penetrate a thickness x of a homogeneous medium without interaction, is given by the exponential law as

$$\phi(x) = \phi(0)e^{-\mu x} \quad (\gamma/\text{cm}^2\text{-sec}) \quad (17)$$

where

$\phi(0)$ = number of photons/ cm^2 -sec incident at $x=0$.

$\phi(x)$ = number of photons/ cm^2 -sec emerging at x .

μ = cross-section appropriate to the interaction effect under consideration; energy dependent.

Thus, it follows that the probability of uncollided photon transmission through a thickness x is given by p , where

$$p = \frac{\phi(x)}{\phi(0)} = e^{-\mu_{TOT}x} \quad (18)$$

Equation (18) is in agreement with Equation (4) of Report-Section (2.2).

Similarly the probability of some kind of interaction occurring in path length x is given by

$$\epsilon_{TOT}(x) = (1 - p) = (1 - e^{-\mu_{TOT}x}) \quad (19)$$

Equations (18) and (19) assume a normally incident parallel or collimated, photon beam. In practice this can only be nearly achieved by narrow-geometry restrictions. For the case of a poorly collimated or uncollimated photon beam it is necessary to introduce a factor to express the increase of the photon number flux at x over the value predicted by Equation (3.4.17). This factor, known as a number Build-Up Factor, $B(x)$, may be defined as.

$$B(x) = \frac{\text{Total Number Flux at } x}{\text{Uncollided Flux at } x} \geq 1.0 \quad (20)$$

which is in agreement with Equation (5) of Report-Section (2.2)

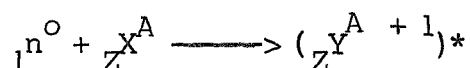
Energy and dose build-up factors may be similarly defined.

That μ is a function of both incident photon energy, E_{γ_0} , and the properties of the traversed medium is apparent from the discussions of sub sections (A-D) and equations (12) to (15). It follows then, that any property, including $B(x)$ which is dependent on μ , is similarly dependent on E_{γ_0} .

II FAST NEUTRON INTERACTION PHENOMENA

Neutrons interact with the nuclei of traversed matter through the mechanism of nuclear force. An interaction is generally referred to as either having scattered or absorbed the incident neutron. The probability of either scattering or absorption varies as a function of the incident neutron energy and the atomic number of the target nuclide, the dependence on atomic number being general and such that for each isotope there is a unique probability, or cross-section (2,28,29).

Perhaps the most convenient and systematic manner of describing neutron interactions consists of invoking the "compound nucleus" concept. According to this concept all interaction modes result in the formation of an intermediate reaction product - a compound nucleus - formed by an absorption of the incident neutron. Symbolically this may be represented as



where, ${}_1n^0$ is the incident neutron, ${}_Z X^A$ the target nucleus before interaction and ${}_Z Y^A + 1$ the compound nucleus formed by the interaction. The asterisk denotes that the compound nucleus will, in general, be left in an excited state for a finite period of time. The energy of the compound nucleus includes both the binding energy and/or part of the kinetic energy of the incident neutron. This energy excess over that of ${}_Z X^A$, distributed in a complex fashion among the nucleons, will cause the compound nucleus system to seek its state of lowest permissible energy in a characteristic "relaxation time", typically about 10^{-20} to 10^{-12} seconds.

The laws of quantum mechanics allow only those reactions to take place which obey certain rigid energy and momentum relationships. This obedience is observed with respect to the available excitation energy of the incident neutron and the distribution of energy levels in the target nucleus, as well as with respect to the symmetry requirements of the interaction,

e. g. parity, baryon number, charge conservation, statistics.

In accord with the compound nucleus concept, scattering and absorption of an incident neutron may be defined in terms of whether or not the compound nucleus emits a neutron during de-excitation. Further and more important, scattering may be separated into two kinds - elastic and inelastic. In elastic scattering the compound nucleus emits a kinetic energy degraded neutron in a very short relaxation time $<10^{-20}$ seconds, and is itself left in exactly the same internal energy state as before the interaction. In inelastic scattering the compound nucleus emits a neutron of partially or totally degraded kinetic energy and is itself left in an internal energy state above that of ${}^A_Z X$; the excess energy is evolved by emission of one or more gamma photons. The degradation of the neutron kinetic energy by scattering is referred to as thermalization. The compound nucleus may be de-excited by emission of particles other than neutrons, such as alphas and betas accompanied by gamma photons in which case neutron absorption is said to have resulted.

The interaction processes reviewed above are summarized:

(i) Elastic Scattering, (n,n) ——A neutron of reduced kinetic energy is emitted by the short-lived compound nucleus which is left in an unexcited state. Kinetic energy is transferred to recoil the target nucleus. In the case of hydrogen target nuclei, for which energy transfer is a maximum, recoil protons result.

(ii) Inelastic Scattering, (n,n') ——A neutron of reduced kinetic energy is emitted by the compound nucleus. The compound nucleus is de-excited by gamma photon emission.

(iii) Radiative Capture, (n,γ) ——The compound nucleus formed by absorption of an incident neutron is de-excited by relatively high energy gamma photon emission.

(iv) Charged Particle Emission, (n,p), (n,d), (n, α)——The compound nucleus formed by absorption of an incident neutron is de-excited by emission of a charged particle such as a proton, deuteron or alpha, accompanied by gamma photons.

(v) Fission, (n,f)——The compound nucleus formed by absorption of an incident neutron breaks into two ionizing fission fragments, and one or more energetic neutrons, accompanied by gamma photon emission. Fission is most probable in heavy nuclei of odd mass number and less so in heavy nuclei of even mass number. It can occur either as the result of an externally incident neutron or as a consequence of quantum mechanical leakage through the Coulomb barrier, ie., spontaneous fission.

(vi) Other Reactions, (α ,n), (γ ,n)——Two interaction processes which give rise to neutron emission and thus which must be identified are (α ,n) and (γ ,n) phenomena in the plutonium-oxide source and its immediate environment. The first reaction proceeds when the energy of an alpha particle exceeds the energetic threshold and Coulomb repulsion barrier for the reaction, and is thus significant only for plutonium alphas (~5.5 meV) incident on light-target nuclei such as beryllium. The second reaction, photo-neutron formation, results from the interaction of high energy gamma photons with light nuclei such as are present in plutonium-oxide as impurities. High energy photons are present in the PuO₂ source through (n,f) reactions and the decay of the Tl²⁰⁸ daughter of the Pu²³⁶ isotope present in plutonium oxide.

APPENDIX II

SUMMARY DESCRIPTION OF SUBPROGRAM NUGAM1

APPENDIX II

SUMMARY DESCRIPTION OF SUBPROGRAM NUGAM1

Code NUGAM1 derived from NUALGAM⁽³⁾, is programmed to predict differential and integral energy-angular fractional gamma photon number transport in cylindrical media geometries. It employs the Monte Carlo technique of following and categorizing a large number of photons from "birth to death". It uses random number and probability theory combined with known interaction distributions to determine such as source and collision site spatial location, as well as trajectory energy and direction throughout each history.

After n interaction events in the source medium, photon number state may be characterized as

$$N_n = N (E_n, \theta_n, \Phi_n, x_n, y_n, z_n; E_m, \theta_m, \Phi_m, x_m, y_m, z_m), \quad (1)$$

where

E = photon energy

θ = polar angle

Φ = azimuth angle

x, y, z = Cartesian co-ordinates

n = subscript to denote nth event

m = n-1, a subscript; 0, 1, ..., m, n, ...

o = subscript to denote photon history origin, i.e. "zero interaction",

which describes the spectrum at the arbitrary point $P_n (x_n, y_n, z_n)$. If interaction site P_n is outside the boundaries of the cylinder of height h and radius ρ , and P_m is within, then the fate of the photon is deemed as escape, and

so tallied by the code. If an escape is recorded at P_n where $P_m = P_0$, then the photon escape energy is unaltered and identical with the initial or birth energy. A typical escape history is indicated in Figure II-1, where escape is shown between P_2 and P_3 . The code employs Cartesian co-ordinates and direction cosines to determine trajectory between interactions.

Although Equation (1) and Figure II-1 characterize photon history state, terminal escape classification is computed with respect to space co-ordinates $(0, 0, \frac{h}{2})$. If a detection band about the Z-axis is assumed at a great distance from the source cylinder then all photons escaping from any point on the source boundary and striking the band may be considered as having the same Z-axis directional cosine. If the detection band subtends the solid angle $d\Omega$ at $\Omega(0, 0, \frac{h}{2})$ then, the photon escape state may be characterized as

$$N = N(E, \Omega) , \quad (2)$$

where

$$E = \text{photon escape energy} .$$

In Equation (2) the understood arguments and subscripts are omitted. Multiplying by differentials in energy and solid angle, the differential angular-energy photon number escape spectrum is given by

$$dN(E, \Omega) = N(E, \Omega) dE d\Omega , \quad (3)$$

keeping in mind that

$$d\Omega = \text{Sin } \theta d\theta d\Phi , \quad (4)$$

where

θ = polar angle between escape vector and Z-axis; $0 \leq \theta \leq \pi$

Φ = azimuth angle of escape vector; $0 \leq \Phi \leq 2\pi$.

Substitution of Equation (4) into Equation (3) and integration over energy and angle between desired limits gives the total photon number escaping from the source. The geometry for photon history escape classification is illustrated in Figure II-2.

The co-ordinates of the source point P_0 , within the source cylinder are chosen by random number selection as⁽¹³⁾

$$\begin{aligned} z_0 &= R_i \cdot h \\ d_0 &= \rho \sqrt{R_{i+1}} \\ \Phi_0 &= (2 R_i + 2 - 1) \pi \end{aligned} \quad (5)$$

where

$$\begin{aligned} d_0 &= (x_0^2 + y_0^2)^{1/2} \\ R_i &= \text{denotes a sequence of pseudo random numbers.} \end{aligned}$$

The initial direction cosines of the source history are determined similarly by random number selection as⁽¹³⁾

$$\begin{aligned} w &= 2 R_i + 3 - 1, \\ u &= \cos \left[(2 R_i + 4 - 1) \pi \right] (1 - w^2)^{1/2}, \\ v &= \cos \left[(2 R_i + 4 - 1) \pi \right] (1 - w^2)^{1/2}. \end{aligned} \quad (6)$$

The direction cosines u , v , w , correspond to co-ordinates (x_0, y_0, z_0) of Equations (5).

Source photons are initiated with a probability of existence or weight W , equal to 1.0. This weight is reduced after each interaction by the ratio of the scattering to total cross-section. Thus photons are not lost to absorption unless their reducing weight drops below an assigned value, 10^{-5} in NUGAM1. Photons may be lost to absorption if their degraded energy drops below an input threshold value.

The path length between interactions, l , is a function of energy and material composition. It may be determined according to the Monte Carlo technique⁽¹⁴⁾ as

$$l = l_1 + l_2 + \dots + l_{j-1} + \lambda_j^{-1} (-\log_e R_i - (\lambda_1 l_1 + \lambda_2 l_2 + \dots + \lambda_{j-1} l_{j-1})) \quad (7)$$

where

l_j = actual path length of photon in medium region j

λ = total mean free path for a photon of given energy in a given medium j .

Energy deposition within the source cylinder at the n^{th} interaction site is determined as

$$I_n = \frac{W_m}{\sigma_t} (E_m (\mu_{pp} + \mu_{pe}) + \mu_s (E_m - E_n)) , \quad (8)$$

where

W_m = weight after m^{th} interaction

E = photon energy

μ = macroscopic interaction cross-section

pp, pe, s, t = subscripts to identify pair production, photoelectric scattering and total cross-sections

$$\mu_t = \mu_{pp} + \mu_{pe} + \mu_s .$$

The macroscopic cross-sections μ_{pp} and μ_{pe} are determined from the microscopic cross-sections σ_{pp} and σ_{pe} input to code NUGAM1, in accord with the well known relationship

$$\mu = A_0 \sum_{i=1}^{i=k} \frac{\rho_i \sigma_i}{A_i} , \quad (9)$$

where

$$A_0 = \text{Avogadro number; } 0.6023 \times 10^{24}$$

$$\rho = \text{material or element density}$$

$$A = \text{material or element atomic weight}$$

$$i = \text{subscript to denote summation for elements, kinds 1 to k}$$

The total macroscopic Compton scattering cross-section per atom is obtained from Equation (9) and

$$\sigma_{si} = Z_i \cdot \sigma_{es} , \quad (10)$$

where

$$Z_i = \text{material or element atomic number}$$

$$\sigma_{es} = \text{total microscopic Compton scattering cross-section per electron .}$$

The scattering cross-section σ_{es} is obtained from the Klein-Nishina relationship as ⁽¹³⁾

$$\sigma_{es} = 2\pi r_0^2 \left[\frac{2}{E^2} + \frac{1+E}{(1+2E)^2} + \ln(1+2E) \left(\frac{E^2 - 2E - 2}{2E^3} \right) \right] , \quad (11)$$

where

$$r_0 = 0.28183 \times 10^{-12} \text{ cm}$$

$$E = \text{photon energy in } m_0 c^2 \text{ (} = 0.51097 \text{ MeV) units .}$$

Direction and energy after a scattering are governed by the angular differential form of the Klein-Nishina distribution, with energy related to direction by the Compton scattering relationship⁽¹³⁾. Code NUGAM1 selects scattering angle and energy in accord with the method outlined by Kahn in reference (30).

At photon energies greater than $2 m_0 c^2$ ($= 1.02$ MeV) pair production results. The code temporarily stores the parent photon characteristics and initiates a daughter photon with isotropically selected direction and energy $m_0 c^2$ ($= 0.51097$ MeV). The daughter is attributed twice the parent weight in order to simulate an actual photon pair. Upon termination of the daughter history, the parent history is recontinued.

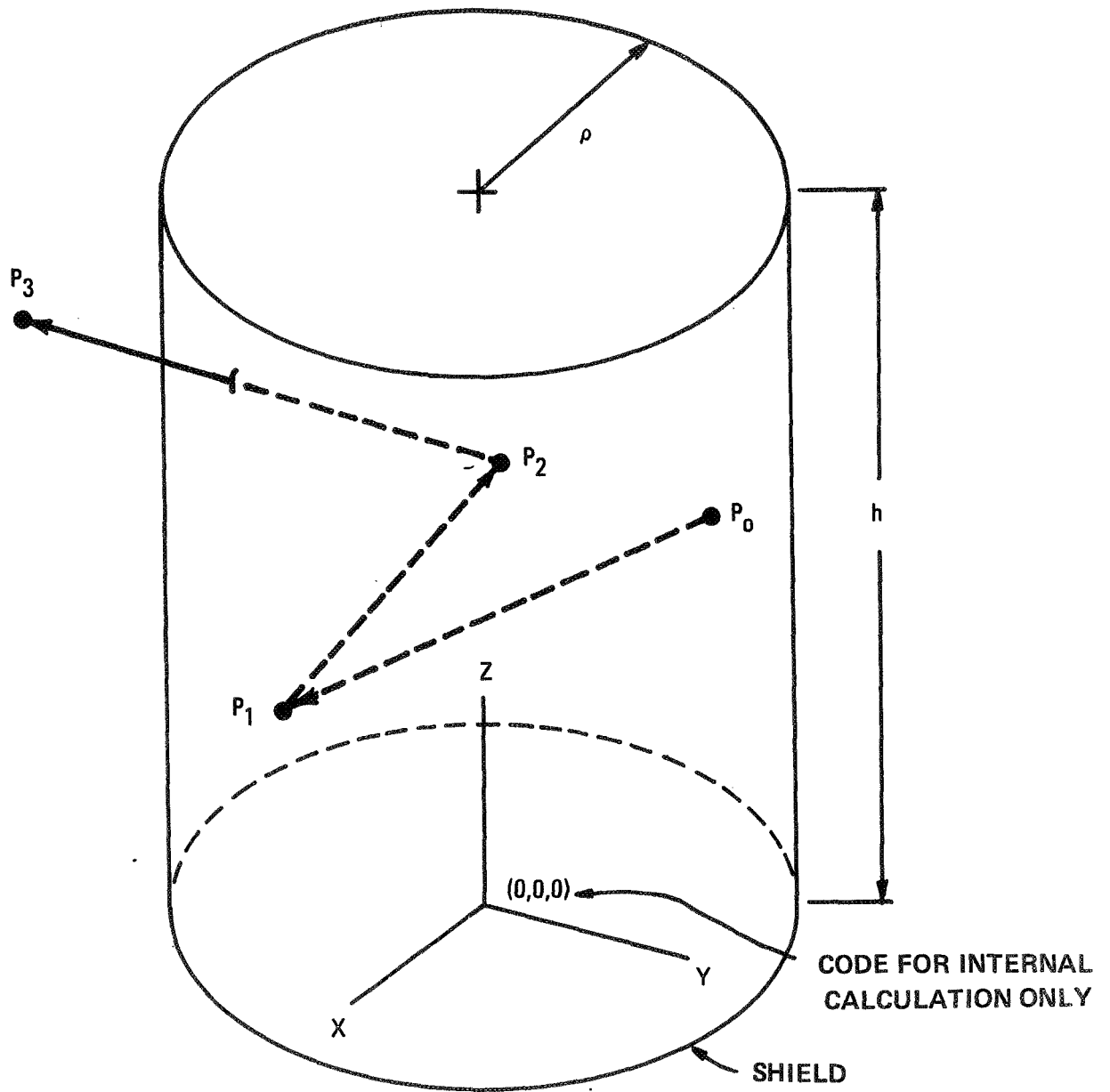


Figure II - 1
 Typical Photon Escape History

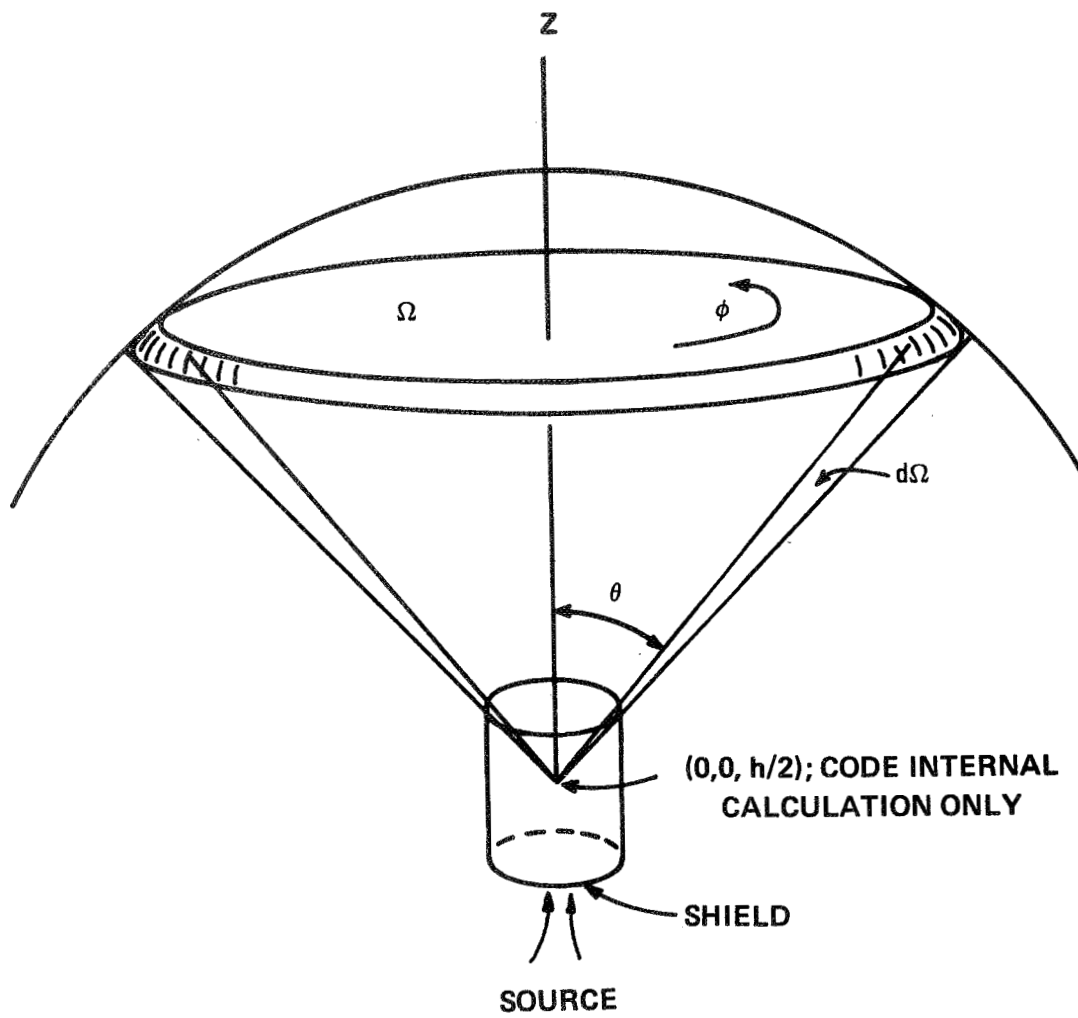


Figure II - 2
 Photon History Escape Classification Geometry

APPENDIX III
CODE SØSC FORTRAN LISTING

```

//71.1 USEC FOR (MID021120A,1,00017,003001),0A5,"SGIFM-F1"
//EXEC PROGRAM=PAR=PC9
//SOURCE,SYS1 IN DD UNIT=2214,SPACE=(CYL,(10,5))
//SOURCE,SYS2 IN DD SPACE=(CYL,(2,1))
//SOURCE,SYS3 IN DD *
C
C PROGRAM SOSC - THE SHIELD OPTIMIZATION STUDY CODE (MOS CORP. DEC.,1969)
C LAMINATED SHIELD
C
C SOSC=MAIN PROGRAM
C
DIMENSION FF(20),MAT(9),Y(9),PA(9),SS(20),SM(20),FA(20),DEMS(6)
DIMENSION TITL(20),SAX(20),SAXX(20),SAXY(20)
COMMON/PARAM/DIR(2),ECT,DIMX(5),MO-
COMMON/RATIO/PA,DE,NME,MN,MC
COMMON/CONST/BVE,RADAP
COMMON/PHLUX/EX,SEY(20),SENX(20),RMH(20),ATTI(20),RU(20),ATTM(20)
COMMON/SOURCE/SS,SM,FE,FM,SSA(20),SSNA(20)
COMMON/CORPS/Y5,Y0,Y5,Y0,Y5,Y0,75,70,CMP1
COMMON/TAI/DIR4(1045),TIME,THA,DIR5(105)
COMMON/OI/OI(20),HEIGHT,RADIUS,RCI,ROR,DIST
COMMON/RAND/RAND,MRANDM
COMMON/LENG/HT(9),PADSO,HRASA(20)
COMMON/INT/MAP
COMMON/DEN/DENSI(9,5),NELE(9),Z7(9,5),UTDEN,EI,DEMT
COMMON/LI/LI(20)
COMMON/STOD/RCM
COMMON/NLP/NRFS,IF(20),NDATH(18)
CPI=2.54
PVE=6.*ATAN(1.0)
RADAP=180.0/PVE
NNE=20
NE=20
MM=0
MG=0
C FACTORS TO CONVERT RADIAL TO AXIAL SPECTRUM
C FATPG=0.08333
C FATPN=0.80
DO 10 K=1,20
SS(K)=0.0
SM(K)=0.0
FE(K)=0.0
FM(K)=0.0
SEY(K)=0.0
SEY(K)=0.0
KUNTER=0
WRITE(6,200)
200 FORMAT(1H, //40X,12H SOURCE DATA)
9 READ(5,350) (NDATH(K),K=1,18)
350 FORMAT(18I4)
KUNTER=KUNTER+1
IF (NDATH(2)-2) 7,5,7
5 READ(5,100) X5,Y5,Z5,X0,Y0,Z0 ,RADIUS,OTST
100 FORMAT(6F10.4,2F6.3)
PSD=SQRT((Y0-Y5)**2+(Z0-Z5)**2)
PC=PSD*CPI
P4=4.*PVE*RCM*PC*
RADIUS=RADIUS*CPI

```

```

DIST=DIST#C#MPI
7 IF (MDPTH(3)-3) 4,P,6
8 READ(5,120)NF,NG,MMF, JMF, MNPT, MPANO, MNFS, AI, TIME, FCT, APOST, TANDEF,
1 ERG,ERN
120 FORMAT(15,6F7.4)
IF (NF.LE.4) GO TO 11
READ(5,121)(LFI(K),K=1,MNFS)
121 FOPB(I)(20)4
11 READ(5,122)(HGAM(K),K=1,MNFS)
122 FORMAT(20F6.0)
6 IF (MDPTH(4)-4) 15,12,15
12 IF (NG-1) 3,2,3
3 NG=NG+1
NG=1
READ(5,101)(FF(I),I=1,NC)
101 FORMAT(12F6.2)
READ(5,130)(SS(I),I=1,NF)
130 FORMAT(7F10.3)
IF (NG.FO.1) GO TO 1
2 MN=1
READ(5,140) (FM(I),I=1,MNF)
140 FORMAT(7F10.4)
READ(5,130) (SM(I),I=1,MNF)
1 S=0.0
SA=0.0
WRITE(6,301)
301 FORMAT(//2X,15HGAMMA SPEC TRUM ,14X,74H ENERGY(MEV) MD,OF GA
1WMA/SEC MD,OF GAMMA/SEC FLUX AT RECTCOR ,4X,14HFLUX AT DE
2TECTOR /55X,8H(RADIAL),12X,7H(AXIAL),12X,8H(RADIAL),12X,7H(AXIAL)
3//)
DO 1000 I=1,NF
SSA(I)=SS(I)*ERG
S=S+SS(I)
SA=SA+SSA(I)
SFX(I)=SS(I)/P4
SFX(I)=SSA(I)/P4
WRITE(6,302)I,FE(I),SS(I),SSA(I),SFX(I),SFX(I)
302 FORMAT(20X,I5,5F20.7)
1000 CONTINUE
TSFX=S/P4
TSFAX=SA/P4
WRITE(6,303) S,SA,TSFX,TSFAX
303 FORMAT(/35X,10H TOTAL= ,4F20.7)
IF (NG.FO.1) GO TO 4
WRITE(6,304)
304 FORMAT(//2X,17HNEUTRON SPEC TRUM ,14X,74H ENERGY(MEV) MD,OF NE
1UT,/SEC MD,OF NEUT,/SEC FLUX AT RECTCOR ,4X,14HFLUX AT DE
2TECTOR /55X,8H(RADIAL),12X,7H(AXIAL),12X,8H(RADIAL),12X,7H(AXIAL)
3//)
SSMAX=0.0
SSM=0.0
DO 2000 J=1,MNF
SSNA(I)=SM(I)*EDM
SSMAX=SSMAX+SSNA(I)
SSN=SSN+SM(I)
SFMX(I)=SM(I)/P4
SFMX(I)=SSNA(I)/P4
WRITE(6,302)I,FM(I),SM(I),SSNA(I),SFMX(I),SFMX(I)
2000 CONTINUE
TSFMX=SSM/P4

```

```

1 SEPARATE=SSMAX/04
WRITE(6,303)SSM,SSMAX,ISEM,ISEMAX,ISEMAX
4 WRITE(6,200) PC%,ALJICE
200 FORMAT(//,38#F12.4,HEI, SOURCE AMPL, DETECTOR (CM)=,F12.4,GY,
125#ALLOWED FLUX AT DETECTOR=,F12.4)
15 IF(NPATH(5)-5) 17,16,18
16 TOTSA=0.0
GO TO 19
17 TOTSA=SAVE
GO TO 19
18 CONTINUE
C. RECALCULATE NEUTRON ALBEDO CALCULATION SET MN=0
MN=0
CALL ALB(TOTSA)
SAVE=TOTSA
MN=1
19 EX=ALLOWE-TOTSA
WRITE(6,110)TOTSA,FX
110 FORMAT(22# TOTAL SCATTERED FLUX=,F12.4,5X,25# ALLOWED ATTENUATED
FLUX=,F12.4)
20 IF(NPATH(6)-6) 30,21,30
21 READ(5,112)(TITLE(I),I=1,80)
112 FORMAT(80A1)
WRITE(6,114)(TITLE(I),I=1,80)
114 FORMAT(1#1,80A1//)
READ(5,111)M0
111 FORMAT(I5)
READ(5,109) (PA(I),NELE(I),I=1,M0)
109 FORMAT(10(F5.2,I2))
IF (NPATH(7)-7)25,23,25
23 DO 250 I=1,M0
NELE=NELE(I)
DENS(I)=0.0
READ(5,112)(Z(I),DEMS(I),I=1,NELE)
112 FORMAT(7(F6.0,F6.6))
DO 149 J=1,NELE
149 DEMS(J)=DEMS(I)+DEMS(I,J)
250 CONTINUE
MORE=
M0=1
CALL GSTICM(I,1,M0,A,A,B)
25 MDEM=0
DO 160 I=1,M0
160 MDEM=MDEM+DEMS(I)*RA(I)
IT=0
M0=1
CALL ALDIP(I,0,RI,RMI,IT)
CALL XEST (M0,X, IT)
55 IT=IT+1
CALL ALDIP(X, RI,RMI,IT)
CALL XEST (M0,XI,IT)
ENDIFF=ABS(XI-X)/XI
WRITE(6,115) ENDFE,APPEST
115 FORMAT(20# ACCURACY FRACTION =,F8.5,7X,21#HARVESTING CAPTUREION =,
I, F8.5)
X=XI
WRITE(6,116)(TITLE(I),I=1,80)
116 FORMAT(//1X,80A1)
IF(IT-GE.3)GO TO 29
IF(ENDFE.GT.APPEST) GO TO 55
29 WRITE(6,117) KUMTEP

```

```

117 FOR=AT(//4Y,SCHEM) DE CALCIUM FOR SUFFID SUBEFL *,12,118)
X0 IE (MPATH(1),55,0) GO TO 5
STOP
END
SUBROUTINE RIIMP(X, RI,RMI,IT)
DIMENSION EN(20),FACTS(20),FACTS(20),F(20),Y(6),Z(6),FMMNPS(20)
DIMENSION RI(20),RMI(20),A1(20),R(20),REX(20)
COMMON/CTOP/ECW
COMMON/TAI/DUM4(1045),IME,IMW,DUM5(1051)
COMMON/SOLPSE/DUMS(40),FF(20),EN, UMSS(60)
COMMON/RATIO/PA(9),NE,MNE,MW,MC
COMMON/CONST/PVF,PAABP
COMMON/RAND/MGAM,NGAMA,NRNDM
COMMON/PARAM/NGAM,NGAMA,EZEPD,ECT,DUM(5),NGM
COMMON/OUTP/MCCL(151),DUM1(604),RVOL(151),DUM7(604)
COMMON/OI/NR,IDENT(18),HEIGHT,RADIUS,HRM,RRR,DISP
COMMON/SPE/ESPEC(20),SPEC(20),NREAD,I,OPR,DUM4(20)
COMMON/PHUX/EX,SEX(20),DUM6(40),ATT(20),DUMPHI(20),ATTM(20)
COMMON/LIC/NOPD
COMMON/DEMT/DENSY(9,5),MELE(9),Z7(9,5),WTDEN,FLDENT
COMMON/FWNO/TEM,TEMPSS
COMMON/WLP/MDS,I=(20),MPATH(18)
COMMON/LEAG/HT(9),RANDO,HGABA(20)
SPECT(1)=1.0
NREAD=1
NDISTM=1
NGAMV=1000
RANCO=RANDIUS*RANDIUS
NMGAM=2.*PVF*(1.-DISP/SORT(DIST*DISP+RANDO))
IF(IT.ME.#0)GO TO 50
DO 20 I=1,20
RI(I)=1.0
RMI(I)=1.0
20 CONTINUE
RETURN
50 HEIGHT=X
RVOL(1)=PVF*HEIGHT*RANCO*WTDEN
RC=RCM-X-NDIST
PACK=1.0/(RC*RC)
DO 51 J=1,NRV
HT(J)=RA(J)*HEIGHT
IF(ME.#F.#4)GO TO 41
IF(NRFS.#F.#ME)GO TO 41
DO 60 J=1,NRFS
JJ=IF(J)
F(J)=FF(JJ)
ESPEC(1)=F(J)
NGAMA=MGAM*HGAMA(J)
CALL MUGAM
FMMNPS(J)=TEMPD/NGAMA
ATT(J)=ATT(JJ)
R(J)=1.+FMMNPS(J)*DMFGAD/ATT(J)
60 CONTINUE
C 1 WRTTE(6,100) DMFGAD,RVOL(1),X,(1,1),F(1),F(1),FMMNPS(1),R(1),
C 1 J=1,NRFS
100 FOR=AT(9H NMGAM=,F12,4,6H RVOL =,F12,4/
165H MUGAM IS CALLED AT ENERGY(NEV) NO IN: FM-COME/STER
20P,OX,16H FOR SUFFID =,F10,5,6H (CM) /
3(1Y,21R,2Y,5F17,7)
55 DO 60 J=1,NR

```

```

FO=FF(J)
CALL TATE( ,F,4,1,MOX,MIN,7,Y,R,2,I,0)
R(I)=TE(5,7,Y,F0)
40 CONTINUE
GO TO 43
41 NOSENE
DO 42 J=1,NMF
ESPECT(I)=FF(J)
NGAMA=NGAMA*HIGAMA(J)
CALL MURAM
EMPS(J)=TEMPS/NGAMA
42 R(I,J)=+EMPS(J)*MFCAD/ATT(J)
43 CONTINUE
44 WRITE(6,10)(J,FF(J),
100 FORMAT(/31H GAMMA
1 CALCULATED R-IP
1 R(I,J),J=1,NMF)
101 FORMAT(/31H NEUTRON
1 CALCULATED R-IP
1 R(I,J),J=1,NMF)
31 RETURN
END
SUBROUTINE XEST(NOM,XXST,I)
DIMENSION VZ(9),FE(20),R(20),PA(9),Z(6),Y(6),UMU(9,20),CUMU(20),
1XSECT(2),FPG(20),XMI(20),EM(20),FG(20),
2XMI(20),FGM(20),CUMU(20),UMU(9,20),FNY(30),XS(30),XNCI(5,30)
COMMON/CONST/VE,RADAP
COMMON/SOURCE/DISSL(40),FF,FM,SS(20),SM(20)
COMMON/DEMT/DUM(9,5),NDUM(9),ZDUM(9,5),WIDEM,F(DEMT)
COMMON/RATIO/PA,NE,MNE,MM,MC
COMMON/PHIUX/EX,SEX(20),SEM(20),RMI(20),ATT(20),R,ATTN(20)
COMMON/EMC/HT(9),RADS0,HIGAMA(20)
COMMON/NLP/NOFS,LF(20),MPATH(18)
IF(IT,NF=0) GO TO 42
IF(MG-1)43,52,43
53 DO 26 J=1,NF
FO=FF(J)/.5)097
UM=0,0
11 DO 25 N=1,NOM
CALL GSTIGM(2,1,N,FO,XSECT)
UM=UM+PA(N)*UMU(N,1)
25 CONTINUE
CUMU(1)=UM
26 CONTINUE
43 IF(MN-1)42,52,42
52 IF(MPATH(7)-7)46,45,46
45 DO 30 N=1,NOM
NRATS=NDUM(N)
CALL MENSIG(NOM,FNY,XS,NRATS)
DO 30 L=N,MMH
30 XMT(M,LN)=XS(L,N)
39 CONTINUE
46 DO 226 J=1,NMF
FO=FM(J)
UM=0,0
DO 225 MN=1,NOM
CALL TATE(FO,FNY,NOM,1,MOX,MIN,7,Y,XS,2,L,0)
Y(1)=XMT(MN,L+1)
Y(2)=XMT(MN,L+2)

```

```

Y(3)=XNC1(MN*1+3)
WRITE(6,9999) MN, ANX, MUM, L, (7(KA), Y(KA), KA=1, 3), F00
MMH(MN, J)=TE(3,7, Y, F00)
IM=IM+RA(MN)*MMH(MN, J)
225 CONTINUE
CUMH(J)=IM
226 CONTINUE
42 CONTINUE
X=1.0
KAY=0
FLU=0.0
FLN=0.0
IF(MG-1)4]5]4]
51 DO 27 J=1, NF
XMH(J)=X*CUMH(J)
FG(J)=R(J)*EXP(-XMH(J))*SEY(J)
27 FLU=FLU+FG(J)
41 IF(MN-1)40,50,40
50 DO 72 J=1, NMF
XMH(J)=X*CUMH(J)
RMH(J)=1.0
FGN(J)=RMH(J)*EXP(-XMH(J))*0.67)*SENY(J)
72 FLN=FLN+FGN(J)
40 FLUS=FLU+FLN
IF(FLUS-EX)28,28,29
29 X=X+1.0
FLU=FLUS
GO TO 31
28 IF(KAY=0)33,32,33
32 FLN=FLUS
KAY=1
X=X+1.0
GO TO 31
33 CONTINUE
Z(1)=FLU
Z(2)=FLN
Z(3)=FLUS
Y(1)=X-2.0
Y(2)=X-1.0
Y(3)=X
XXST=TE(3,7, Y, EX)
DO 60 J=1, NE
ATT(J)= EXP(-CUMH(J)*XXST)
60 CONTINUE
WRITE(6,99)
99 FORMAT(1H0/,)25H J ENERGY(MEV) MTD=MH(CM-1) MTD=MH*X
1 NO.AT SOURCE RAPE FLUX AT 0 RUINDIP FACT. ATT,FLUX AT 0 ATT.
2FAC(XFST) )
WRITE(6,100)(I, FF(I), CUMH(J), XMH(J), SS(I), SEY(J), R(J), FG(J), ATT(J)
) J=1, NF)
300 FORMAT(12H GAMMA-DATA /12X, I3, RF15.4)
IF(MN-1)90,90,90
80 DO 70 I=1, NMF
70 ATN(I)= EXP(-CUMH(I)*XXST)
WRITE(6,200)(I, FM(I), CUMH(J), XMH(J), SN(I), SENX(J), RMH(J), FGN(J),
) ATN(J), J=1, NMF)
200 FORMAT(14H NEUTRON-DATA /12X, I3, RF15.4)
90 WRITE(6,10)XXST, EX, (Y(I), 7(I), I=1, 3)
101 FORMAT(14H 2X, 47HDEFLECTED FLUX AS A FUNCTION OF SHIELD THICKNESS
) //PX, 34H X-FST, (CM) FLUX(MD/C:MC:SEC) /12(4X, F14.5))

```



```

MPL=XXST*WTDEN
WT=MPL*PYE*RADSO
WRITE(6,102) IT,XXS1,WTDEN,WT
102  FORMAT(//154 ITERATION NO.=,I3,/214  SHIELD LENGTH(CM) =,F10.4,
1)  5X,204  WEIGHTED DENSITY=, F8.6,5X,12H WT,(CRXMS)=,F12.4)
RETURN
END
SUBROUTINE MENSIG(MOM,FNY,XS,MELF)
DIMENSION FNY(30),XS(30),FNN(30),XSM(30),7(6),Y(6)
COMMON/DENT/DUM(100),FLDENT
FLDENT=0.0
DO 5 L=1,30
XS(L)=0.0
TDENS=0.0
DO 49 KM=1,NELF
FINT=0.1
FN=0.0
N=0
READ(15,1000)MM,DEMSY,ATOMNO,ANDAW,(FNN(I),XSM(I),I=1,MM)
FORMAT(I2,3F10.5/(10F7.2))
ADEN=0.6023*DEMSY/ANDAW
FLDEN=ADEN*ATOMNO
7  FN=EN+FINT
CALL TA(FN,FNN,MM,1,MOX,MINI,7,Y,XSM,2,L,0)
XNN=TF(3,Z,Y,FN)
N=N+1
FNY(N)=FN
XS(N)=XS(N)+XNN*ADEN
IF(FN.GF*.99)FINT=0.5
IF(FN.GF*.49) FINT=1.0
IF(FN>12.0) 7,9,9
9  N=N+1
FLDENT=FLDENT+FLDEN
49  CONTINUE
C  WRITE(6,501)(FNY(LL),XS(LL),LL=1,NM)
501  FORMAT(16H NEUTRON X-SECT.,4(2X,2E12.4))
RETURN
END
SUBROUTINE GENSIG(K1,FLOW,MINT,NERAN,ERG,MRANGE,XSECT,NMED)
SUB GENERATES CROSS-SECTIONS
COMMON/ID/MOPT
COMMON/ST/NDR
COMMON/DENT/DEMS(9,5),MEL(9),ZZ(9,5),WTDEN,FLDENT
DIMENSION F(40),SIGPF(40),SIGPP(40),XSECT(40),ERG(20)
1  ,ENERGY(100)
READ(15,1)MINT,LOW,HIGH
1  FORMAT(3I5)
LEMO=1
KP=K1+1
MINT=2*MINT
NERAN=MINT*(HIGH-LOW)+1
GO TO (2,3),KP
2  MRANGE=2*NERAN
GO TO 4
3  MRANGE=3*NERAN
4  FLOW=2.*LOW
XNINT=2.*MINT
MRANGE=MRANGE*NMED
DO 37 J=1,NMED

```

```

JFNC=MRANGE*(J-1)
J1=JFNC+1
J2=JFNC+MRANGE
NELF=NEFL(1)
FLDENT=0.0
DO 5 K=J1,J2
5 XSECT(K)=0.
IF(NOPT,FO,0) GO TO 401
WRITE(6,201)MINT,LOW,HTIGH,NELF,MNP
201 FORMAT(1H), //40X,30H GENERATED CROSS-SECTION DATA //
1 RH MINT = ,15,6X,7HLOW = ,15,6X,8HHTIGH = ,15,6X,14HNO,FLF
2 MENTS = ,15,6X,6HNO = ,15)
401 DO 3 LL=1,NELF
3 READ(5,7)NE,DENSTY,ATOMNO,ANDAW
7 FORMAT(15,5X,3F10.5)
IF(NOPT,FO,0) GO TO 402
WRITE(6,999)NE,NERAW,ATOMNO,DENSTY,MNINT,ANDAW
999 FORMAT(30H NO,CROSS-SECTION ENERGIES ,15,6X,26HNO,ENERGY SURTIN
TERVALS ,15,12X,13HATOMIC NUMBER,11X,F12.5/1X,15HDENSITY (GM/CC)
,7X,F12.5,6X,26HINTERVALS/ENERGY GROUP ,15,12X,13HATOMIC WE
IGHT ,11X,F12.5)
402 DO 50 JK=1,LFMNO
50 READ(5,6)(F(K),SIGP(K),SIGPP(K),K=1,NE)
IF(NOPT,FO,0) GO TO 50
WRITE(6,206)(F(K),SIGP(K),SIGPP(K),K=1,NE)
50 CONTINUE
6 FORMAT(9F,3)
206 FORMAT(42H MICROSCOPIC CROSS-SECTION TABLE (INPUT) /(1X,6F18.7))
ADEN=(0.6023/ANDAW)*DENSTY
FLDEN=ADEN*ATOMNO
FLDENT=FLDENT+FLDEN
IF(NOPT,FO,0) GO TO 403
WRITE(6,8)ADEN,FLDEN
8 FORMAT(18H ADEN= ,F14.7,10H FLDEN= ,F14.7//
112X,RHSIGMA-TL,7X,RHSIGMA-PP,7X,RHSIGMA-PF,7X,RHSIGMA-SC,7X,6HNER
25Y /)
403 DO 3000 K=1,NE
3000 IF(SIGP(K)) 3001,3001,3001,3001,3000
3001 KAY=K
CAY=(SIGP(K-2)*F(K-2)**3+SIGP(K-1)*F(K-1)**3)/2.0
IF(NOPT,FO,0) GO TO 3003
WRITE(6,2999)KAY,CAY
2999 FORMAT(4H KAY=,15,7H CAY= ,F14.7)
3000 CONTINUE
GO TO 3005
3003 DO 3004 K=KAY,NE
3004 SIGP(K)=CAY/F(K)**3
3005 CONTINUE
DO 9 K=1,NE
SIGPP(K)=ADEN*SIGP(K)
F(K)=F(K)/.51097
ASIG=SIGMA*(F(K))*FLDEN
SIGP(K)=SIGP(K)*ADEN
ATOTAL=SIGP(K)+SIGPP(K)+ASIG
IF(NOPT,FO,0) GO TO 9
WRITE(6,88)ATOTAL, SIGP(K),SIGPP(K),ASIG,F(K),K
88 FORMAT(4X,5F15.7,110)
9 CONTINUE
DEL=FLDW/XMINT

```

```

FM=FLNW
I=1
L=1
M=1
10 IF(F(I+1)-FLNW)/11.100
11 I=I+1
GO TO 10
100 GO TO (12,101),KP
101 IPP=I
102 IF(SIGPP(IPP))103,104,105
103 CALL FRROR(SIGPP(IPP))
104 IPP=IPP+1
GO TO 102
105 SPP=ALOG(SIGPP(IPP+1)/SIGPP(IPP))/ALOG(F(IPP+1)/F(IPP))
C
C WRITE(3,915)IPP,SPP
C FORMAT(10H GFMSIG-6 /1X,110,10X,F14.7)
12 S=ALOG(SIGPF(I+1)/SIGPF(I))/ALOG(F(I+1)/F(I))
C
C WRITE(3,916),KP,S
C
C 916 FORMAT(10H GFMSIG-7 /1X,2110,10X,F14.7)
13 GO TO (19,14),KP
14 IF(IPP-1)7,19,19
17 IPP=1
SPP=ALOG(SIGPP(IPP+1)/SIGPP(IPP))/ALOG(F(IPP+1)/F(IPP))
19 O=FN-E(I+1)
IF(O)23,20,20
20 I=I+1
EYE=I
IF(I-NF)12,22,21
21 CALL FRROR(EYE)
22 I=I-1
23 MT=M+JFNC
MS=MT+NERAN
AS=SIGMAS(FN)*FIDFN
XSECT(MS)=XSECT(MS)+AS
FFF=F(I+1)
C
C WRITE(3,950)I,MS,M,MT,NERAN,NE,IPP,IFNC,KP,O,FN,FFF,FLDEN,SPP,
C
C 950 FORMAT(10H GFMSIG-8 /1X,9110/1X,7F14.7)
AP=O.0
GO TO (26,24),KP
24 IF(FN-2.)26,26,25
25 MP=MS+NERAN
AP=SIGPP(IPP+1)*EXP(SPP*ALOG(FN/F(IPP+1)))
XSECT(MP)=XSECT(MP)+AP
26 ENERGY(M)=EN*O.51097
AT=AF+AP+AS
XSECT(MT)=XSECT(MT)+AT
IF(M-NERAN)27,31,28
27 M=M+1
FN=FN+DEL
FL=L
WRITE(3,960)I,M,NERAN,MP,MS,IPP,MNINT,FL,FN,DFL,XSECT(MP)
IF(L-MNINT)30,29,28
28 CALL FRROR(FI)
29 DFL=2.*DFL
L=L+1
GO TO 19
31 CONTINUE

```

```

00 35 K=1,NFRAN
MT=K+JFENC
MS=MT+NFRAN
XSECT(MS)=XSECT(MS)/XSECT(MT)
WRITE(3,980)K,MT,JFENC,MS,XSECT(MS)
C 980 FORMAT(10H GENSIG=10 /1X,4I10,5X,F14.7)
IF(XSECT(MS)-1.)33,33,32
32 XSECT(MS)=1.
33 GO TO (36,34),KP
34 MP=MS+NFRAN
XSECT(MP)=XSECT(MP)/XSECT(MT)
IF(XSECT(MP)-1.)36,36,35
35 XSECT(MP)=1.
36 CONTINUE
37 CONTINUE
NGROUP=HIGH-LOW
DO 60 J=2,NGROUP
FRG(J)=ELW
60 FRG(J)=FRG(J-1)*2.
DO 302 JK=1,NMFD
NER=NRANGE*(JK-1)+1
NFRAN=NFR+NFRAN-1
IF(MDPT.EQ.0) GO TO 2001
WRITE(6,1999)
1999 FORMAT(1H,3X,19HCROSS SECTION TABLE //18X,5HTOTAL,2XX,
1 LOHSCAT/TOTAL,20X,9HP-P/TOTAL,14X,12HENERGY (MEV) //)
DO 302 J=NER,NFRAN
JJ=J+J0
JJJ=JJ+J0
K=J-(JK-1)*MRANGE
WRITE(6,2000)J,XSECT(J),JJ,XSECT(JJ),JJJ,XSECT(JJJ),ENERGY(K)
2000 FORMAT(1X,3(I10,F20.5),F20.5)
302 CONTINUE
IF(MDPT.EQ.0)GO TO 2001
WRITE(6,920) NGROUP,HIGH,LOW,(FRG(J),J=1,NGROUP)
920 FORMAT(12H GENSIG END,3110(1X,5F20.5))
2001 RETURN
END
SUBROUTINE NUGAM1
C NUGAM1 - PROGRAM FOR POINT SOURCE OUTSIDE OF THE CYLINDER
C FOR PARALLEL SOURCE IF DIST EQUALS TO ZERO
COMMON/RAND/NRAND,NRNDNM
COMMON/PARAM/MGAMA,EZFR0,ECT,FE,HRR,HL,FAK,HARS,TOTCOL,NMFD
COMMON/OUTP/ACOL,I(51),OMI(1359)
COMMON/OI/NR,INENT(18),HEIGHT,RAD(US,HOL,ROR,DIST
COMMON/GAMMA/DUM(6),FR,WR,DUM3(4),IMFD,IRFG,DUM4,NAME
COMMON/STRT/TSECT(5),SPOR(5),PPOR(5)
COMMON/FOR/III
COMMON/XINDEF/ENL0
COMMON/SPE/ESPECT(30),SPECT(30),NLGRP,LGRP,NLIMP,NIMP(20)
COMMON/CONST/PYE,RADAP
COMMON/NST/NOR
COMMON/LI0/NOPT
COMMON/PPP/PPIMS(20),PPIC,PPFC,PPPF,PPPT0,HRRT,HF1,HP,QUINTOT,PSTOT
COMMON/TAL/F(25),A(20),PM(25,20),R0M(25,20),IME,INM,PE(25,20),
1 P5(25,20),F4(25),PEM(25),P5}
COMMON/PIIT/PIITOT,PIITOT,PPFEW
COMMON/FWNO/FEW,TEWPS
DIMENSION CSECT(3),R(3)

```

```

I11=0
FOLD=0.0
WRITE(6,50)
50 FORMAT(1H1)
CALL SPECTM(1)
CALL NCOMP(1)
PMTOT=0.0
PWTOT=0.0
MLP=1
LCPN=NLP
IMFD=1
IFCG=1
CALL SPECTM(2)
HF=0.
HRP=0.
HLFAK=0.
HARS=0.
TOTCN=0.
DO 3 M=1,NMFD
CALL GSIW(3,1,M,FZFRQ,CSECT)
1SECT(M)=CSECT(1)
SPFR(M)=CSECT(2)
PFR(M)=CSECT(3)
C 200 WRITE(3,200)M,FZFRQ,(CSECT(1),I)=1,3)
C 200 FORMAT(1H MAIN-1 /10X,15,10X,4F14.7)
3 CONTINUE
NARG=1
10 NAME=NAME+1
SCAT=0.0
HP=0.0
HF1=1.0
HRR1=1.0
IF(NOPT,FO,0)GO TO 2001
WRITE(6,250)NAME
250 FORMAT(26H CURRENT HISTORY NUMBER = ,I10)
2001 IF(NAME=NGAMA)11,11,21
11 CALL SOURCE
IM=1
C 30 WRITE(3,270)NAME
30 IE(FR-ECT)12,12,13
12 HF=HF+HF1
NARG=3
22 CONTINUE
IF(NOPT,FO,0)GO TO 23
WRITE(6,260)LOW,NAME,NARG,FATE,HLFAK,HRP,HARS,TOTCN
260 FORMAT(7H MAIN-2 /1X,3I5,5X,5F14.7)
23 CALL NCOMP(4)
GO TO 10
13 CALL TESTWT(LOW)
C 15 WRITE(2,270)NAME
15 IE(LOW)15,15,16
HRR=HRR+HRR1
NARG=3
GO TO 23
16 CALL CALLIS(FATE,IM)
C 17 WRITE(3,270)NAME
C 270 FORMAT(22H SOURCE HISTORY NO. = ,I10)
17 HARS=HARS+1.
NARG=3

```

```

GO TO 23
HLFAK=HLFAK+1.
NAPC=3
WARS=1.0-WA-HB
CALL TALLY(SCAT,FR,WARS,0,1,0)
GO TO 23
19 TITCOL=TITCOL+1.
SCAT=FAIF
CALL NCOMP(3)
GO TO 30
21 NAME=NAME-1
CALL NCOMP(5)
WRITE(6,50)
IF(NLP-MLNPD)1010,1000,1000,1000
1010 NLP=NLP+1
CALL NCOMP(1)
GO TO 2000
1000 CONTINUE
2000 GO TO 100
100 RETURN
END
SUBROUTINE AZI(PHI,PHIS)
COMMON/RAND/N,NM
COMMON/CONST/PVF,PADAP
PHI=2.*PVF*RRIGEN(N)
PHIS=COS(PHI)
PHIS=SIGN(PHI)
RETURN
END
SUBROUTINE CKMAT(PATH,I,TX,MM,EL)
DIMENSION TX(9)
COMMON/OI/NR,IOFNT(IR),HEIGHT,RADIIIS,HOL,ROR,DISt
COMMON/LIN/NRPT
COMMON/GAMR/XR,YR,ZR,ALPR,RETR,GAMR,DIW(10)
COMMON/PARAM/NG,F(7),NMEN
COMMON/LENG/HT(9),RADSO,HGAMA(20)
HT=0.0
FLDL=0.
SL=0.
TSAVE=HT(I)
AGAMR=ARS(GAMR)
IF(ZR)12,11,12
11 PPL=0.0
GO TO 3
12 DO 1 J=1,I
1 THT=THT+HT(J)
PPL=THT-ZR
IF(GAMR)2,3,3
2 PPL=HT(I)-PPL
K=I
II=1
GO TO 4
3 K=NMEN
II=1
4 IF(ZR) 5,6,5
5 HT(I)=PPL
6 DO 10 JK=II,K
IF(GAMR)20,20,20
20 J=I-JK+1
GO TO 40

```

```

30 J=JK
40 IF(I,IT,1) GO TO 60
   IF(I-1) 43,47,42
42 JJI=J-1
   GO TO 44
43 JJI=J+1
44 SI=SI+HT(JJI)/AGAMB
   X=XR+SJ*ALPH
   Y=YR+SL*RETR
   IF((X*X+Y*Y).GT.RADSO ) GO TO 60
47 FLDL=FLDL+ HT(J)*TY(J)/AGAMB
   FLDL=FLDL+ HT(J)*TY(J)/AGAMB
10 CONTINUE
C  IF PASSES THROUGH 10 THEN ESCAPED
60 MM=0
   GO TO 70
50 JI=J
35 FL=SL+(PATH=FLDL*M)/TX(JI)
   MM=JI
70 IF(NOPT,EO,0) GO TO 80
   WRITE(6,100)MM,I,K,II,JI, 7P,DPL,PATH,GAMB,AGAMB,FLDL,FLDL*M,SL,
   IFL,X,Y,XR,YR,RADSO,
   I (HT(I),TX(I),I=1,MMED)
100 FORMAT(12H CKMAT MM=,5I4/TF12.5,7F12.5/(1X,6F15.4))
   RETURN
   END
SUBROUTINE COLLIS(FATE,IM)
DIMENSION XSECT(3),TX(9),SX(9),PPX(9),PEX(9)
COMMON/RAND/IN,NI
COMMON/GAMB/XR,YR,ZR,ALPR,RETR,GAMB,ER,WR,SIGTA,SPRR,PPRR,
1PHRR,TIMEA,IREGR,NIIM(2)
COMMON/GAMB/XA,YA,ZA,NIIM(3),FA,WA,SIGTA,SPRDA,PPRDA,PHPRDA,
1IMEA,IREGA,NIIM(2)
COMMON/PARAM/NG,F(7),NMED
COMMON/ENGFM/REF,NHIST
COMMON/LI/NOPT
COMMON/PPP/PPRMS(20),PPMC,PPEC,PPPE,PTOT,HRR1,HF1,HP,PIINTOT,PSTOT
NHIST=NIIM(2)
DO 15 M=1,MMED
CALL CTSIG(3,1,M,ER,XSECT)
REF=ER
TX(M)=XSECT(1)
SX(M)=XSECT(2)
PPX(M)=XSECT(3)
PEX(M)=1.-SX(M)-PPX(M)
15 CONTINUE
J=IM
PATH=-ALG(RNGEN(N))
CALL CKMAT(PATH,I,TX,MM,TPATH)
IF(MM) 1R,1R,19
19 XA=XR+TPATH*ALPR
   YA=YR+TPATH*RETR
   ZA=ZR+TPATH*GAMB
CALL GFOM(FATE)
IF(NOPT,EO,0)GO TO 2001
WRITE(6,200) ER, PATH,ZA,YA,XA,GAMB,RETR,ALPR,7R,YR,XR,FATE,
1(TX(I),SX(I),PPX(I),PEX(I),I=1,MMED)
200 FORMAT(10H COLLIS=1, RE12.4/1X,RE12.4/(1X,4F12.4))

```

```

60 TO 200)
10 FATE=0.0
2001 IF(FATE.F0.0.)GO TO 39
IMEDH=MM
CALL KIFIN(THETC)
CALL A7I(DHIC,PHIS)
CALL ROT(THETC,PHIC,PHIS)
SIGTS=TX(TMEDH)
SPRR=SX(IMFDR)
PPRR=PPX(IMFDR)
PHPRR=PEX(IMEDH)
WA=WR*SPRR
I=J%ENA
IF(MOPT.F0.0)GO TO 3000
WRITE(6,300)FA,THETC,PHIC,PHIS,SIGTS,SPRR,PPRR,WA
300 FORWAT(104,COLLS=3, F16.7/1X.7F14.7)
3000 CALL PAIR(1)
IM=1
39 RETURN
END
SUBROUTINE DCMP(MARG)
COMMON/GAMMA/DUM(6),ER,WR,DUM1(4),IMED,MPGR,NMU,NAME
COMMON/GAMMA/DUM2(6),FA,WA,DUM3(4),IMEDA,NRGA,MMU,NAMEA
COMMON/PI/WR,TOPT(18),HEIGHT,RADIUS,HOL,RRR,RTST
COMMON/UNIT/MGOLI(15),ROXAV(15),ROXSO(15),ROXVR(15),COEFF(15)
1 RVOL(15),COLL(15),AF(15),O(15),VARE(15)
COMMON/PARAM/NC,FZER,DUM5(4),NMED
COMMON/DC/DVEV
COMMON/TAL/F(25),A(20),RM(25,20),ROM(25,20),INF,IMA,PF(25,20),
1 RS(25,20),EM(25),PEM(25),P5)
COMMON/SPE/SPECT(30),SPEC1(30),NREAD,LDPAN,NMGA(20)
COMMON/NWFGA/NRM(25,20),OROM(25,20),FORM(25,20),FORM(25,20),FOROM(25,20),
1 TRM(25),TRM(25),PRM(25),TOTRM,TOTRM,PERM
COMMON/LI/MSPT
COMMON/PPP/PPINS(20),PPMC,PPFC,PPPE,PPPT,HPRI,HEI,HP,PRINTPT,PSINT
COMMON/EHNO/TOTEM,TEUPS
ZEPDS FOR MARG=1 (FIRST CALL FROM MAIN)
AVE=NAME
60 TO (1,2,3,4,5),MARG
1 DO 6 I=1,151
6 NCOLL(I)=0
RLNV=RVOL(I)
II=0
DO 7 I=1,1359
7 ROXAV(I)=0.
RVOL(I)=RLNV
DO 40 I=1,4
DUM(I)=0.
40 DUM2(I)=0.
WR=0.
FA=0.
WA=0.
IMED=0
NRGR=0
NMU=0
NAME=0
IMEDA=0
NRGA=0
MMU=0

```



```

NAVFA=0
DO 41 I=1,4
DIM2(I)=0.
41 DIM3(I)=0.
C 200 FORMAT(16H DCOMP, 7ERD CALL, 20X,2110)
2 RETURN
3 DMEV=DEACT(ADDFP)
IF(INOPT,FO,0)GO TO 3000
WRITE(6,210)DMEV,ADDER,NR
210 FORMAT(16H DCOMP, MARG 3-1, 20X,2F14.7,110)
3000 IF(NR-1)2000,2000,2001
2000 JJ=1
JS=151
GO TO 11
2001 CONTINUE
IF(JJ,5F,NR)GO TO 120
COLL(JJ)=COLL(JJ)+DMEV
COLL(JS)=COLL(JS)+DMEV
NCOLL(JJ)=NCOLL(JJ)+1
NCOLL(JS)=NCOLL(JS)+1
DO 13 I=1,12
DIM2(I)=DIM2(I)
13 DIM2(I)=0.
NRGR=NRGA
IF(INOPT,FO,0)GO TO 120
WRITE(6,250)JJ,JS,NRGR,COLL(JJ),COLL(JS),NCOLL(JJ),NCOLL(JS)
250 FORMAT(16H DCOMP, MARG 3-2, 3110,2F20.7,2110)
120 RETURN
4 FO=ZFERO*.51097
IF(INOPT,FO,0)GO TO 3001
WRITE(6,265)(COLL(I),ROXAV(I),I=1,NR)
265 FORMAT(16H DCOMP, MARG 4-1, 2F20.5/11X,2F20.5))
3001 DO 20 I=1,NR
ROXAV(I)=ROXAV(I)+COLL(I)
DEFI)=(AF(I)+ROXAV(I)/FO)/AMF
ROXSO(I)=ROXSO(I)+COLL(I)**2
COLL(I)=0.
20 NRGR=1
NRGA=1
DO 21 I=1,12
DIM2(I)=0.
21 DIM2(I)=0.
IF(INOPT,FO,0)GO TO 3002
WRITE(6,260)NAME,FO,(ROXAV(I),4F(I),ROXSO(I),I=1,NR)
260 FORMAT(16H DCOMP, MARG 4-2, 110,4F20.5/(1X,3F20.5))
3002 RETURN
5 DO 30 I=1,NR
ROXAV(I)=ROXAV(I)/AMF
COLL(I)=ROXAV(I)**1.60207E-R
AMF1=NAME-1
ROXVR(I)=(ROXSO(I)/AMF-ROXAV(I)**2)/AMF1
IF(ROXVR(I))30,30,31
31 SRVR=SQRT(ROXVR(I))
CDEFV(I)=SRVR/ROXAV(I)
VARE(I)=2.566628285E-16*SRVR*SRVR
30 CONTINUE
IF(INOPT,FO,0)GO TO 3003
WRITE(6,275)NAME,(ROXAV(I),O(I),ROXVR(I),CDEFV(I),VARE(I),I=1,NR)
275 FORMAT(16H DCOMP, MARG 5 /110/11X,5F14.7)

```

```

3003  T0TR0M=0.0
      DO 400 I=1, N2FA0
        TR0M(I)=0.0
      DO 390 J=1, IMA
        TR0M(I)=R0M(I,J)+TR0M(I)
390  CONTINUE
      T0TR0M=TR0M(I)+T0TR0M
400  CONTINUE
      T0TR0M=0.0
      PERM=0.0
      DO 420 I=1, IMF
        TRM(I)=0.0
        PRM(I)=0.0
      DO 410 J=1, IMA
        TRM(I)=PRM(I,J)+TRM(I)
        PRM(I)=PRM(I,J)+PRM(I)
410  CONTINUE
      T0TRM=TRM(I)+T0TRM
      PERM=PRM(I)+PERM
420  CONTINUE
      FNG=NG
      SINM=INM
      DO 60 J=1, IMA
      DO 50 I=1, IMF
        ORM(I,J)=RM(I,J)/ OMGD(J)
50  FORM(I,J)=ORM(I,J)/FNG
      DO 60 I=1, NBEAD
        OR0M(I,J)=R0M(I,J)/ OMGD(J)
60  FOR0M(I,J)=OR0M(I,J)/FNG
        WRITE(6,26)
          I=L0PM
          WRITE(6,25)FPECT(I)
          WRITE(6,27)(J,A(J),A(J+1),OMGA(J),R0M(I,J),ORM(I,J),FOR0M(I,J),
          ]
          SUMA=0.0
          PUNTOT=0.0
      DO 6550 J=1, IMA
        PUNTOT=PUNTOT+PPHMS(J)
6550  SUMA=SUMA+OR0M(I,J)
          SUMA=SUMA/SINM
65  CONTINUE
        WRITE(6,70)TR0M(I),SUMA,PUNTOT,P51
      T0TR0M=0.0
      PSTOT=0.0
        WRITE(6,26)
        WRITE(6,25)FPECT(I)
      DO 66 I=1, IMF
        WRITE(6,28)F(I),F(I+1),I
        WRITE(6,72)(J,A(J),A(J+1),OMGA(J),R0M(I,J),ORM(I,J),FOR0M(I,J),
          ]
          R5(I,J), J=1, IMA)
        PPSTOT=0.0
          SUMA=0.0
      DO 6551 J=1, IMA
        PPSTOT=PPSTOT+PS(I,J)
6551  SUMA=SUMA+ORPM(I,J)
          SUMA=SUMA/SINM
        FWTOT=FW(I)+PFW(I)
        FTPS=FWTOT/OMGA(IMA)
        WRITE(6,71)TR0M(I),PRM(I),SUMA,PPSTOT,FWTOT,FWTOT,FW(I),PFW(I),FTPS
        PSTOT=PPSTOT+PPSTOT

```

```

      TEMPS=TOTEMP+EMTOT+P51
      TEMPS=TOTEMP/UNSCA(1)NA)
66 CONTINUE
24 FORMAT(1H) ,30H TALLY UNSCATTERED ESCAPES //)))
25 FORMAT(1H0//46X ,18H SOURCE ENERGY = ,F8.5,4H MEV)
26 FORMAT(1H) ,30H TALLY SCATTERED ESCAPES //)))
27 FORMAT(1H0//110H J ANGLES A(J) TO 4(J+1) SOLID ANGLE =
1 NUMBER NUMBER/STER FRACT/STER PAIR PHOTONS //
2 (1X,(14,2F12.5,5F15.5)))
28 FORMAT(1H0//41X ,24H ESCAPE ENERGY INTERVAL ,F8.5,4H TO ,F8.5,
1 8H INDEX ,15)
70 FORMAT(1H0//25H UNSCATTERED ESCAPES = ,F12.5//
1 25H NUMBER AV/STER = ,F12.5
2 //25H PAIR PHOTON ESCAPES = ,F12.5,
3 //25H NO. P IN END CONE = ,F12.5)
71 FORMAT(1H0//23H SCATTERED ESCAPES = ,F12.5//
1 23H P.F. ABSORPTIONS = ,F12.5//
2 23H NUMBER AV/STER = ,F12.5
3 //25H PAIR PHOTON ESCAPES = ,F12.5
4 //23H NUMBER IN END CONE = ,3F12.5
5 //23H NO. IN END CONE/STER = ,F12.5)
72 FORMAT(1H0//110H J ANGLES A(J) TO 4(J+1) SOLID ANGLE //
1 NUMBER NUMBER/STER FRACT/STER PAIR PHOTONS //
2 (1X,(14,2F12.5,5F15.5)))
      PAPER=95(L,00PN,1)
      CALL OUTPUT(INF,PAPER)
      RETURN
      END
      FUNCTION DEACT(X)
      COMMON/GAMMA/DUM(6),ER,WR,SIGTA,SPRR,PPRR,PHPROR,DUM(4)
      COMMON/GAMMA/DUM2(6),FA,WA,SIGTA,SPR0A,PPR0A,PHPR0A,DUM2(4)
      COMMON/LIN/NDPT
      AN0=(ER-2.)*PPPRR
      AN02=FA*PHPRR
      AN03=(ER-FA)*SPRR
      DEACT=WR*.51097*(AN01+AN02+AN03)
      IF(NDPT.EQ.0)GO TO 10
      WRITE(6,3)AN01,AN02,AN03,PPRR,PHPRR,SPRR,WR,FA,ER
3 FORMAT(7H DEACT /1X,7F14.7/1X,2F14.7)
10 RETURN
      END
      SUBROUTINE ERROR(X)
      COMMON/ERROR/I
      I=I+1
      WRITE(6,11)*X
1 FORMAT(17H ERROR NUMBER = ,I4,10X,19H VARIABLE VALUE = ,F14.7)
      CALL EXIT
      RETURN
      END
      SUBROUTINE EQUARD(IE4)
      COMMON/GAMMA/XR,YR,ZR,ALP,REFI,GAM,RDUM(10)
      COMMON/OI/DUM(19),HEIGHT,RADII5,HEL,ROP,DIST
      COMMON/LIN/NDPT
      COMMON/LENG/ZHT(9),SORAD,HGAMA(20)
      IE4=0
      DZ=HEIGHT-7R
      DL=ZD/GAM
      XR=XR+DL*ALP
      Y=YR+DL*REFI
      SOX=X*X

```

```

SOY=Y*Y
IF((SOX+SOY).LE.SOPAD)JFH=1
IF(MOR.FI,0) GO TO 10
WRITE(6,110)IF(.AND.DL,X,Y,XR,YR,ZH,SOX,SOY,SOPAD,HEIGHT
110 FORMAT(10H FORWARD ,I5.6F12.5/15X,5F12.5)
10 RETURN
END
SUBROUTINE GENO(FATE)
COMMON/GAMMA/X,Y,Z,RHM(10),NORM,DIRM(2)
COMMON/OI/NO,INERT(14),HEIGHT,PAN(15),HFL,RRP,DIST
COMMON/ENGENG/F,N
COMMON/LENG/HT(6),RANSG,HGAMA(20)
1 IF(X*Y*Y*CT.RANSG)GO TO 6
2 IF(Z.GT.0..AND.Z.LE.HEIGHT)GO TO 3
GO TO 6
3 FATE=1.
NORM=1
GO TO 7
6 FATE=0.
7 CONTINUE
C WRITE(3,200)N,KEY,FATE,X,Y,Z,RANSG,F
C 200 FORMAT(6H GENO ,10X,2I10/1X,6F14.7)
RETURN
END
SUBROUTINE GTISN (U,V,W,RHO,PHI)
COMMON/RAND/N,NH
COMMON/CONST/PYE,RADAP
W=RNGEN(N)*2-1.
RHO=SQRT (1. -W*W)
PHI=(RNGEN(N)*2. -1.)*DYE
U=COS (PHI)*RHO
V=SIN (PHI)*RHO
WRITE(3,3)U,V,W,RHO,PHI
C 3 FORMAT(6H GTISN /1X,5F14.7)
RETURN
END
SUBROUTINE GTSIG(I,K1,MED,F,SIGMA)
SUB RETRIEVES CROSS-SECTIONS
COMMON/NSI/MOR
DIMENSION XSFCI(830),SIGMA(3),KK(3),FRG(20)
GO TO (1,3,3),J
1 IF(MOR.GT.0)GO TO 40
CALL GENSIG(K1,FLOW,NTINT,NFRAN,FRG,MRANGE,XSFCI,MFO)
40 MOR=MOR-1
MMINT=2**NINT
MEDOT=NFRAN*(2+K1)
WRITE(3,20)MMINT,MEDOT,K1,I,(FRG(J),J=1,20)
CALL INDEX(KK,K1,0.,FLOW,NINT,MED,MEDOT,MMINT,NFRAN,FRG)
RETURN
3 CALL INDEX(KK,K1,F,FLOW,NINT,MED,MEDOT,MMINT,NFRAN,FRG)
WRITE(3,20)MMINT,MEDOT,K1,I,(FRG(J),J=1,20)
C 20 FORMAT(9H GTISGN-1 /1X,4I10/1X,5F14.7)
5 L=2
GO TO 7
6 L=3
7 DO 10 M=1,L
N=KK(V)
SIGMA(M)=XSFCI(V)
10 CONTINUE

```

```

C      WRITE(2,201),KK(1),KK(2),KK(3),SIGMA(1),SIGMA(2),SIGMA(3)
C      FORMAT(9H GSTIGM=2 /1X,4I10/1X,3F14.7)
C      RETURN
C      END
C      SUBROUTINE KLEIN(THETA)
C      COMMON/PARAM/N,NM
C      COMMON/GAMMA/H(16)
C      COMMON/GAMMA/RA(16)
C      COMMON/LI/NOPT
C      TEM=R(7)+R(7)
C      TERP1=TER+1.
C      WRITE(3,200)TER,TERP1,R(7)
C      FORMAT(9H KLEIN=1,10X,3F14.7)
C      IF(R(7).GT.7.)GO TO 11
C      CRI=TERP1/(TER+9.)
C      IF(RNGEN(N).GT.CRI)GO TO 2
C      R2=PMGEN(N)
C      Y=1.+TER*R2
C      IF(NOPT.EQ.0)GO TO 2000
C      WRITE(6,210)R2,Y,CPI
C      FORMAT(9H KLEIN=2,3F14.7)
C      2000 IF(PMGEN(N).LT.4./Y-4./(Y*Y))GO TO 9
C      GO TO 10
C      2 R2=PMGEN(N)
C      CONST=1.+TER*R2
C      Y=TERP1/CONST
C      CAS=1.+(2.*R2-2.)/CONST
C      IF(NOPT.EQ.0)GO TO 2001
C      WRITE(6,230)CAS,Y,CONST,P2
C      230 FORMAT(9H KLEIN=3,4F14.7)
C      2001 IF(RNGEN(N).GT.5*(CAS*CAS+1./Y))GO TO 10
C      8 RA(7)=R(7)/Y
C      THETA=CAS
C      RETURN
C      9 RA(7)=R(7)/Y
C      THETA=1.-2.*R2
C      RETURN
C      11 R1=PMGEN(N)
C      X=TERP1**R1
C      TEMP1=1.-X
C      TEMP2=1./X
C      CAS=(CAS*CAS-TEMP1+TEMP2)*.5*TEMP2
C      IF(NOPT.EQ.0)GO TO 2002
C      WRITE(6,220)TX,R1,X,TEMP1,CAS,TEMP2
C      220 FORMAT(9H KLEIN=4,5F14.7)
C      2002 IF(RNGEN(N).GT.TX)GO TO 11
C      12 RA(7)=R(7)/X
C      THETA=CAS
C      RETURN
C      END
C      SUBROUTINE INDEX(IX,K1,F,FIOW,NINT,NEO,MEOTOT,MININT,NERAM,ERG)
C      COMMON/XINDEX/FOLO
C      DIMENSION ERG(20),IX(3)
C      ER=MNJNT
C      NK=2+K1
C      IF(F-FOLO)5,5,10
C      5 IX(1)=(NEO-1)*MEOTOT+1
C      GO TO 15
C      10 IF(F-FOLO)1,11,1

```

```

7  FOLD=F
   J=ALOG(F/FLN0)/.4914718+1.
   I=FW*F/ERG(I)-EM+1.49
11  IX(I)=(J-I)**60/INT+(I+(MFD-1)*F)DTON
15  DO 20 K=2,NK
20  IX(K)=IX(K-1)+MERAN
C   WRITE(3,200)NK,K1,J,I,MEDT0T,MERAN,MINT,F,FLN0,ERGI,IX(K),
C   IK=I,NK)
C 200  FORMAT(7H INDEX /1X,7I5,3E14,7/(1X,I10))
      RETURN
END
SUBROUTINE OUTPUT(JNF,PAPP0)
COMMON/PARAM/NGAMA,EZERO,FCI,HE,HPR,HEAK,HARS,TOICOL,MMED
COMMON/OUTP/NCOLL(151),ROXAV(151),HOXS0(151),ROXVR(151),COFEV(151)
1,AVOL(151),COLL(151),AF(151),F(151),VARF(151)
COMMON/OI/NR,IDENT(18),HEIGHT,PADJUS,HOL,POR,DIST
COMMON/STRT/TSECT(5),SPROR(5),PPROR(5)
COMMON/PUT/PDONT,PMT0T,PPER%
COMMON/OMEGA/DUMR(2050),PRM(25),TOTR0W,TOTRM,PERM
COMMON/PPP/PBIMS(20),PPWC,PPFC,PPPE,PDONT,MRP1,HE1,HP,PIINT0T,PST0T
COMMON/FWNO/TOTEM,TEMPS
SUMP=0.*0
DO 65 I=1,INE
65  SUMP=PRM(I)+SUMP
    FCT=FCI*.51097
    EZERO=EZERO*.51097
    AGAMA=NGAMA
C 202  WRITE(3,202)(IDENT(I),I=1,12)
C 202  FORMAT(1H,12A5)
    WRITE(4,200)NGAMA,EZERO,FCI,NCOLL(NR)
200  FORMAT(1H1,76HND, 0F HISTORIES INITIAL ENERGY CUT-OFF ENERGY
1  TOTAL NO. OF COLLISIONS // 110,9X,F10.3,8X,F10.3,11X,I10 //)
C   WRITE(3,9)
C 9  FORMAT(1H0,45H TOTAL XSECT SCAT PROR PAIR PROR /)
C   WRITE(3,10)(I,TSECT(I),SPROR(I),PPROR(I),I=1,MMED)
C 10  FORMAT(1H,15,3(13X,F10.4))
    PPE=PERM-PPERM
    RMT=TOTR0W-RMT0T
    RMT=TOTRM-RMT0T
    RARS=HF+HRR+BPPE
    IF(TOTR0W-RMT)50,50,51
50  PIMS=0.*0
51  PMS=SUMP-PIMS
    HARS=HF+HRR+PIMS
    HL=RMT+RMT
    WRITE(4,2000)
2000  FORMAT(1H0,30HTERMINATION PRIMARY PHOTONS // )
    FHU=HL/AGAMA
    FPM=RMT/AGAMA
203  WRITE(4,203)HE,HRR,HL,FHU,HARS, RMT,ER0, RMT,ERM, PMS,PDONT
    FORMAT(
15H 1. ENERGY .F12.5///
2, 2, WEIGHT .F12.5///15H 3. ESCAPE .F12.5,
17X, 24H (3./NO. OF HISTORIES) .F12.5,///
4, 4, ARSOREO .F12.5//22H 5. TOTAL UNSCATTERED ESCAPES .
3E12.5,24H (5./NO. OF HISTORIES) F12.5//32H 6. TOTAL SCATTERED E
4SCAPES .F12.5,24H (6./NO. OF HISTORIES) F12.5//32H 7. PAIR
5ELECTRIC ABSORPTIONS .F12.5,
6, 32H 8. PAIR PRODUCTION PHOTONS .F12.5/// )
    WRITE(4,100)TOTEM,TEMPS

```

```

100 FORMAT(36H TOTAL ESCAPES IN END 10-DEG. COME=F12.5,10X,
123HTOTAL IN END COME/STEP=F12.5)
C WRITE(3,1000)PPE,PARS
C1000
FORVAT(//2F12.5//)
PDESC=PIINTOT+PSTOT
PARS=PPEC+PPEC+PPE
CHECK=(PPARS+PDESC)/2.0+PARS+HL
WRITE(4,3000)
3000 FORMAT(10H,24HTERMINATION PAIR PHOTONS // )
WRITE(4,201)PPEC,PPEC,PDESC,PDESC,PINTOT,PSTOT,PPE,PSTOT
201 FORMAT(
15H 1. ENERGY F12.5//
15H 2. WEIGHT F12.5//
15H 3. FSCAPE F12.5//
215H 4. ARSORDER F12.5//
324H 5. TOTAL UNSCATTERED ESCAPES
3E12.5 //
324H 6. TOTAL SCATTERED F
4SCAPES F12.5. //
324H 7. PHOT
5ELECTRIC ABSORPTIONS F12.5.
6 32H 8. PAIR PRODUCTION PHOTONS F12.5 // )
WRITE(4,4000) CHECK
4000 FORMAT(15H TALLY CHECK = F12.5)
PMTOT=TOTRNM
RMTOT=TOTRMI
RPEM=PERM
DO 3 I=1,NR
RCOMV=1.60207E-8/RVOL(I)
ROXAV(I)=ROXAV(I)*RCOMV
IF(ROXV(I))4,4,5
5 ROXV(I)=SORT(ROXV(I))*RCOMV
4 CONTINUE
C WRITE(4,204)
204 FORMAT(11H,108H AV,DOSF(RADS) DOSE STD. COEF. VAR.
)
3 CONTINUE
C WRITE(6,206) ROXV(I),ROXV(I),COEFV(I), RVOL(I),F(I),
1VARF(I),AF(I) F(G-RADS) VAR. OF F ARSD. FRAC. /
C206 FORMAT(11H, 10X,2(F10.3,3X),F10.3, 13X,3(F10.3,3X),-1PFI0.4)
PIMS=SIMP
RETURN
END
SUBROUTINE PAIR(IM)
DIMENSION TR(12),NTR(4),TA(12),NTA(4)
DIMENSION XSECT(3),TX(9),SX(9),PPX(9),PEX(9)
COMMON/ROAND/NR,NL
COMMON/GAMMA/AFTER(12),NR(4)
COMMON/GAMMA/AFTER(12),NA(4)
COMMON/PARAM/NU,DD,ECT,DI(5),NMED
COMMON/LIO/LOPT
COMMON/PPP/PPIMS(20),PPMC,PPE,PSTOT,HRR1,HF1,HIP,PIINTOT,PSTOT
IF(NOPT.EQ.0)GO TO 2000
WRITE(4,300)REFOR(7)
300 FORMAT(8H PAIR= 10X,F14.7)
2000 IF(REFOR(7).LE.2.)GO TO 2
SCAT=0.0
DO 3 I=1,12
TR(I)=REFOR(I)
3 TA(I)=AFTER(I)
DO 4 J=1,4
NTR(I)=NR(I)
4 NTA(I)=NA(I)
DO 11 J=1,3
11 REFOR(I)=AFTER(I)

```

```

IF(NOPT.F0.0)GO TO 2001
WRITE(6,350)INTR(J,I),NTA(J,I),MTA(J,I),J,I=1,4),(TR(I),TA(I),I=1,12)
350 FORMAT(8H PAIR-2 /1X,RI10/(1X,6F14.7))
2001 CALL GISIN(REFER(4),REFER(5),REFER(6),ROW,FILE)
REFER(7)=1.
REFER(8)=2.*REFER(8)*REFER(11)
TOR=REFER(8)
PPTOT=PPTOT+TOR
HRR1=HRR1-TOR/2.0
HF1=HF1-TOR/2.0
HP=HP+TOR/2.0
J=1*W
10 REFER(12)=0.
DO 15 M=1,NMEN
CALL GTSIGM(3,1,M,REFER(7),XSECT)
TX(M)=XSECT(1)
SX(M)=XSECT(2)
PPX(M)=XSECT(3)
PEX(M)=0.
15 CONTINUE
PATH=-ALOG(PNGEN(M))
CALL CKMAT(PATH,J,TX,MM,TPATH)
IF(MM) 18,18,19
19 DO 20 K=1,3
20 AFTER(K)=REFER(K)+TPATH*REFER(K+3)
CALL GFORM(FATE)
IF(NOPT.F0.0)GO TO 2002
WRITE(6,360)MM, PATH,AFTER(1),AFTER(2),AFTER(3),REFER(1),
1)REFER(2),REFER(3), (TX(I),SX(I),PPX(I),PEX(I),I=1,MMEN)
360 FORMAT(8H PAIR-3 .10X,15/1X,7F14.7/(1X,4F14.7))
GO TO 2002
18 FATE=0.0
2002 IF(FATE.E0.0.)GO TO 6
MED=MM
CALL KLFIN(THFTC)
CALL AZI(PHIC,PHIS)
CALL ROT(THFTC,PHIC,PHIS)
REFER(9)=TX(MED)
REFER(10)=SX(MED)
REFER(11)=PPX(MED)
AFTER(8)=REFER(8)*SX(MED)
SCAT=FATE
CALL DCOMP(3)
J=MED
IF(NOPT.F0.0)GO TO 2003
WRITE(6,380)PPOR,FATE,THFTC,PHIC,PHIS,THFTC,(REFER(I),I=R,11)
380 FORMAT(8H PAIR-5 /1X,5F14.7)
2003 IF(REFER(7).I.FCT)GO TO 60
7 CALL TESTMT(LNW)
IF(LNW)160,160,10
6 CONTINUE
ES=REFER(7)
WARS=TOR-REFER(8)
CALL TALLY(SCAT,ES,WARS,1,TOR)
600 DO 23 I=1,12
REFER(I)=TR(I)
23 AFTER(I)=TA(I)
DO 24 I=1,4
NR(I)=NTA(I)
24 NA(I)=NTA(I)

```



```

GO TO 2
PPFC=PPFC+TOR
GO TO 600
160 PPWC=PPWC+TOR
GO TO 600
2 RETURN
END
SUBROUTINE ROT(THETC,PHIC,PHIS)
COMMON/GAMMA/RUM(3),A,R,C,RUM1(10)
COMMON/GAMMA/DUM(3),AA,AR,AC,DUM1(10)
COMMON/LIN/NOPT
IF(C)1,2,3
1 IF(C+1.0)6,4,6
4 THETS=SQRT(1.0-THETC*THETC)
AA=-PHIC*THETS
AR=PHIS*THETS
AC=-THETC
GO TO 20
3 IF(C-1.0)6,5,6
5 THETS=SQRT(1.0-THETC*THETC)
AA=PHIC*THETS
AR=PHIS*THETS
AC=THETC
GO TO 20
2 THETS=SQRT(1.0-THETC*THETC)
AI=A
AA=-R*PHIS*THETS+AI*THETC
AR=AI*PHIS*THETS+R*THETC
AC=-PHIC*THETS
GO TO 20
6 THETS=SQRT(1.0-THETC*THETC)
AI=A
AA=AI*PHIC*THETS/T-R*PHIS*THETS/T+AI*THETC
AR=R*PHIC*THETS/T+AI*PHIS*THETS/T+R*THETC
AC=-T*PHIC*THETS+C*THETC
20 CONTINUE
IF(NOPT.EQ.0)GO TO 2000
WRITE(6,300)AA,AR,AC,THETS,C,A,B
300 FORMAT(5H ROT /IX,7F14.7)
2000 RETURN
END
FUNCTION RNGFN(IX)
IY=IX*65539
IF(IY)5,6,6
5 IY=IY+2147483647+1
6 YFL=IY
YFL=YFL*.4656613E-9
IX=IY
RNGFN=YFL
RETURN
END
FUNCTION SIGMAS(A)
SIGMAS=.49895*(2.0/(A**2)+(1.+A)/(1.+{2.*A})**2)+ALOG(1.+(2.*A))*
1(1.-2.*(1.+A)/(A**2))/(2.*A))
RETURN
END
SUBROUTINE SOURCE
COMMON/RAND/N,NW
COMMON/GAMMA/X,Y,7,ALP,RFT,GAM,FNER,HGT,DUM(5),NRG,DUM(2)

```

```

COMMON/PARAM/NUM1,FZERO,NUM2(6),MMF1
COMMON/OI/NR,IDENT(18),HEIGHT,RADIUS,HOL,POR,DIST
COMMON/LI/NOPT
COMMON/LENG/HT(6),CORAD,NGAMA(20)
COMMON/CONST/PYE,RADAP
IF(DIST)21,20,21
20 CALL SPAR
RETURN
21 W2=DIS1/(SORT(DIST*DIST+SORAD))
GAM=1-(1.-W2)*PGEN(N)
RT=DIS1/GAM
PHI=(RNGFN(N)*2.-1.)*PYE
EL=SORT(R1*PI-RT*DIST)
X=EL*COS(PHI)
Y=EL*Sin(PHI)
Z=0.0
ALP=X/PI
RT=Y/R1
FNER=FZERO
WGT=1.
NRG=1
IF(NOPT.EQ.0)GO TO 200
WRITE(6,100)W2,PHI,X,Y,Z,ALP,RT,GAM,FNER,HEIGHT,RADIUS,HOL,POR
1 ,FL, R1
100 FORMAT(18H SOURCE ,7X,7F14.5/1X,8F14.5)
200 RETURN
END
SUBROUTINE SPAR
COMMON/RAND/N,NM
COMMON/GAMM/X,Y,Z,ALP,RT,GAM,FNER,WGT,NUM(5),NRG,NUM(2)
COMMON/PARAM/NUM1,FZERO,NUM2(6),MMF1
COMMON/OI/NR,IDENT(18),HEIGHT,RADIUS,HOL,POR,DIST
COMMON/LI/NOPT
COMMON/CONST/PYE,RADAP
D=SORT(RNGFN(N))*RADIUS
Z=0.0
PHI=(RNGFN(N)*2.-1.)*PYE
X=D*COS(PHI)
Y=D*Sin(PHI)
GAM=1.0
ALP=0.0
RT=0.0
WGT=1.0
FNER=FZERO
NRG=1
IF(NOPT.EQ.0)GO TO 200
WRITE(6,100)7,0,PHI,X,Y,Z,ALP,RT,GAM,FNER,HEIGHT,RADIUS,HOL,POR,RNW
1 ,FIF
100 FORMAT(18H PARALLEL SOURCE ,7X,7F14.5/1X,8F14.5)
200 RETURN
END
SUBROUTINE SPECTM(K)
COMMON/RAND/RAND,MRNDMM
COMMON/PARAM/NGAMA,EZERO,FACT,NUM1(5),MMFD
COMMON/SPEZSPECT(30),SPECT(30),NRFAD,ICORN,OMCA(20)
COMMON/OI/NR,IDENT(18),HEIGHT,RADIUS,HOL,POR,DIST
COMMON/TAL/F(25),A(20),RM(25,20),RNM(25,20),IME,INA,PF(25,20),
1 R5(25,20),FW(25),Psw(25),P51
COMMON/CONST/PYE,RADAP
COMMON/OUTP/NCOLL(151),NUM5(606),RVOL(151),NUM6(606)

```

```

COMMON/ IIN/NDPT
COMMON/PPP/PPRINS(20),PPWC,PPPF,PPPTOT,HPR1,HF1,HP,PHINTOT,PSTAT
NDPTM=1
GO TO (I+2),K
1 IF(NDPT-1)2450,2400,2400
2400 NGAMA=100
2450 WRITE(6,2501)NGAMA,NRAD,HEIGHT,NRFAD,NDISTM,RADIIH,INE,ECT,
1 HVOI(1),DIST
2501 FORMAT(1H0,2RHNUMBER OF PHOTON HISTORIES ,15,6X,26HINITIAL PARAM
IM NUMBER ,110,7X,24HCYLINDER HEIGHT (CM) ,F12.5 / 1X,
2RHNO. SOURCE SPECTRUM ENERGIES ,15,6X,26HCENTRAL PARAMETER-NDISTM
3 ,15,12X,24HCYLINDER RADIIH (CM) ,F12.5 / 1X,2RHNO. EQUAL ENR
4RGY INTERVALS ,15,6X,25HLOW ENERGY CUTOFF (MEV) ,F12.5,6X,
524HCYLINDER VOLUME (CM**3) ,F12.5/
660X,16HPPOINT SOURCE IS F12.5,32H (CM) BELOW THE CYLINDER Z-AXIS)
INA=1R
AIN=IMA
IM=JNA+1
IN=IN
IN=INE+1
REN=INE+1
NR=I
NRAD=1
NLAYER=1
WRITE(6,3001)(ESPECT(I),I=1,NRFAD)
3001 FORMAT(1H ,25HSOURCE SPECTRUM ENERGIES / (1X,6F15.5))
3002 WRITE(6,3002)(SPECT(I),I=1,NRFAD)
3002 FORMAT(1H ,40HSOURCE SPECTRUM INTENSITY DISTRIBUTIONS /
1 (1X,6F15.5))
2850 ECT=ECT/0.51097
EXT=ECT
NRNDNM=NRAMD
AD=NRAD
ROR=RADIUS/AD
AYER=NLAYER
HOL=HEIGHT/AYER
EDIF=((ESPECT(1)/0.51097)-0.0)/(REN-1.0)
DO 10 I=1,IN
XK=IN-I
10 A(I)=XK*DYF/AIN
DO 100 I=1,11N
XK=JIN-I
100 F(I)=EDIF*XK
F(1)=ESPECT(1)/0.51097
F(11M)=0.0
A(11M)=0.0
NN=11N
988 IF(ECT-F(MM))999,909,9999
9999 MM=NN-1
GO TO 988
999 NN=NN+1
F(NN)=ECT
909 COMTIME
WRITE(6,3005)(F(I),I=1,11M)
3005 FORMAT(1H ,32HESCAPE SPECTRUM ENERGIES (MC**2) / (1X,6F15.5))
WRITE(6,3006)(A(I),I=1,11N)
3006 FORMAT(1H ,34HESCAPE SPECTRUM ANGLES (RADIAN) / (1X,6F15.5))
DO 20 J=1,11NA
ANGD(J)=2.0*DYF*(COS(A(J+1))-COS(A(J)))
PPRINS(J)=0.0

```

```

00 15 I=1,INE
FW(I)=0.0
PEW(I)=0.0
PF(I,J)=0.0
R5(I,J)=0.0
RDM(I,J)=0.0
15 RW(I,J)=0.0
20 CONTINUE
PPFC=0.0
PPWC=0.0
PPPF=0.0
PPTAT=0.0
P5I=0.0
RETURN
2 FZFRN=ESPECT(LORPN)/0.51097
FCT=EXT
IF(NOPT.EQ.0)GO TO 2000
WRITE(6,3003)FDIF,INE,INA
3003 FORMAT(10H SPECTIM-4 ,F15.5,2I5)
2000 RETURN
END
SHARPTIME TALLY(SCAT,FS,WARS,MPP,TOR)
COMMON/TAL/F(25),A(20),RM(25,20),RDM(25,20),INF,IMA,PF(25,20),
1 R5(25,20),FW(25),PEW(25),P5I
COMMON/GAMR/DUM(5),GAMR,DUMER,WR,DUMZ(R)
COMMON/SPF/ESPECT(30),SPECT(30),NREFAD,LORPN,OMGA(20)
COMMON/CONST/PVE,RADAP
COMMON/LIO/NOPT
COMMON/PPP/PPHMS(20),PPWC,PPFC,PPPF,PPTAT,HRR1,HF1,HP,PIINTOT,PSTOT
IFW=0
ANGLE=ARCS(GAMP)
200 DO 3 J=1,INA
IF(ANGLE-A(J))11,11,12
11 IF(ANGLE-A(J+1))2,14,14
14 IF(SCAT)1,2,1
2 IF(NPP)23,22,23
22 RDM(LORPN,J)=RDM(LORPN,J)+TOR
GO TO 24
23 PPHMS(J)=PPHMS(J)+TOR
IF(J.EQ.IMA)CALL FORWARD(IFW)
IF(IFW.FO.1)P5I=P5I+TOR
24 IF(NOPT.EQ.0)GO TO 2000
WRITE(6,21)NPP,J,ANGLE,GAMR,FS,RDM(LORPN,J),PPHMS(J),SCAT,A(J),FS,
1WR,WARS
21 FORMAT(9H TALLY 2 ,2I5,4F15.5/4F15.5)
GO TO 2000
J IF(J.EQ.IMA)CALL FORWARD(IFW)
DO 4 I=1,INE
IF(FS-F(I))11,11,121
11 IF(FS-F(I+1))21,21,141
141 IF(NPP)43,42,43
42 RW(I,J)=RM(I,J)+WR
PF(I,J)=PF(I,J)+WARS
IF(IFW.FO.1)FW(I)=FW(I)+WR
GO TO 5
43 R5(I,J)=R5(I,J)+WR
PPPF=PPPF+WARS
IF(IFW.FO.1)PEW(I)=PEW(I)+WR
GO TO 5
121 CONTINUE

```

```

4 CONTINUE
I=IME
12 CONTINUE
3 CONTINUE
J=IMA
5 CONTINUE
IF(NOPT.EQ.0)GO TO 2000
WRITE(6,20)LODPM,J,I,ANGLE,CAMR,FS,ROM(LODPM,J),RM(I,J),SCAT,
1 A(J),F(I),WR,PE(I,J),R5(LODPM,J),WARS,NRP,TOR
20 FORMAT(9H TALLY 1 ,3I5,6F15.5/4F15.5,1I0,F15.5)
2000 RETURN
END
SUBROUTINE TA(F,X,M,MM,MOX,MIN,Z,Y,P,NDEGRE,L,LL)
DIMENSION X(200),Z(6),Y(6),R(200)
MOX=MM
MIN=MM
7 XDFI=(MOX-MIN)/2
8 IF(KDFL)R,14,1P
1R KP=MIN+KDFL
DIF=X(KP)-F
IF(X(KP).GT.X(KP+1))DIF=-DIF
IF(DIF)12,12,11
11 MOX=KP
GO TO 7
12 DIF=F-X(KP)
IF(X(KP).GT.X(KP+1))DIF=-DIF
IF(DIF)24,24,13
13 MIN=KP
GO TO 7
24 MIN=KP
MOX=KP+1
14 IF(MOX-M)4,5,4
5 L=MIN-2
GO TO 6
4 L=MIN-1
6 MN=NDEGRE+1
IF(LL)15,2,15
2 DO 3 I=1,MN
J=I+1
7(I)=X(J)
3 Y(I)=P(J)
15 RETURN
END
FUNCTION TF(N,X,Y,FO)
DIMENSION X(6),Y(6)
S=0.0
I=1
28 IF(I-M)21,21,22
21 P=Y(I)
J=1
27 IF(J-M)23,23,24
23 IF(I-J)25,26,25
25 P=P*(FO-X(J))/(X(I)-X(J))
26 J=J+1
GO TO 27
24 S=S+P
I=I+1
GO TO 28
22 IF=S
RETURN

```

```

END
SUBROUTINE TESTWT(LNW)
COMMON/RAVD/N,NM
COMMON/GAMMA/DIR(7),WR,DIRW(8)
COMMON/LIN/NPRT
IF(WR-1,0F-5)1,1,3
1 IF(WR)4,2,4
2 LNW=0
IF(NPRT.F0.0)GO TO 2000
WRITE(4,100)WR,LNW
100 FORMAT(10H TESTWT=1 ,F20.7,110)
2000 RETURN
4 IF(PNGFN(N)-1,0F-5)5,5,2
5 WR=WR*1,0F5
3 LNW=1
WRITE(2,200)WR,LNW
C 200 FORMAT(10H TESTWT=2 /1X,F14.7,110)
RETURN
END
SUBROUTINE AGRW(IP,X,Y,Z,THETA,THETA,THETS,R,RS,AREA,NT)
COMMON/COROS/XX(2),YY(2),ZZ(2),CMP1
COMMON/CXZ/XC,YC,ZC
DIMENSION X(4),Y(4),Z(4),
SUMX=0.,0
SUMY=0.,0
SUMZ=0.,0
DO 10 K=1,1P
SUMX=SUMX+X(K)
SUMY=SUMY+Y(K)
SUMZ=SUMZ+Z(K)
10 CONTINUE
XC=SUMX/IP
YC=SUMY/IP
ZC=SUMZ/IP
CALL INVTOR(IP,X,Y,Z,UX,UY,UZ,AREA,NT)
DO 20 KK=1,2
PX =XX(KK)-XC
RY =YY(KK)-YC
RZ =ZZ(KK)-ZC
CALL ANGTHE(RX,RY,RZ,UX,UY,UZ,THE)
THA(KK)=THE
WRITE(4,100)UX,UY,UZ,XC,YC,ZC,RX,RY,RZ,KK
1001 FORMAT(10H UX,UY,UZ, 3F15.5/10H XC,YC,ZC= 3F15.5/10H RX,RY,RZ= ,
1 3F15.5,5X,2HK=,13)
IF(KK.F0.2) GO TO 15
R1=RX
R2=RY
R3=RZ
20 CONTINUE
15 CALL ANGTHE(RX,RY,RZ,R1,R2,R3,THETS)
AREA=AREA#CMP1#CMP1
R=SQRT(RX*RX+RY*RY+RZ*RZ)#CMP1
R5=SQRT(R1*R1+R2*R2+R3*R3)#CMP1
THETS=THA(1)
THETA=THA(2)
WRITE(4,1000)THA(1),THA(2),THETS,R,RS,AREA
1000 FORMAT(5X,15HINCIDENT ANGLE=F,10.5,5X,17HREFLECTING ANGLE=F,10.5,
15X,5H THETS = ,F10.5/3X,2HR= ,F10.4,5H R5= ,F10.4,7H AREA=F12.4)
RETURN
END

```

```

SURFOUTIME AIR(TOTSAA)
DIMENSION X(40),Y(40),Z(40),PX(40),PY(40),PZ(40),P1(40),P2(40),P3(40),P4(40),P5(40),P6(40),P7(40),P8(40),P9(40)
DIMENSION XSEC(13),FPA(20),YQ(6),ZQ(6),FMY(30)
DIMENSION STRUC(8),POINT(8),SM(20),FF,FM,DIFFSS(40)
COMMON/SURFSE/ZSS(20),SM(20),FF,FM,DIFFSS(40)
COMMON/RATIO/PA,ME,NMF,MN,MC
COMMON/CORRIS/XS,YO,YS,YO,ZS,ZO,CMP1
COMMON/RDIA/TROD,RL
COMMON/CORNST/PVF,RADAP
COMMON/GANXS/FMY,XSC,MM
COMMON/RII/RII,IRI
COMMON/MENT/DUM1(45),MELL(9),DUM2(47)
COMMON/RSTOS/SCOR,ROTOR
XSOL=XS
YSOL=YS
ZSOL=ZS
XOOL=XD
YOOL=YD
ZOOL=ZD
TOTSAA=0.0
MOLD=0
WRITE(6,97)
97 FORMAT(1H,40X,6HALFEDN //13JH INPUT STRU, NAME MATERIAL THIC
1K(CM) LFMGTH(CM) RADIUS(CM) AREA(CM**2) DIST(FR,S) DIST(F
2P,D) MDRDRC FLUX S-SC FLUX /)
READ(5,99)NORF
99 FORVAT(12)
DO 10 NSS=1,NORF
READ(5,98)STRUC(I),I=1,8), (POINTS(I),I=1,8), (RMAT(I),I=1,6)
98 FORMAT(RA1,2X,8B1,2X,6A1)
READ(5,100)NMIN,M,IP,IK,I2,TI,TR,M1,(X(I),Y(I),Z(I),I=1,IP)
98 FORMAT(I1,I4,2I5,3F10,5,I5,/(9F8,3)
ALRF=0.0
TLSS=0.0
XS=XSOLD
YS=YSOLD
ZS=ZSOLD
XD=XDOLD
YD=YDOLD
ZD=ZDOLD
MX=0
M7=0
IC=0
FRMM=0
I=(I2-TI)*CMP1
IF (TR,ME,0.0)FRMM=I
IF (M,FO,MFLD) GO TO 2
MFL(1)=I
IF (NMIN,ME,0)MFL(1)=NMIN
NOR=0
CALL GTSIGW(1,1,1,4,8)
IF (MN-1)82,81,81
81 NMIN=MFL(1)
82 MOLD=M
CALL NFNISI(NOR,FMY,XSC,MNIN)
1 IF(IP,FO,4,OR,IP,FO,3) GO TO 4
1 CALL CKTRAN(IP,IK,X,Y,Z,IXY,RHO,P1,P2,P3,IPP)
IF(IP,IF,2) GO TO 12

```

```

RHO2=0.0
ROUT=0.0
PARFA=0.0
PSOC=PSOCNA*CMPI
RDIR=RDIRNA*CMPI
IRDP=4
IF(IK.F0.3)IRDP=3
IC=IC+1
IA=(IC-1)*IRDP
DO 40 K=1,IRDP
X(K)=PI(IA+K)
Y(K)=P2(IA+K)
Z(K)=P3(IA+K)
GO TO 7
12 IF(IXY.NE.0) GO TO 14
3 CALL ROTATE(X,Y,Z,IXY,RHO)
14 CALL DIVIDE(IXY,RHO,PX,PY,PZ,N,NLA,JP)
ROUT=TP*CMPI
RHO2=RHO*2.0*CMPI
PARFA=0.0
PSOC=PSOCNA*CMPI
RDIR=RDIRNA*CMPI
NAA=NLA-1
NN=2*N
20 MX=MX+1
X(1)=PX(MX)
X(2)=X(1)
X(3)=PX(MX+1)
X(4)=X(3)
IF(IXY.E0.1) GO TO 8
Y(1)=PY(MX)
Y(2)=Y(1)
Y(3)=PY(MX+1)
Y(4)=Y(3)
IF(IXY.E0.2) GO TO 8
Z(1)=PZ(MX)
Z(2)=Z(1)
Z(3)=PZ(MX+1)
Z(4)=Z(3)
8 M7=M7+1
IF(IXY-2)21,21,22
21 Z(1)=PZ(MZ)
Z(2)=PZ(MZ+1)
Z(3)=Z(2)
Z(4)=Z(1)
IF(IXY-2)22,9,22
22 Y(1)=PY(MZ)
Y(2)=PY(MZ+1)
Y(3)=Y(2)
Y(4)=Y(1)
IF(IXY-2)7,9,9
9 X(1)=PX(M7)
X(2)=PX(MZ+1)
X(3)=X(2)
X(4)=X(1)
7 IP=4
4 CALL AGFNM(IP,X,Y,Z,THETA,THETA,THS,R,PS,AREA,NT)
IF(IK.NE.0) GO TO 60
ROUT=0.0
RHO2=0.0

```



```

PAREA=AREA
KSCC=PS
PDTA=PB
60 IF (IRDM,EO,1) GO TO 50
   IF (THETA,GT,90.,OR,THETA,GT,90.) GO TO 5
   ALRG=0.0
   DO 25 KF=1,NF
     EQ=EF(KF)
     NS=SS(KF)
     FG=FO/0.51097
     CALL GSTIG(3,1,1,FG,XSFC)
     UMI=XSFC(1)
     CALL ALRFD(FO,M,THETA,THETA,THETA,THS,T,ALRFD)
     ALFLUX=0.0/COS(THETA/RADAP)*ALRFD*AREA/14.*PYE*RS*PS**R)
     ALRG=ALRG+ALFLUX
   C   WRITE(6,150)FO,UMI,DO,ALFLUX,ALRG
   150 FORMAT(AH AT F=,F7.3,6H MI=,F12.5,10H NO. OF GAM.SOURCE F12.4,
     110H ALFLUX=,F12.4,14H ACC.ALFLUX=,F12.4)
   25 CONTINUE
     ALRXN=0.0
     IF (MN,EO,0) GO TO 16
     DO 30 KFN=1,NNF
       FDN=FN(KFN)
       DO=SN(KFN)
       CALL TA(FDN,FNY,NMN,1,MAX,MIN,ZO,YO,XSC,2,L,0)
       UMI=TF(3,ZO,YO,FDN)
   C   ASSUME NO ALRFD DUE TO NEUTRON REFLECTION
     ALREN=0.0
     ANFLUX=0.0/COS(THETA/RADAP)*ALREN*AREA/14.*PYE*RS*PS**R)
     ALRXN=ALRXN+ANFLUX
   30 CONTINUE
     GO TO 16
     5 ALRG=0.0
     ALRXN=0.0
   16 ALRE=ALRG+ALRG+ALRXN
   C   WRITE(6,200)ALRG,ALRXN,ALRE,IC,MZ,MX,(X(1),Y(1),Z(1),I=1,IP)
   200 FORMAT(15H FLUX(G,N,1),3F12.4,11H IC,MX,M7,3F15.7/(3F10.4))
     GO TO 15
   50 CALL SINGSC (JK,T2,T1,THS,R,RS,PHLUSS,PHLUSN,AREA)
     TLSS=TLSS+PHLUSS+PHLUSN
   C   WRITE(6,250)IC,MX,MZ,PHLUSS,PHLUSN,TLSS
   250 FORMAT(18H SINGLE SCATTERING,3F15.3E12.6)
     15 IF (MZ,EO,0) GO TO 11
     IF (MZ,LT,MAA) GO TO 8
     MZ=0
     IF (MX,LT,MM) GO TO 20
   11 CONTINUE
     IF (IC,EO,0) GO TO 6
     IF (IA,LT,(IPP-4)) GO TO 23
   6   WRITE(6,600)NSS,(STRUCT(I),I=1,R),(POINTS(I),I=1,R),(RMAT(I),I=1,6)
     1),T,PHO2,KOIT,PAREA,PSOC,RDTR,ALRE,TLSS
   600 FORMAT(1X,I2,2X,8A1,1X,8A1,1X,6A1,8(F13.4))
   C   6   WRITE(6,300)ALRE
   C   300 FORMAT(9H ALREN=,F15.6)
   C   WRITE(6,400)TLSS
   C   400 FORMAT(23H TOTAL SINGLE SCATT.=,F15.6)
     19 TOTSA=ALRE+TLSS+TOTSA
   10 CONTINUE
     WRITE(6,500)TOTSA

```

```

500  F0RMA7(  //
1  70X, 35H 7OTAL CALCULATED SCATTERED FLUX = ,F13.5// )
  R0TURN
  EN0
  SUBROUTINE ALR0D(C0,M,TH,TH0,THS,T,ALR0D)
  DIMENSION FF(3),CAMP(3,10),MN(10),D(3),7(3),Y(3)
  COMMON/COMMON/DIRM(6),CAMP
  COMMON/COMMON/TH0,TH,THS,T,ALR0D
  DATA FF/0.412,0.662,1.25/
  DATA DANN/0.095,0.125,0.111, 0.082,0.117,0.102,
1  0.056,0.091,0.100, 0.044,0.072,0.095,
2  0.00975,0.016,0.053, 0.00976,0.011,0.044/
  DATA MN/6.13,22.26,50.92/
  K00=1
  TT=T
  GF=THICK(F0,IMH,TT)
  DO 30 I=1,6
  IF(M,F0,MN(I)) GO TO 1
  IF(M,LT,MN(I+1),ΔMP,M,GT,MN(I)) GO TO 2
30  CONTINUE
  WRITE(6,222)
222  F0RMA7(44H  CHARGE NO. OF THE MATERIAL IS GT 92 OR LT 6 )
  R0TURN
1  K00=0
2  N=1
  DO 3  J=1,3
  D(J)=DANN(J,M)
3  CONTINUE
  IF(F0,GT,FF(2)) GO TO 4
  L=0
  GO TO 5
4  L=1
5  7(1)=FF(L+1)
  7(2)=FF(L+2)
  Y(1)=D(L+1)
  Y(2)=D(L+2)
  WRITE(6,220)F0,L,7(J),Y(J),J=1,2)
  DALPH0=TF(2,Z,Y,F0)
  F0RMA7(8H  TA=DATA,F12.3, I5.4F12.3)
  C  220  F0RMA7(6,111)DALPH0,M,N
  F0RMA7(10H  DALPH0-1 ,F15.5,5H  M= ,I3.5H  N= ,I3)
  IF(K00,F0,0) GO TO 50
  DO 20  K=1,3
  D(K)=DANN(K,N+1)
20  CONTINUE
  Y(1)=D(L+1)
  Y(2)=D(L+2)
  DALP=TF(2,Z,Y,F0)
  ZM=EM
  7(1)=MN(N)
  7(2)=MN(N+1)
  Y(1)=DALPH0
  Y(2)=DALP
  DALPH0=TF(2,Z,Y,7M)
50  ALR0D=DALPH0*COS(TH/RADAP)*COS(TH0/RADAP)*GF
  C  112  F0RMA7(6,112)F0,DALPH0,GF,ALR0D
  F0RMA7(7H  ALR0D ,4F15.5)
  R0TURN
  EN0

```

C AL
TT FF
SW II

```

SUBROUTINE ANGLE=(X1,Y1,Z1,X2,Y2,Z2,THE)
COMMON/CONST/PVF,RADAP
VCT1=SQRT(X1**2+Y1**2+Z1**2)
VCT2=SQRT(X2**2+Y2**2+Z2**2)
THE=ARCOS((X1*X2+Y1*Y2+Z1*Z2)/(VCT1*VCT2))
WRITE(6,1)VCT1,VCT2,THE
1 FORMAT(31H ANGLE=V1,V2,ANGLE(IN RADIAN) ,3F14.5)
THE=THE/RADAP
RETURN
END

FUNCTION SIGMA(F,THE)
EFFECT IS IN THE UNIT OF M*CM*CM
COMMON/CONST/PVF,RADAP
AT=COS(THF/RADAP)
A=1.-AT
R=1.+AT*AT
FA=F**A
SIGMA=(2.*R/R**3)**2/2.*R/(1.+FA)**2*(1.+FA*FA/(R*(1.+FA)))
WRITE(6,11)AT,A,R,FA,CIGMA
111 FORMAT(8H CIGAM ,4F15.5)
RETURN
END

SUBROUTINE CKTRM(IP,K,X,Y,Z,IXY,RHO,FX,PY,IPP)
DIMENSION X(24),Y(24),Z(24),PX(40),PY(40),PZ(40)
COMMON/COROS/XX(2),YY(2),ZZ(2),C,MP1
COMMON/RSTOS/RS,RD
OX=0.,OY=0.,OZ=0.
DO 1 J=1,JP
PX(J)=0.0
PY(J)=0.0
PZ(J)=0.0
DELX=X(2)-X(1)
DELY=Y(2)-Y(1)
DELZ=Z(2)-Z(1)
IPP=0
IF(IP-2) 5,5,10
IXY=0
IF(DELX.EQ.0.0.AND.DELY.EQ.0.0)IXY=3
IF(DELZ.EQ.0.0.AND.DELX.EQ.0.0)IXY=2
IF(DELZ.EQ.0.0.AND.DELY.EQ.0.0)IXY=1
OY=(Y(1)+Y(2))/2.0
OX=(X(1)+X(2))/2.0
OZ=(Z(1)+Z(2))/2.0
RHO=SQRT((X(1)-OX)**2+(Y(1)-OY)**2+(Z(1)-OZ)**2)
IF(IXY)2,2,4
10 IPP=IP
XSUM=0.0
YSUM=0.0
ZSUM=0.0
DO9 J=1,IPP
XSUM=XSUM+X(J)
YSUM=YSUM+Y(J)
ZSUM=ZSUM+Z(J)
CONTINUE
OX=XSUM/IPP
OY=YSUM/IPP
OZ=ZSUM/IPP
DO 19 J=1,IPP

```

```

PX(1)=X(1)-OX
PY(1)=Y(1)-OY
PZ(1)=Z(1)-OZ
19 CONTINUE
4 DO 20 K=1,2
XX(K)=XX(K)-OX
YY(K)=YY(K)-OY
ZZ(K)=ZZ(K)-OZ
20 CONTINUE
1000 FORMAT(7H IX= ,I2,9H WH= ,F10.4/(6X,6F12.4))
RS=SQRT(XX(1)**2+YY(1)**2+ZZ(1)**2)
RD=SQRT(XX(2)**2+YY(2)**2+ZZ(2)**2)
C 2 WRITE(6,1000)IX,RHD,DFIX,DFLY,DFLZ,OX,OY,OZ,(XX(L),YY(L),ZZ(L),L=
C 11,2)
2 CONTINUE
RETURN
END
SURROUTINE DIVIDE(IX,RHD,PX,PY,PZ,N,NA,T2)
DIMENSION PX(40),PY(40),PZ(40)
COMMON/COMMON/PVF,RADAP
COMMON/COMMON/IR,DL
COMMON/COMMON/XS,XD,YS,YD,ZS,ZD,C,MP1
RADAP=T2
C CYLINDER IS DIVIDED INTO NL SECTIONS OF DL LENGTH
RD=SQRT(XD**2+YD**2+ZD**2)
RS=SQRT(XS**2+YS**2+ZS**2)
SN=2.0
1 DL=RHD/SN
SS=(RS-DL)/5.0
DD=(RD-DL)/5.0
IF(DL.LF.SS.AND.DI.LF.DD) GO TO 2
SN=SN+1.
GO TO 1
2 N=RHD/DL
NL=2*SN+1
C ANGLE IS DIVIDED INTO NA-DEGREES INTERVALS
C WRITE(6,3000) IR
3000 FORMAT(5X,4HIP= ,I2)
IF(IR)4,4,3
3 NA=2
AINT=PIF
GO TO 4
4 NA=45.0
5 AINT=DA/RADAP
A=AI*PI/RADAP
IF(A.LF.SS.AND.A.LF.DD) GO TO 6
NA=NA-15.0
IF(DA.LT.10.0) NA=10.0
GO TO 5
6 NA=360.0/DA+1.
C WRITE(6,2000)NL,DL,NA,DA,AINT,A,SS,DD
2000 FORMAT(16H DIVIDE DATA= ,2(I3,F9.4),4F12.3)
8 IF(IXY-2)9,30,60
9 DO 10 I=1,NL
10 PX(I)=(I-1)*RHD/N
DO 20 I=1,NA
FCOS=COS((I-1)*AINT)
FSIN=SIN((I-1)*AINT)
IF(ABS(FCOS).LE.1.0E-05)FCOS=0.0
IF(ABS(FSIN).LE.1.0E-05)FSIN=0.0

```

```

PY(I)=RADARR*FCOS
PZ(I)=RADARR*FSIN
CONTINUE
GO TO 90
30 DO 40 I=1,ML
40 PY(I)=(I-1-M)*RH0/M
DO 50 I=1,NA
FCOS=COS((I-1)*AINT)
FSIN=SIN((I-1)*AINT)
IF(ABS(FCOS).LE.1.0E-05)FCOS=0.0
IF(ABS(FSIN).LE.1.0E-05)FSIN=0.0
PX(I)=RADARR*FCOS
PZ(I)=RADARR*FSIN
CONTINUE
GO TO 90
60 DO 70 I=1,ML
70 PZ(I)=(I-1-M)*RH0/M
DO 80 I=1,NA
FCOS=COS((I-1)*AINT)
FSIN=SIN((I-1)*AINT)
IF(ABS(FCOS).LE.1.0E-05)FCOS=0.0
IF(ABS(FSIN).LE.1.0E-05)FSIN=0.0
PX(I)=RADARR*FCOS
PY(I)=RADARR*FSIN
CONTINUE
80 CONTINUE
90 WRITE(6,1000)ML,OL,NA,DA,RHO
1000 FORMAT(14H DIVIDE DATA ,2(I5,F10.5),5X,4HRHO=,F10.5)
CONTINUE
90 RETURN
END
SUBROUTINE ROTATE(X,Y,Z,IXY,RHO)
DIMENSION X(4),Y(4),Z(4),R(2)
COMMON/RTNS/RS,RO
COMMON/CORNS/XX(2),YY(2),ZZ(2),CMPI
J=2
IXY=1
OX=(X(1)+X(2))/2.0
OY=(Y(1)+Y(2))/2.0
OZ=(Z(1)+Z(2))/2.0
IF(X(1).GT.X(2)) J=1
OXY=X(J)-OY
OYX=Y(J)-OY
OYZ=Z(J)-OZ
RHO=SQRT(OOX*OOX+OOY*OOY+OOZ*OOZ)
F11=OOX/RHO
F12=OOY/RHO
F13=OOZ/RHO
IF(ABS(OOX).LT.ARS(OOY)) GO TO 10
RHOZX=SQRT(OOX*OOX+OOZ*OOZ)
F31=-OOZ/RHOZX
F32=0.0
F33= OOX/RHOZX
F21=F32*F13-F33*F12
F22=F33*F11-F31*F12
F23=F31*F12-F32*F11
GO TO 15
10 IXY=2
F21=F11
F22=F12
F23=F13

```

```

RH07Y=SQRT((OY*OY+007*007)
F31=0*0
F32=-007/RH07Y
F33= OY/RH07Y
F11=F22*F33-F23*F32
F12=F23*F31-F21*F33
F13=F23*F32-F22*F31
00 20 K=1,2
R(K)=SQRT((X(K)-OX)**2+(Y(K)-OY)**2+(Z(K)-OZ)**2)
XX(K)=(XX(K)-OX)*F11+(YY(K)-OY)*F12+(ZZ(K)-OZ)*F13
YY(K)=(XX(K)-OX)*F21+(YY(K)-OY)*F22+(ZZ(K)-OZ)*F23
ZZ(K)=(XX(K)-OX)*F31+(YY(K)-OY)*F32+(ZZ(K)-OZ)*F33
CONTINUE
20 RS=B(1)
30 RP(2)
C WRITE(6,1)IXY,OX,OY,OZ,F11,F12,F13,F21,F22,F23,F31,F32,F33,
C 1(X(K),Y(K),Z(K),XX(K),YY(K),ZZ(K),K=1,2)
1 FORMAT(/,4H IXY=,I2/(5X,6E10.5))
REFIHPN
END
SUBROUTINE SIMGSC (IK,T2,T1,THS,R,RS,PHLUSN,AREA)
DIMENSION FF(20),FM(20),Y(6),Z(6),RA(9),XSECT(3)
COMMON/RATIO/RA,NF,MNF,MW,MC
COMMON/SOURCE/SS(20),SMI(20),FF,FM,DIUMSS(40)
COMMON/DEMT/DIUM(100),FLDEN
COMMON/CORNS/DIUM(6),CMPI
COMMON/CORNST/PYE,RANDAP
COMMON/RDMM/IR,NI
COMMON/GAMXS/ENV(30),XSC(30),NOM
P4R=4*0**PVE**R*RS**RS
IF (IK,EO,0) GO TO 3
VOL=PVE*DL*(T2-T1)*TI*CMPI**3
GO TO 4
3 VOL=AREA*(T2-T1)*CMPI
4 PHLUSN=0*0
IF (MG)6,6,5
5 00 10 I=1,NF
DO=SS(I)
EN=FF(I)/0.51097
CALL GTSIGN(3,1,1,EN,XSECT)
IUMI=XSECT(1)
XKS=CIGMA(EN,THS)
SSFLXG=DO*FLDEN*IUMI*XKS*VOLI*1.0E+24/P4R
PHLUSN=PHLUSN+SSFLXG
WRITE(6,11)EN,DO,XKS,IUMI,SSFLXG,PHLUSN
10 CONTINUE
6 PHLUSN=0*0
IF (MN)9,9,7
7 00 8 J=1,MNF
ENJ=EN(J)
DN=SM(J)
CALL TA(FND,ENV,NOM,1,MNX,MIN,7,Y,XSC,2,f,0)
IUMI=FE(3,7,Y,FND)
XKSN=0*0
SSFLXN=DN*VOLI*XKS*FI DEN*1.0E+24/P4R*IUMI
PHLUSN=PHLUSN+SSFLXN
8 CONTINUE
C 9 WRITE(6,11)TR,THS,P4R,FLDEN,PHLUSN,PHLUSN

```

```

111 FORMAT(24H SINGLE SCATTERING DATA ,I2,4F12.4)
C
CONTINUE
RETURN
END
FUNCTION THICK(F0,UMI,T)
C= -ALOG(1.-0.99)*UMI/P.
THICK=1.-EXP(-C*T)
WRITE(6,2000)F0,UMI,C,T,THICK
C
2000 FORMAT(13H THICK=DATA ,4F12.4)
RETURN
END
SUBROUTINE HVFTRP(K,X,Y,Z,UX,UY,UZ,AREA,NT)
DIMENSION X(4),Y(4),Z(4),DX(3),DY(3),DZ(3)
COMMON/CXYZ/XC,YC,ZC
KF=K-1
DO 10 I=1,KF
L=I
L1=I+1
DX(L)=X(L1)-X(I)
DY(L)=Y(L1)-Y(I)
DZ(L)=Z(L1)-Z(I)
10 CONTINUE
KI=1
K2=2
GO TO 7
8 KI=2
K2=1
7 VX=DY(K1)*DZ(K2)-DY(K2)*DZ(K1)
VY=DX(K1)*DZ(K2)-DX(K2)*DZ(K1)
VZ=DX(K1)*DY(K2)-DX(K2)*DY(K1)
IF(VX*XC) 8,6,4
5 IF(VY*YC) 8,4,4
6 IF(VY*YC) 8,5,5
4 V=SQRT(VX*VX+VY*VY+VZ*VZ)
AREA=V
IF(KF.F0.2)AREA=0.5*V
C
9 WRITE(6,50)VX,VY,VZ,V
50 FORMAT(22H V-VECTOR VX,VY,VZ,V ,4F14.4)
UX=VX/V
UY=VY/V
UZ=VZ/V
RETURN
IF (NT.LT.0) GO TO 20
20 UX=-UX
UY=-UY
UZ=-UZ
RETURN
END
/*

```

APPENDIX IV
CODE SØSC SAMPLE INPUT DATA LISTING


```

// EXEC LINKGO,RECFORM,COND=250K
//CO,PTOAF001 DD SYSOUT=A,DCR=(PREFCE=VR0,{PFC[=]37,PIKSI7=7265}),
//          SPACE=(CVL,(5,5))
//SYSDUMP DD SYSOUT=A,SPACE=(TRK,(10))
//CO.DATAS DD *
1 2 3 4 6 6 7
0.0 0.0 0.0 0.0 240.0 0.0 0.1 0.15 2.0 0.5839 3.94
18 2 16 2 0 77 4 5.0 0.08322 0.8
1 7 12 18
10.0 7.5 5.0 3.0
0.25 0.35 0.45 0.55 0.65 0.75 0.85 0.95 1.10 1.30 1.50 1.70
1.90 2.50 3.50 4.50 5.50 6.50
1.6200E074.7047E077.9331E071.8418E088.4814E073.2661E089.7972E07
5.0233E077.0597E074.5001E076.0440E073.9699E073.9455E076.7414E08
9.1278E052.7067E058.1041E042.7755E04
.1615 0.266 0.4285 0.524 0.801 1.03 1.325
1.70 2.18 2.795 3.575 4.25 4.82 5.92
7.605 9.275
1.1044E062.1724E063.6796E063.7262E066.0516E068.1468E069.2204E06
8.4488E061.3835E072.3046E071.6815E071.7579E064.5018E054.4579E05
1.2893E054.0482E04
20
R00M J-I-I IR0M
26 2 1 0.406 0.312 1.0 5.0
7.5 42.5 19.0 3 70.0
6 -3 4 1 26.0
24 7.87 26.0 55.85
.01 16500. .015 5380. .02 2380.
.03 729. .04 308. .05 155.
.06 91. .08 38. .10 19.1
.15 5.4 .20 2.23 .30 .66
.40 .29 .50 .16 .60 .10
.80 .05 1.0 .03 1.5 .032
2.0 0.0 .12 3.0 0.0 3.503 4.0 0.0
5.0 0.0 0.753 6.0 0.0 0.915 8.0 0.0 1.181
R0X 00NF IR0M
26 24 0 0.2 0.0
85.0 30.0 85.0 -5.0 50.0 85.0 5.0 50.0
5.0 5.0 85.0 -5.0 50.0 85.0 5.0 50.0
95.0 5.0 30.0 95.0 5.0 50.0 85.0 30.0
85.0 5.0 30.0 95.0 5.0 30.0 95.0 5.0
85.0 5.0 50.0 85.0 -5.0 30.0 95.0 30.0
95.0 -5.0 50.0 85.0 -5.0 50.0 95.0 30.0
95.0 -5.0 50.0 85.0 5.0 50.0 95.0 30.0
PLANE A-2 IR0M
26 4 0 0.125 0.0 0.0 0.0
23.8 13.75 2.5 23.8 13.75 27.5 23.8 2.5
13.75 23.8 27.5
IR0M
PLANE A-3 IR0M
26 4 0 0.125 0.0 0.0 0.0
13.75 23.8 2.5 13.75 23.8 27.5 23.8 2.5
0.0 27.5 27.5
IR0M
PLANE A-1 IR0M
26 4 0 0.125 0.0 0.0 0.0
27.5 0.0 2.0 27.5 0.0 27.5 23.8 2.5
23.8 13.75 27.5
IR0M
PLANE M-F IR0M
26 2 1 0.406 0.312 1.0 5.0
23.8 13.75 27.5 27.5 46.875 32.5
R00M J-K IR0M
26 2 1 0.406 0.312 1.0 5.0
7.5 42.5 19.0 -7.5 42.5 19.0
R00M N-0 IR0M
26 2 1 0.406 0.312 1.0 5.0
97.5 3.75 40.0 47.5 23.75 12.5
R00M P-0 IR0M
26 2 1 0.406 0.312 1.0 5.0
87.5 2.5 25.0 47.5 23.75 12.5
R00M C-0 DL
13 2 1 0.406 0.312 1.0 5.0

```

47.5	22.5	47.5	23.75	12.5					
6	-3	4	13.00	26.98					
24	0.01	1170.0	0.0	0.015	343.0	0.0	0.02	141.0	0.0
	0.03	39.0	0.0	0.04	15.2	0.0	0.05	7.3	0.0
	0.06	4.0	0.0	0.08	1.61	0.0	0.10	.78	0.0
	0.15	.21	0.0	0.20	0.08	0.0	0.30	.02	0.0
	0.40	0.01	0.0	0.50	0.0	0.0	0.60	0.0	0.0076
	0.80	0.0	0.0	1.0	0.0	0.0	1.5	0.0	.1406
	2.00	0.0	.03	3.0	0.0	0.0862	4.0	0.0	.30
	5.0	0.0	.187	6.0	0.0	.229	8.0	0.0	
	CYLINDER	02-01	AL						
	13	1	8.0	7.5	0.0	0.0	71.25		
	0.0	0.0	32.5	0.0	0.0	0.0			
	ANTENNA	T-II	AL						
	13	1	1.875	1.275	1.0	36.25			
	42.5	0.0	40.00	7.5	0.0	0.0			
	CYLINDER	02-03	AL						
	13	1	11.5	11.0	0.0	0.0			
	0.0	0.0	71.25	0.0	0.0	106.25			
	ANTENNA	P-T	AL						
	13	1	1.25	0.75	1.0	40.0			
	81.0	0.0	61.25	42.5	0.0	0.0			
	ANTENNA	R1-T1	AL						
	13	1	1.25	0.75	1.0	40.0			
	70.02	40.5	61.25	36.8	21.25	40.0			
	ANTENNA	T-II	AL						
	13	1	1.875	1.275	1.0	36.25			
	36.8	21.25	40.00	6.49	3.75	36.25			
	RNDM	01-C1	AL						
	13	2	0.406	0.312	1.0	32.5			
	232.5	0.0	95.0	47.5	22.5	32.5			
	RNDM	R1-R2	AL						
	13	1	0.406	0.312	1.0	63.75			
	146.875	12.50	63.75	146.875	-12.5	63.75			
	RNDM	G-H	AL						
	13	1	0.406	0.312	1.0	28.75			
	22.5	63.75	18.75	-26.75	11.25	28.75			
	RNDM	L-F	AL						
	13	1	0.406	0.312	1.0	32.5			
	13.75	23.8	27.5	27.5	46.875	32.5			
	THE SHIELD CONSISTS OF 0.1%LEAD AND 0.9%IIR								
	0.1	1	0.9	2					
	82.	11.35							
	1.00	1040	3.00	7159					
	6	-3	4						
	27	11.35	82.0	207.21					
	0.01	27500.0	0.0	0.1307	13200.0	0.0	0.1586	45400.0	0.0
	0.02	24000.0	0.0	0.03	7620.0	0.0	0.04	3310.0	0.0
	0.05	1740.0	0.0	0.06	1040.0	0.0	0.08	444.0	0.0
	.088229	334.0	0.0	0.08823	2510.0	0.0	0.10	1780.0	0.0
	0.15	596.0	0.0	0.20	275.0	0.0	0.30	93.6	0.0
	0.40	45.7	0.0	0.50	26.1	0.0	0.60	17.3	0.0
	0.80	9.5	0.0	1.0	6.2	0.0	1.5	3.0	0.55
	2.0	2.0	1.72	3.0	1.1	3.931	4.0	0.80	5.764
	5.0	0.60	7.259	6.0	0.49	8.49	8.0	0.35	10.53
	24	0.1040	1.0	1.008					
	0.01	0.046	0.0	0.15	0.0011	0.0	0.02	0.0	0.0
	0.03	0.0	0.0	0.04	0.0	0.0	0.05	0.0	0.0
	0.06	0.0	0.0	0.08	0.0	0.0	0.10	0.0	0.0
	0.15	0.0	0.0	0.20	0.0	0.0	0.30	0.0	0.0
	0.40	0.0	0.0	0.50	0.0	0.0	0.60	0.0	0.0
	0.80	0.0	0.0	1.0	0.0	0.0	1.5	0.0	0.00044
	2.00	0.0	0.0018	3.0	0.0	0.0052	4.0	0.0	0.0087
	5.0	0.0	0.0012	6.0	0.0	0.0015	8.0	0.0	0.0022
	24	0.7159	3.0	6.94					
	0.01	1.0	0.0	0.015	0.3	0.0	0.02	0.1	0.0
	0.03	0.03	0.0	0.04	0.01	0.0	0.05	0.006	0.0
	0.06	0.003	0.0	0.08	0.002	0.0	0.1	0.0	0.0
	0.15	0.0	0.0	0.2	0.0	0.0	0.3	0.0	0.0
	0.4	0.0	0.0	0.5	0.0	0.0	0.6	0.0	0.0
	0.8	0.0	0.0	1.0	0.0	0.0	1.5	0.0	0.004

2.0	0.0	.0016	3.0	0.0	.0048	4.0	0.0	.0018
5.0	0.0	.0011	6.0	0.0	.0014	8.0	0.0	.0018
18	11.35	207.21	82.0					
0.1	10.01	0.2	8.0	0.3	7.0	0.34	5.2	0.26
0.40	6.0	0.5	3.2	0.55	5.0	0.70	6.8	0.75
0.80	5.6	1.0	6.0	1.5	5.4	2.20	6.0	3.0
5.0	7.2	8.0	5.3	10.0	5.0			7.6
17	0.1041	1.008	1.0					
0.1	12.5	0.2	9.6	0.24	8.8	0.26	8.5	0.28
0.32	7.8	0.5	6.2	0.80	4.8	1.0	4.25	2.0
3.0	2.25	4.2	1.83	5.0	1.5	6.0	1.42	7.0
9.0	1.05	12.0	0.8					1.13
17	0.7159	6.94	3.0					
0.1	1.0	0.2	1.7	0.24	7.0	0.26	10.0	0.28
0.32	2.0	0.5	1.0	0.98	1.4	1.0	1.5	2.0
3.0	2.0	4.2	2.3	5.0	2.25	6.0	2.1	7.0
9.0	1.6	12.0	1.5					1.8
-1			6	7				
THE SHIELD CONSISTS OF 0.9*LIH AND 0.1*LEAD								
2								
0.9	2	0.1	1					
1.00	1040	3.00	7159					
82	11.35							
6	-3	4						
24	0.1040	1.0	1.008					
0.1	.0046	0.0	.015	0.0	.02	0.0	0.0	0.0
0.3	0.0	0.0	.04	0.0	.05	0.0	0.0	0.0
0.6	0.0	0.0	.08	0.0	.10	0.0	0.0	0.0
1.5	0.0	0.0	.20	0.0	.30	0.0	0.0	0.0
4.0	0.0	0.0	.50	0.0	.60	0.0	0.0	0.0
8.0	0.0	0.0	1.0	0.0	1.5	0.0	0.0	.000044
2.00	0.0	.00018	3.0	0.0	.00052	4.0	0.0	.000087
5.0	0.0	.0012	6.0	0.0	.0015	8.0	0.0	.00022
24	.7159	3.0	6.94					
0.01	1.0	0.0	0.015	0.3	0.0	0.02	0.1	0.0
0.03	0.03	0.0	0.04	0.01	.0	0.05	0.006	0.0
0.06	0.003	0.0	0.08	0.002	.0	0.1	0.0	0.0
0.15	0.0	0.0	0.2	0.0	0.0	0.3	0.0	0.0
0.4	0.0	0.0	0.5	0.0	0.0	0.6	0.0	0.0
0.8	0.0	0.0	1.0	0.0	0.0	1.5	0.0	.00004
2.0	0.0	.0016	3.0	0.0	.0048	4.0	0.0	.0008
5.0	0.0	0.011	6.0	0.0	0.014	8.0	0.0	0.018
27	11.35	82.0	207.21					
0.01	27500.0	0.0	.01307	13200.0	0.0	.01586	45400.0	0.0
0.02	24000.0	0.0	0.03	7620.0	0.0	0.04	3310.0	0.0
0.05	1740.0	0.0	0.06	1040.0	0.0	0.08	444.0	0.0
.088229	334.0	0.0	0.08823	2510.0	0.0	0.10	1780.0	0.0
0.15	596.0	0.0	0.20	275.0	0.0	0.30	93.4	0.0
0.40	45.7	0.0	0.50	26.1	0.0	0.60	17.3	0.0
0.80	9.5	0.0	1.0	6.2	0.0	1.5	3.0	0.55
2.0	2.0	1.72	3.0	1.1	3.931	4.0	0.80	5.764
5.0	0.60	7.259	6.0	0.49	8.469	8.0	0.35	10.53
17	0.1041	1.008	1.0					
0.1	12.5	0.2	9.6	0.24	8.8	0.26	8.5	0.28
0.32	7.8	0.5	6.2	0.80	4.8	1.0	4.25	2.0
3.0	2.25	4.2	1.83	5.0	1.6	6.0	1.42	7.0
9.0	1.05	12.0	0.8					1.13
17	0.7159	6.94	3.0					
0.1	1.0	0.2	1.7	0.24	7.0	0.26	10.0	0.28
0.32	2.0	0.5	1.0	0.98	1.4	1.0	1.5	2.0
3.0	2.0	4.2	2.3	5.0	2.25	6.0	2.1	7.0
9.0	1.6	12.0	1.5					1.8
18	11.35	207.21	82.0					
0.1	10.01	0.2	8.0	0.3	7.0	0.34	5.2	0.36
0.40	6.0	0.5	3.2	0.55	5.0	0.70	6.8	0.75
0.80	5.6	1.0	6.0	1.5	5.4	2.20	6.0	3.0
5.0	7.2	8.0	5.3	10.0	5.0			7.6
/*								

APPENDIX V
CODE SØSC SAMPLE OUTPUT DATA LISTING

SOURCE DATA

GAMMA SPECTRUM	ENERGY(MEV)	NO. OF GAMMA/SEC (RADIAL)	NO. OF GAMMA/SEC (AXIAL)	FLUX AT DETECTOR (RADIAL)	FLUX AT DETECTOR (AXIAL)
1	0.051000E 00	0.162000E 08	0.149945E 07	0.279050E 01	0.2274566E 02
2	0.351200E 01	0.474600E 08	0.702424E 07	0.792710E 01	0.6615685E 03
3	0.430000E 01	0.799300E 08	0.6652314E 07	0.130509E 02	0.1102070E 03
4	0.550000E 01	0.184100E 09	0.1534771E 08	0.313300E 02	0.2586096E 01
5	0.650000E 01	0.840100E 08	0.7775916E 07	0.143740E 02	0.1102239E 01
6	0.750000E 01	0.326600E 08	0.2721639E 08	0.5873156E 02	0.4535776E 01
7	0.850000E 01	0.979700E 08	0.816474E 07	0.165761E 02	0.1375579E 01
8	0.950000E 01	0.523200E 08	0.4195913E 07	0.846392E 01	0.7352981E 00
9	0.100900E 01	0.705600E 08	0.5898445E 07	0.1109512E 02	0.8912198E 00
10	0.120900E 01	0.450300E 08	0.3749931E 07	0.7582363E 01	0.6318398E 01
11	0.150000E 01	0.474000E 08	0.3369864E 07	0.6813967E 01	0.5677992E 01
12	0.170000E 01	0.396900E 08	0.330116E 07	0.6689712E 01	0.5939595E 01
13	0.190000E 01	0.354600E 08	0.328778E 07	0.664790E 01	0.5939692E 01
14	0.240000E 01	0.574130E 08	0.561760E 08	0.113998E 03	0.9465284E 01
15	0.350000E 01	0.912700E 08	0.7670189E 07	0.153797E 03	0.128191E 01
16	0.450000E 01	0.276700E 06	0.225492E 05	0.456747E 01	0.390735E 02
17	0.550000E 01	0.810100E 05	0.6753145E 04	0.1355486E 01	0.1117999E 02
18	0.650000E 01	0.278500E 05	0.2312923E 04	0.4678524E 02	0.396604E 03
TOTAL=		0.179761E 10	0.1407947E 09	0.312995E 03	0.252394E 02

NEUTRON SPECTRUM,	ENERGY(MEV)	NO. OF NEUT./SEC (RADIAL)	NO. OF NEUT./SEC (AXIAL)	FLUX AT DETECTOR (RADIAL)	FLUX AT DETECTOR (AXIAL)
1	0.161500E 01	0.110400E 07	0.8893199E 06	0.186.839E 01	0.1488671E 01
2	0.260000E 01	0.217200E 07	0.1737919E 07	0.3660347E 00	0.2929270E 01
3	0.438500E 01	0.367960E 07	0.2943579E 07	0.6196877E 01	0.4959900E 01
4	0.524000E 01	0.372620E 07	0.2987950E 07	0.6278395E 01	0.5922714E 01
5	0.811000E 01	0.615100E 07	0.4841279E 07	0.1019653E 01	0.8157228E 00
6	0.113000E 01	0.916680E 07	0.6593439E 07	0.1976756E 01	0.110094E 01
7	0.132500E 01	0.922400E 07	0.7376319E 07	0.1553575E 01	0.1249860E 01
8	0.170000E 01	0.843800E 07	0.6799009E 07	0.123306E 01	0.119985E 01
9	0.217999E 01	0.138300E 08	0.1106800E 08	0.2331103E 01	0.1864982E 01
10	0.279499E 01	0.239460E 08	0.1918678E 08	0.4438739E 01	0.3227786E 01
11	0.357500E 01	0.168140E 08	0.134109E 08	0.283212E 01	0.2266569E 01
12	0.425000E 01	0.176790E 07	0.1414319E 07	0.2074792E 00	0.239332E 00
13	0.482000E 01	0.450180E 06	0.3601439E 06	0.7585227E 01	0.6168182E 01
14	0.571999E 01	0.445780E 06	0.3568319E 06	0.7511238E 01	0.6090078E 01
15	0.760500E 01	0.128930E 06	0.1131439E 06	0.2172183E 01	0.1737900E 01
16	0.927500E 01	0.474820E 05	0.323866E 05	0.6682045E 02	0.546753E 02
TOTAL=		0.999942E 08	0.7999044E 08	0.168021E 02	0.134793E 02

DIST. BET. SOURCE AND DETECTOR (CM)= 0.6872E 03 ALLOWED FLUX AT DETECTOR= 0.50E 01



AL9500

INPUT STRU.	NAME	MATERIAL	THICK(CM)	LENGTH(CM)	RADIUS(CM)	AREA(CM**2)	DIST(FP.S)	DIST(FP.D)	NO ABDN FLUX	S-SC FLUX
1	ROOM	J-1	0.2398E 00	0.866E 02	0.1031E 01	0.0000	0.751E 02	0.652E 03	0.0	0.1724E-01
2	BOX	ONE	0.591E 00	0.0	0.0	0.120E 04	0.333E 03	0.394E 03	0.0	0.0
3	PLANE	A-2	0.3175E 00	0.0	0.0	0.2292E 04	0.1604E 03	0.5905E 03	0.1736E 00	0.0
4	PLANE	A-3	0.3175E 00	0.0	0.0	0.2297E 04	0.1467E 03	0.6295E 03	0.1129E 00	0.0
5	PLANE	A-1	0.3175E 00	0.0	0.0	0.2343E 04	0.2028E 03	0.5816E 03	0.0	0.0
6	ROOM	M-F	0.2398E 00	0.8561E 02	0.1031E 01	0.0000	0.1632E 03	0.5742E 03	0.0	0.2297E-01
7	ROOM	J-K	0.2398E 00	0.3810E 02	0.1031E 01	0.0000	0.1091E 03	0.6486E 03	0.0	0.1492E-01
8	ROOM	N-O	0.2398E 00	0.1313E 03	0.1031E 01	0.0000	0.251E 03	0.4731E 03	0.0	0.1545E-01
9	ROOM	P-Q	0.2398E 00	0.1103E 03	0.1031E 01	0.0000	0.2478E 03	0.4803E 03	0.0	0.1733E-01
10	ROOM	C-O	0.2398E 00	0.5000E 02	0.1031E 01	0.0000	0.1986E 03	0.5259E 03	0.0	0.7919E-02
11	CYLINDER	O2-O1	0.1270E 01	0.9842E 02	0.2032E 02	0.0000	0.2443E 03	0.6194E 03	0.9578E-01	0.0
12	ANTENA	T-U	0.1270E 01	0.8941E 02	0.4762E 01	0.0000	0.2361E 03	0.5649E 03	0.0	0.2951E-01
13	CYLINDER	O2-O3	0.1270E 01	0.8900E 02	0.2921E 02	0.0000	0.3052E 03	0.6098E 03	0.4574E-01	0.0
14	ANTENA	R-T	0.1270E 01	0.1117E 03	0.3175E 01	0.0000	0.2889E 03	0.4666E 03	0.0	0.2227E-01
15	ANTENA	R-T*	0.1270E 01	0.1115E 03	0.3175E 01	0.0000	0.2262E 03	0.4935E 03	0.0	0.3182E-01
16	ANTENA	T-U*	0.1270E 01	0.8941E 02	0.4762E 01	0.0000	0.2066E 03	0.5741E 03	0.0	0.4554E-01
17	ROOM	D1-C1	0.2398E 00	0.4903E 03	0.1031E 01	0.0000	0.4290E 03	0.2677E 03	0.0	0.1765E-01
18	ROOM	B1-B2	0.2398E 00	0.6350E 02	0.1031E 01	0.0000	0.4556E 03	0.2496E 03	0.0	0.1162E-02
19	ROOM	G-H	0.2398E 00	0.1846E 03	0.1031E 01	0.0000	0.1260E 03	0.6482E 03	0.0	0.9633E-02
20	ROOM	L-F	0.2398E 00	0.6940E 02	0.1031E 01	0.0000	0.1483E 03	0.5881E 03	0.0	0.3745E-02

TOTAL CALCULATED SCATTERED FLUX = 0.60812E 00

TOTAL SCATTERED FLUX= 0.6081E 00 ALLOWED ATTENUATED FLUX= 0.4392E 00



D

NOTE: The following output corresponds to the second shield case in the Appendix IV input sample data.

THE SHIELD COMPOSES OF 40%LEAD AND 60%CONCRETE

J	ENERGY (eV)	WTD-MU(CM-1)	WTD-MU(X)	NUCL. SOURCE MADE FLUX AT C	BUILDUP FACT.	ATT. FLUX AT D	ATT. FACT (BEST)
GAMMA-DATA							
1	0.05 E	1.60 E	0.1178E 02	0.277E 07	0.1 E 1	0.333E 05	0.190E-04
2	0.35 E	0.370E 01	0.632E 01	0.666E 01	0.1 E 1	0.348E 02	0.275E-02
3	0.45 E	0.26 E	0.443 E	0.495E 0	0.1 E 1	0.300E 01	0.102E-01
4	0.55 E	0.264E 01	0.359E 01	0.238E 01	0.1 E 1	0.349E 01	0.349E-01
5	0.65 E	0.174E 01	0.34E 01	0.70E 0	0.1 E 1	0.310E 01	0.617E-01
6	0.75 E	0.160E 01	0.260E 01	0.590E 0	0.1 E 1	0.310E 01	0.870E-01
7	0.85 E	0.140E 01	0.241E 01	0.565E 0	0.1 E 1	0.280E 01	0.172E 00
8	0.95 E	0.120E 01	0.223E 01	0.510E 0	0.1 E 1	0.270E 01	0.128E 00
9	1.1 E	0.112E 01	0.192E 01	0.480E 0	0.1 E 1	0.151E 01	0.156E 00
10	1.3 E	0.1 E	0.170E 01	0.470E 0	0.1 E 1	0.117E 01	0.149E 00
11	1.5 E	0.08 E	0.150E 01	0.537E 0	0.1 E 1	0.119E 01	0.238E 00
12	1.7 E	0.073E 01	0.150E 01	0.557E 0	0.1 E 1	0.127E 01	0.353E 00
13	1.9 E	0.062E 01	0.146E 01	0.548E 0	0.1 E 1	0.253E 01	0.593E 00
14	2.5 E	0.047E 01	0.131E 01	0.561E 0	0.1 E 1	0.337E 01	0.325E 00
15	3.5 E	0.037E 01	0.127E 01	0.767E 0	0.1 E 1	0.410E 01	0.330E 00
16	4.5 E	0.027E 01	0.116E 01	0.295E 0	0.1 E 1	0.364E 01	0.346E 00
17	5.5 E	0.02 E	0.113E 01	0.274E 0	0.1 E 1	0.317E 01	0.350E 00
18	6.5 E	0.018E 01	0.112E 01	0.231E 0	0.1 E 1	0.316E 01	0.350E 00
NEUTRON-DATA							
1	0.141E 01	0.330E 01	0.1410E 02	0.140E 06	0.177E 01	0.110E 04	0.145E-05
2	0.266 E	0.870E 01	0.146E 02	0.178E 07	0.170E 01	0.416E 05	0.197E-06
3	0.438E 01	0.870E 01	0.377E 01	0.490E 07	0.410E 01	0.471E 05	0.118E-03
4	0.624 E	0.464E 00	0.790E 01	0.208E 07	0.120E 01	0.254E 02	0.650E-03
5	0.811 E	0.421E 00	0.719E 01	0.208E 07	0.120E 01	0.673E 02	0.188E-02
6	1.037 E	0.431E 00	0.417E 01	0.433E 07	0.111E 01	0.450E 02	0.407E-03
7	1.325 E	0.457E 00	0.478E 01	0.470E 07	0.110E 01	0.672E 02	0.720E-03
8	1.7 E	0.391E 00	0.748E 01	0.470E 07	0.110E 01	0.775E 02	0.982E-03
9	2.13 E	0.430E 00	0.748E 01	0.517E 08	0.110E 01	0.132E 01	0.149E 02
10	2.73E 01	0.448E 00	0.750E 01	0.510E 08	0.11 E 1	0.237E 01	0.820E-03
11	3.37E 01	0.629E 00	0.786E 01	0.226E 08	0.110E 01	0.115E 01	0.665E-03
12	4.85 E	0.450E 00	0.782E 01	0.238E 08	0.11 E 1	0.125E 02	0.693E-03
13	6.82 E	0.447E 00	0.780E 01	0.410E 08	0.11 E 1	0.374E 03	0.856E-03
14	9.22 E	0.447E 00	0.780E 01	0.356E 08	0.110E 01	0.571E 03	0.150E-02
15	1.265E 01	0.338E 00	0.504E 01	0.401E 08	0.110E 01	0.460E 03	0.280E 02
16	1.747E 01	0.314E 00	0.510E 01	0.324E 08	0.11 E 1	0.169E 03	0.450E 02

DETECTED FLUX AS A FUNCTION OF SHIELD THICKNESS

X-FAST (CM)	FLUX(INP/CM/CM/SEC)
0.1691 E 02	0.4010E 06
0.1500 E 02	0.4774E 06
0.1600 E 02	0.4780E 06
0.1700 E 02	0.4995E 06

ITERATION NO. = 15.9 C3 WEIGHTED DENSITY = 1.8720 WT. (GRAMS) = 0.1574 F 4



0.15817E-02
 0.40237E 01
 CYLINDER HEIGHT (CM)
 CYLINDER RADIUS (CM)
 CYLINDER VOLUME (CM**3)
 POINT SOURCE IS 0.10000E 02 (CM) BELOW THE CYLINDER Z-AXIS

523506365
 1
 INITIAL RANDOM NUMBER
 CONTROL PARAMETER-NDISTN
 LOW ENERGY CUTOFF (MEV)
 POINT SOURCE IS 0.10000E 02 (CM) BELOW THE CYLINDER Z-AXIS

10000
 1
 NUMBER OF PHOTON HISTORIES
 ND SOURCE SPECTRUM ENERGIES
 2
 ND FOVAL ENERGY INTERVALS

SOURCE SPECTRUM ENERGIES

0.25770E 04

SOURCE SPECTRUM INTENSITY DISTRIBUTIONS

0.10000E 01

ESCAPE SPECTRUM ENERGIES (MC**2)

0.48927E 00

0.24463E 00

0.19571E 00

0.31416E 01

0.27925E 01

0.26187E 01

0.24435E 01

0.20944E 01

0.19199E 01

0.17453E 01

0.13963E 01

0.10472E 01

0.87256E 01

0.69813E 00

0.34907E 00

0.0

0.0

0.0

0.17453E 00



TALLY UNSCATTERED ESCAPES

SOURCE ENERGY = 0.25300 MEV

J	ANGLES A(J) TO A(J+1)	SOLID ANGLE	NUMBER	NUMBER/STER	FRACT/STER	PAIR PHOTONS
1	3.14159	0.95457E-01	0.0	0.0	0.0	0.0
2	2.96706	1.28347E-00	0.0	0.0	0.0	0.0
3	2.79253	1.46287E-00	0.0	0.0	0.0	0.0
4	2.61799	1.62820E-00	0.0	0.0	0.0	0.0
5	2.44346	1.77445E-00	0.0	0.0	0.0	0.0
6	2.26893	1.89716E-00	0.0	0.0	0.0	0.0
7	2.09439	1.99262E-00	0.0	0.0	0.0	0.0
8	1.91986	2.06579E-01	0.0	0.0	0.0	0.0
9	1.74533	2.10911E-01	0.0	0.0	0.0	0.0
10	1.57180	2.13962E-01	0.0	0.0	0.0	0.0
11	1.39826	2.1579E-01	0.0	0.0	0.0	0.0
12	1.22173	2.16472E-00	0.0	0.0	0.0	0.0
13	1.04720	2.16726E-00	0.0	0.0	0.0	0.0
14	0.87266	2.16981E-00	0.0	0.0	0.0	0.0
15	0.69813	2.17236E-00	0.0	0.0	0.0	0.0
16	0.52360	2.17490E-00	0.15620E-04	0.33530E-04	0.33530E-00	0.0
17	0.34907	2.17745E-00	0.4320E-04	0.14224E-05	0.14224E-01	0.0
18	0.17453	0.95457E-01	0.79000E-02	0.82761E-03	0.82761E-01	0.0

UNSCATTERED ESCAPES = 0.56630E-04

NUMBER AV/STER = 0.10225E-04

PAIR PHOTON ESCAPES = 0.0

NO. P P IN FWD CONE = 0.0

(E)

SOURCE ENERGY = 1.25 MeV

ESCAPE ENERGY INTERVAL = 1.4927 TO 1.8443 INDEX 1

J	ANGLE'S A(J) TO AL(J+1)	SOLID ANGLE	NUMBER	NUMBER/STEP	FRACT/STEP	PAIR PHOTONS
1	3.14159	0.35776	0.18090E+01	0.1993E+0	0.1993E-01	0
2	2.66774	0.29376	0.71334E+0	0.25165E+0	0.25165E-01	0
3	2.73253	0.41730	0.11411E+0	0.4621E+0	0.4621E-01	0
4	2.61700	0.44346	0.15680E+0	0.24651E+0	0.24651E-01	0
5	2.44746	0.28293	0.77485E+0	0.13434E+0	0.13434E-01	0
6	2.24903	0.16430	0.9716E+0	0.1927E+0	0.1927E-01	0
7	2.12435	1.01290	0.92429E+0	0.2174E+0	0.2174E-01	0
8	1.81946	1.74513	1.74513E+0	0.17579E+0	0.17579E-01	0
9	1.57780	1.87483	1.87483E+0	0.19683E+0	0.19683E-01	0
10	1.39624	1.30426	1.30426E+0	0.24434E+0	0.24434E-01	0
11	1.28173	1.23173	1.23173E+0	0.23191E+0	0.23191E-01	0
12	1.16722	1.16722E+0	0.27184E+0	0.2747E+0	0.2747E-01	0
13	1.07266	0.9216E+0	0.27184E+0	0.33789E+0	0.33789E-01	0
14	0.97324	0.6913E+0	0.27529E+0	0.35636E+0	0.35636E-01	0
15	0.89312	0.5246E+0	0.27709E+0	0.4425E+0	0.4425E-01	0
16	0.83306	0.4037E+0	0.2826E+0	0.48566E+0	0.48566E-01	0
17	0.78977	0.17457E+0	0.51997E+0	0.19040E+0	0.19040E-01	0
18	0.74553	0.04455E+0	0.14999E+0	0.15714E+0	0.15714E-01	0

SCATTERED ESCAPES = 0.1121E+0

P.F.ABSORPTIONS = 0.3377E+0

NUMBER AV/STEP = 0.2373E+0

PAIR PHOTON ESCAPES = 0

NUMBER IN FWD CONE = 0

NO. IN FWD CONE/STEP = 0

ESCAPE ENERGY INTERVAL = 1.2463 TO 1.9571 INDEX 2

J	ANGLE'S A(J) TO AL(J+1)	SOLID ANGLE	NUMBER	NUMBER/STEP	FRACT/STEP	PAIR PHOTONS
1	3.14159	0.35776	0.18090E+01	0.63949E+0	0.63949E-02	0
2	2.66774	0.29376	0.71334E+0	0.25229E+0	0.25229E-02	0
3	2.73253	0.41730	0.11411E+0	0.43221E+0	0.43221E-02	0
4	2.61700	0.44346	0.15680E+0	0.51941E+0	0.51941E-02	0
5	2.44746	0.28293	0.77485E+0	0.24211E+0	0.24211E-02	0
6	2.24903	0.16430	0.9716E+0	0.39334E+0	0.39334E-02	0
7	2.12435	1.01290	0.92429E+0	0.29378E+0	0.29378E-02	0
8	1.81946	1.74513	1.74513E+0	0.27455E+0	0.27455E-02	0
9	1.57780	1.87483	1.87483E+0	0.23174E+0	0.23174E-02	0
10	1.39624	1.30426	1.30426E+0	0.29475E+0	0.29475E-02	0
11	1.28173	1.23173	1.23173E+0	0.31722E+0	0.31722E-02	0
12	1.16722	1.16722E+0	0.16808E+0	0.1903E+0	0.1903E-02	0
13	1.07266	0.9216E+0	0.16808E+0	0.11631E+0	0.11631E-02	0
14	0.97324	0.6913E+0	0.16808E+0	0.11322E+0	0.11322E-02	0
15	0.89312	0.5246E+0	0.16808E+0	0.11322E+0	0.11322E-02	0
16	0.83306	0.4037E+0	0.16808E+0	0.08781E+0	0.08781E-02	0
17	0.78977	0.17457E+0	0.16808E+0	0.11747E+0	0.11747E-02	0
18	0.74553	0.04455E+0	0.16808E+0	0.11747E+0	0.11747E-02	0

SCATTERED ESCAPES = 0.3117E+0

P.F.ABSORPTIONS = 0.1504E+0

NUMBER AV/STEP = 0.2465E+0

PAIR PHOTON ESCAPES = 0

NUMBER IN FWD CONE = 0

NO. IN FWD CONE/STEP = 0

F

NO. OF HISTORIES INITIAL ENERGY OUT-OF-ENERGY TOTAL NO. OF COLLISIONS
 1 100.000000 1.0 1000000

TERMINATION PRIMARY PHOTONS

- 1. ENERGY 1741 6 9
- 2. WEIGHT 112 6 9
- 3. ESCAPE 1.0943E-4 (3. AND. OF HISTORIES) 1.0943E-4
- 4. ABSORBED 1.2157E-3
- 5. TOTAL UNSCATTERED ESCAPES 1.5743E-4 (5. AND. OF HISTORIES) 1.5743E-4
- 6. TOTAL SCATTERED ESCAPES 1.213E-4 (6. AND. OF HISTORIES) 1.213E-4
- 7. PHOTOELECTRIC ABSORPTIONS 1.3447E-12
- 8. PAIR PRODUCTION PHOTONS 0

TOTAL ESCAPES IN FWD 1st-DEG. CONE= 1.5743E-4

TERMINATION PAIR PHOTONS

- 1. ENERGY 0
- 2. WEIGHT 0
- 3. ESCAPE 0
- 4. ABSORBED 0
- 5. TOTAL UNSCATTERED ESCAPES 0
- 6. TOTAL SCATTERED ESCAPES 0
- 7. PHOTOELECTRIC ABSORPTIONS 0
- 8. PAIR PRODUCTION PHOTONS 0

TALLY CHECK = 1.090000E-4



NOTE: Output pages (D), (E) and (F) omitted for 0.85, 1.70 and 6.50 MeV source energies.

NO. OF HISTORIES INITIAL ENERGY CUT-OFF ENERGY TOTAL NO. OF COLLISIONS
 76 0.2511 0.110 5430

TERMINATION BY ENERGY PHOTONS

1. ENERGY 0.418 E 3
 2. WEIGHT 0.176 E 3
 3. ESCAPE 0.6041E 4 (3./NO. OF HISTORIES) 0.02064E
 4. ABSORBED 0.5357E 7
 5. TOTAL UNSCATTERED ESCAPES 0.4987E 4 (5./NO. OF HISTORIES) 0.0647E 4
 6. TOTAL SCATTERED ESCAPES 0.7006E 4 (6./NO. OF HISTORIES) 0.2074E 4
 7. PHOTOELECTRIC ABSORPTIONS 0.1119E 12
 8. PAIR PRODUCTION PHOTONS 0.0

TOTAL ESCAPES IN END 1-ORF. CONF 0.1342E 02 TOTAL IN END 1-ORF. CONF 0.1342E 02

TERMINATION BY PAIR PHOTONS

1. ENERGY 0.0
 2. WEIGHT 0.0
 3. ESCAPE 0.0
 4. ABSORBED 0.0
 5. TOTAL UNSCATTERED ESCAPES 0.0
 6. TOTAL SCATTERED ESCAPES 0.0
 7. PHOTOELECTRIC ABSORPTIONS 0.0
 8. PAIR PRODUCTION PHOTONS 0.0

TALLY CHECK = 0.750E 04

G

NO. OF HISTORIES INITIAL ENERGY CUT-OFF ENERGY TOTAL NO. OF COLLISIONS
 17.571 1.12E 448E

TERMINATION PRIMARY PHOTONS

- 1. ENERGY 1.14542E 12
- 2. WEIGHT 1.5747E 12
- 3. ESCAPE 1.0729E 14 (3./NO. OF HISTORIES) 1.0016E 12
- 4. ABSORBED 1.26025E 12
- 5. TOTAL UNSCATTERED ESCAPES 1.7675E 14 (5./NO. OF HISTORIES) 1.735E 12
- 6. TOTAL SCATTERED ESCAPES 1.11048E 14 (6./NO. OF HISTORIES) 1.21916E 12
- 7. PHOTOELECTRIC ABSORPTIONS 1.56224E 12
- 8. PAIR PRODUCTION PHOTONS 1.37930E 12

TOTAL ESCAPES IN FWD 1-DEG. CONES 1.14132E 12 TOTAL IN FWD CONES/STEPS 1.14075E 12

TERMINATION PAIR PHOTONS

- 1. ENERGY 1.12545E 12
- 2. WEIGHT 1.04172E 11
- 3. ESCAPE 1.1361E 12
- 4. ABSORBED 1.24221E 12
- 5. TOTAL UNSCATTERED ESCAPES 1.1235E 12
- 6. TOTAL SCATTERED ESCAPES 1.13949E 11
- 7. PHOTOELECTRIC ABSORPTIONS 1.22587E 11
- 8. PAIR PRODUCTION PHOTONS 1.37630E 12

(6)

TALLY CHECK = 1.53005E 14

NO. OF HISTORIES INITIAL ENERGY CUT-OFF ENERGY TOTAL NO. OF COLLISIONS
 3.000 0.050E 01 0.100 251

TERMINATION PRIMARY PHOTONS

1. ENERGY	.31855E 02	
2. WEIGHT	0.11801E 02	
3. ESCAPE	.07755E 04	(3.7NO. OF HISTORIES) .02520E 02
4. ABSORBED	.04100E 02	
5. TOTAL UNSCATTERED ESCAPES	.04370E 04	(5.7NO. OF HISTORIES) .01933E 02
6. TOTAL SCATTERED ESCAPES	.03300E 03	(6.7NO. OF HISTORIES) .01120E 02
7. PHOTOELECTRIC ABSORPTIONS	.07510E 01	
8. PAIR PRODUCTION PHOTONS	.03050E 03	

147 TOTAL ESCAPES IN FWD 1-DEG. CONE .12300E 02 TOTAL IN FWD CONE/STRE 0.12300E 02

TERMINATION PAIR PHOTONS

1. ENERGY	.13170E 03	
2. WEIGHT	0.45762E 02	
3. ESCAPE	0.12421E 03	
4. ABSORBED	.02157 E 02	
5. TOTAL UNSCATTERED ESCAPES	.09265E 02	
6. TOTAL SCATTERED ESCAPES	0.04067E 02	
7. PHOTOELECTRIC ABSORPTIONS	.01396E 02	
8. PAIR PRODUCTION PHOTONS	.02000E 02	

(6)



APPENDIX VI
SUMMARY OF NUS-600 DETAIL EVALUATION

APPENDIX VI
SUMMARY OF NUS-600 DETAIL EVALUATION

Sample results obtained with the SØSC component codes are reviewed. They consist of shield thickness and weight evaluations for assumed typical SNAP-27 RTG source strengths and spectral distributions. Example results obtained for the scattering from spacecraft structural members are presented, and the significance of various factors discussed.

The calculations described in this Appendix are generally based on a RTG gamma photon emission distribution similar to that of the Martin Cronus⁽³²⁾ (thermal loading of 4100 watts) normalized to a total emission of 1×10^9 λ /sec. The RTG fast neutron emission distribution was based on SNAP-27-1 reported data from reference (1); a source emission rate of 5.7×10^8 n/sec was assumed. For both fast-neutrons and gamma photons, axial and axially perpendicular emission rates were taken as identical, although this is not true in fact. This assumption was necessitated by the lack of actual encased RTG source data in the early phase of the work program. The assumed source emission spectrum is given in Table VI-1 for gamma photons and in Table VI-2 for fast neutrons.

The typical spacecraft for which the calculations were carried out is that of Figure 1 (section 2.1 of this report). The dimensions of this spacecraft were obtained from NASA-GSFC preliminary drawings. Figure VI-1 shows a schematic outline of the spacecraft for the discussions in this section.

Gamma photon cross-section data were taken from references (17) through (21). Neutron cross-section data were obtained from reference (22).

The Table VI-1 source spectrum is that for a three (3) year old PuO_2 SNAP-27 as opposed to the five (5) year PuO_2 used in section 3.3.5 of this report. Calculations in reference (32) indicate that the total gamma emission rate increases by a factor of ~ 4 over the first 18 years. Table VI-3, reproduced from the reference, indicates that the energy groups 0.2 to 0.3, and 2.0 to 3.0 MeV are the most critical, e.g. the 2.0 to 3.0 MeV group (2.62 MeV ThC") increases by a factor of more than 100 in the first 10 years. This age effect on shielding requirements was not studied during this report period because of lack of reliable source data.

The scattering of source gamma photons to the detector by aluminum boom tubing proximate to the source (or the detector) was investigated. The boom axis was assumed as perpendicularly bisecting a 16" long unit (1 γ /sec) source of 0.75 MeV photons. The calculations assumed a line source and a single scattering model for a boom tube volume of 0.79 cc/cm. The results of the calculations are shown in Figure VI-2 along with the calculation geometry. In the figure it may be seen that the calculations considered boom tubing coming as close as 10 cm to the source whereas GSFC drawings indicated actual closest point of boom as 25 cm distant. The detector-incident flux scattered by a typical boom, boom (1,2) in Figure VI-1, is obtained from Figure VI-2 after integration over r , between 25 and 80 cm, as $\phi_{\alpha S}(E_{\alpha}) = 1.3 \times 10^{11}$ $\gamma/\text{cm}^2\text{-sec}$. Assuming boom (1,2) as typical, where r_1 ranges from 25 to 80cm, i.e. a length of 55cm, the total scattered flux from 6 such booms (6 per side) and 4 sources would be $\sim 3 \times 10^{-10}$ $\gamma/\text{cm}^2\text{-sec}$. If the actual source strength are taken as 10^9 γ/sec , then < total flux of ~ 0.3 $\gamma/\text{cm}^2\text{-sec}$ is obtained. The use of the single scattering model as opposed to the albedo method for boom structure calculations, was investigated. A 1 cm length of 1 inch diameter aluminum boom was considered as located 100 cm from both a point source and a detector, with source and detector 141 cm apart. For

$E_0 = 0.75$ MeV, a unit source (1 γ /sec), a boom wall thickness of 0.04 inches and a boom volume 0.79 cc/cm, the calculated fluxes at the detector were

$$\begin{aligned} \text{and } \phi_{\alpha S}(E_\alpha) &= 3.6 \times 10^{-12}, \gamma/\text{cm}^2\text{-sec,} \\ \phi_{\alpha SS}(E_\alpha) &= 6.4 \times 10^{-12}, \gamma/\text{cm}^2\text{-sec.} \end{aligned}$$

The difference in these calculations diminishes if it is assumed, in the case of the albedo result, that photons penetrating the relatively thin (0.04") tube frontal wall may be backscattered from the tube interior wall surface ie, if either the wall thickness or scattering area is doubled for the calculation, then

$$\phi_{\alpha S}(E_\alpha) = 7.0 \times 10^{-12}, \gamma/\text{cm}^2\text{-sec.}$$

This result indicates a very good agreement between the single scatter and albedo methods for small finite geometries.

A similar calculation for a large iron cylinder, in the physical position of the spacecraft cupola, was also carried out. The cylinder dimensions were taken as 20" x 38.5" x 0.5" (dia. x lt. x thickness). A unit source of 0.75 MeV photons was assumed. The source, detector and cupola were located per the spacecraft dimensions.

$$\begin{aligned} \text{and } \phi_{\alpha S}(E_\alpha) &= 2.4 \times 10^{-9} \gamma/\text{cm}^2\text{-sec,} \\ \phi_{\alpha SS}(E_\alpha) &= 2.7 \times 10^{-9} \gamma/\text{cm}^2\text{-sec.} \end{aligned}$$

The same configuration for an aluminum cylinder of 1 inch wall thickness, gave a single scatter flux of

$$\phi_{oss}(E_{\alpha}) = 1.8 \times 10^{-9} \text{ } \gamma/\text{cm}^2\text{-sec.}$$

Taking an actual cupola "flat", A, as in Figure VI-1, with the dimensions 13.2" x 25.5" x 1" (width x ht. x thickness) and assuming the material to be aluminum, the albedo and single scatter fluxes were determined as

$$\phi_{\alpha s}(E_{\alpha}) = 1.8 \times 10^{-10} \text{ } \gamma/\text{cm}^2\text{-sec.}$$

and

$$\phi_{\alpha s}(E_{\alpha}) = 1.9 \times 10^{-10} \text{ } \gamma/\text{cm}^2\text{-sec.}$$

The above calculations were based on a single RTG source of 1 photon/sec, and $E_0 = 0.75$.

Figures VI-3 and VI-4 are sodium-iodide scintillation detector spectra reproduced from reference (). They indicate the energy distribution of backscattered photons as a function of t , θ_s and θ_0 , respectively, for graphite as the backscattering material. The prominent peak in these spectra corresponds to single scatter the 'arrow-indicated' peak corresponds to double scatter and the continuum represents multiple scatter.

If this photon scattering is considered significant enough to require shielding ($\sim C$, the criterion flux) then such shielding would be a minimum weight if designed to attenuate the scattered photons as opposed to the primaries. Figures VI-3 and VI-4 show that the scattered photon energies will generally be in the range, 0.10 to 0.5 MeV, and thus can be readily attenuated by a relatively thin and thus low weight, shield located at the detector.

Examples of energy-integrated shield-scattered photon angular distributions are presented in Figure VI-5. The angular categorization in this figure is referenced to the shield geometric center. The distributions were deter-

mined by an early version of the Monte Carlo subprogram: NUGAM1. The current code version additionally determines the photon distribution to which the detector is specifically exposed, i.e., photons escaping from the side of the shield cannot intercept the detector.

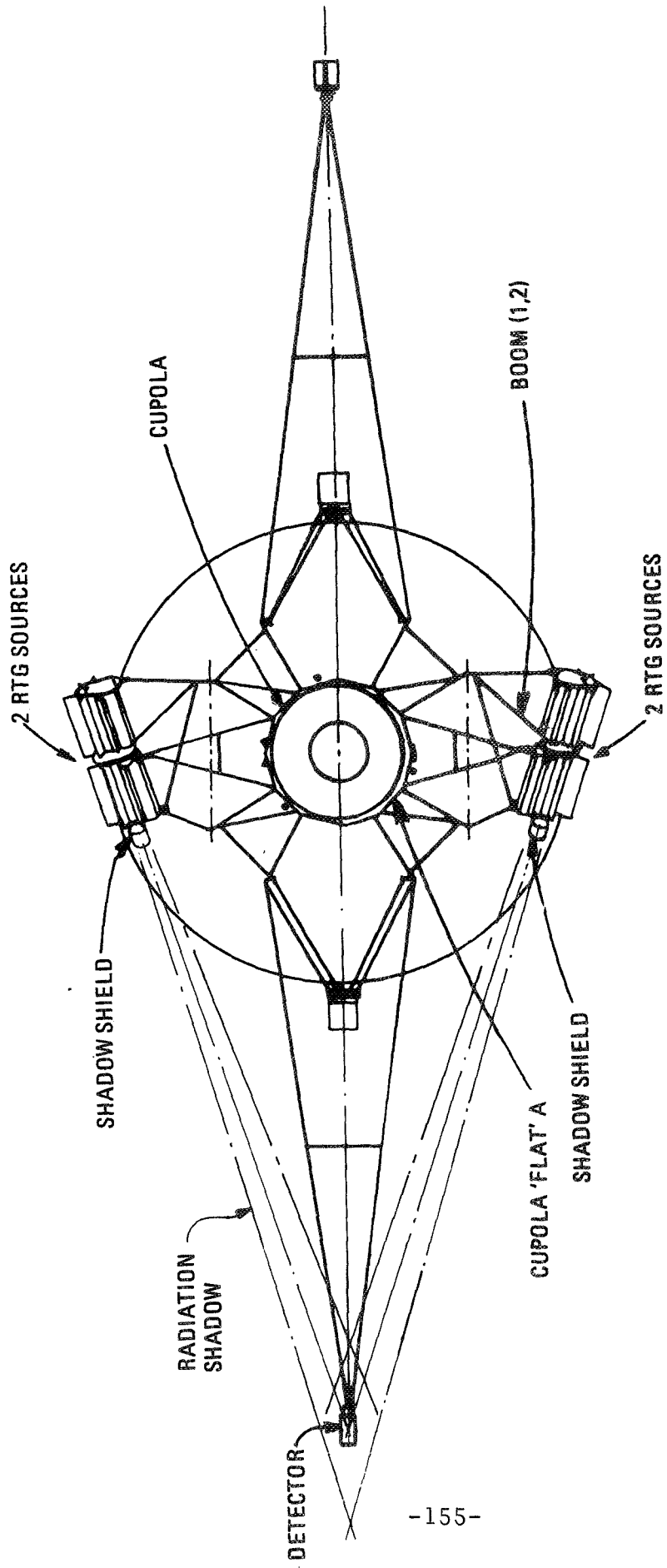


FIGURE VI-1
 SCHEMATIC DRAWING OF SPACECRAFT
 SHOWING SPECIFIC STRUCTURAL MEMBERS

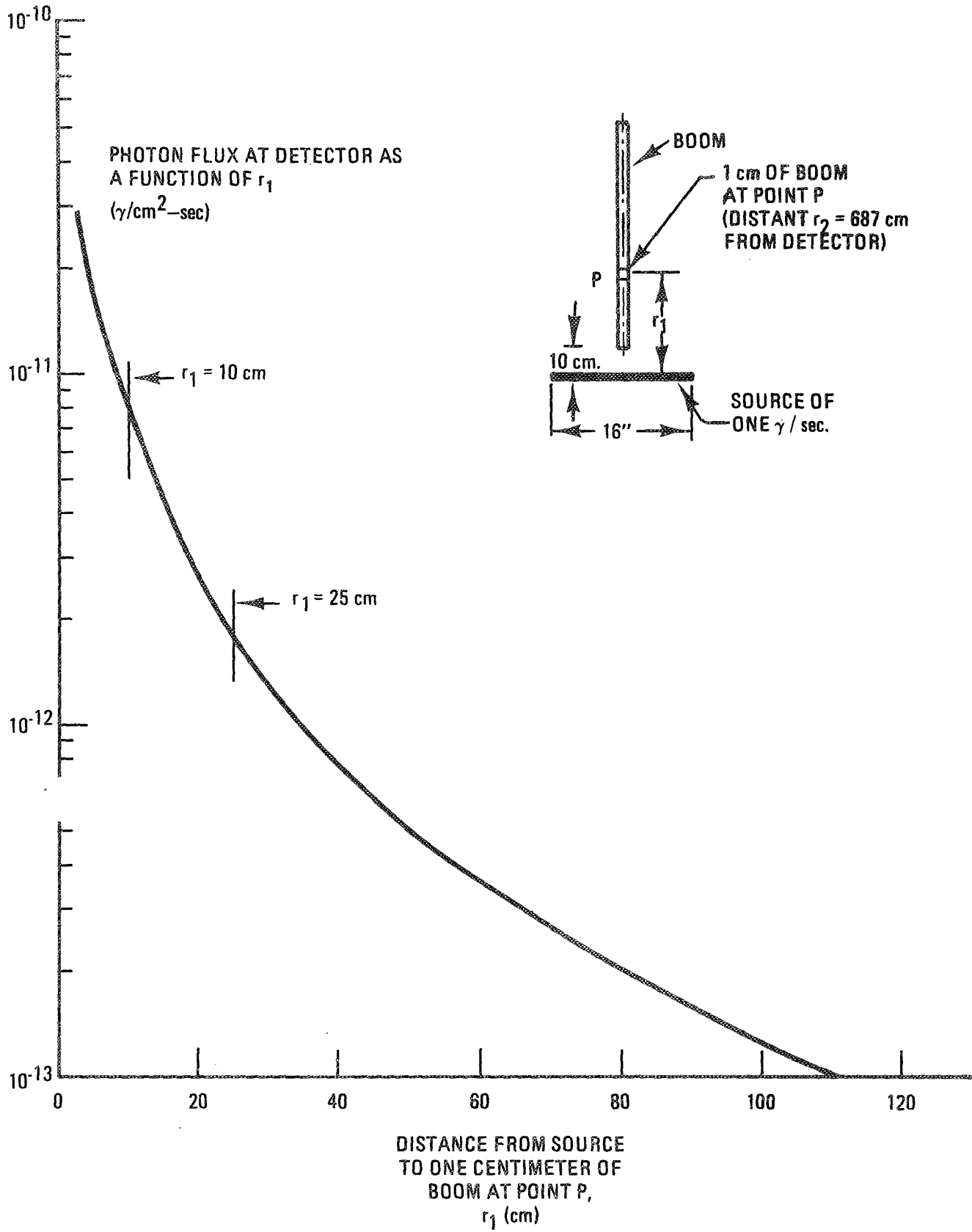


FIGURE VI - 2
BOOM SCATTER INTENSITY AS A FUNCTION
OF SOURCE-TO-BOOM DISTANCE

400 Min; X = Material Thickness

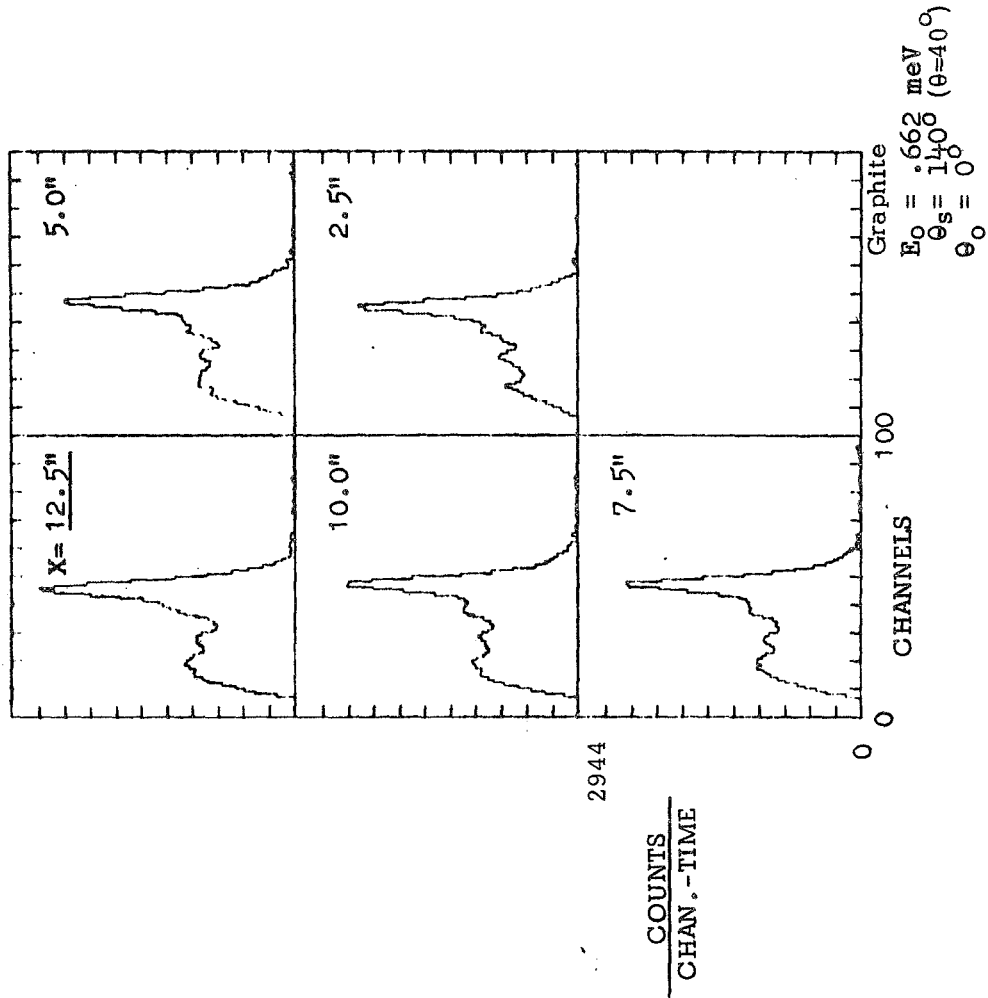
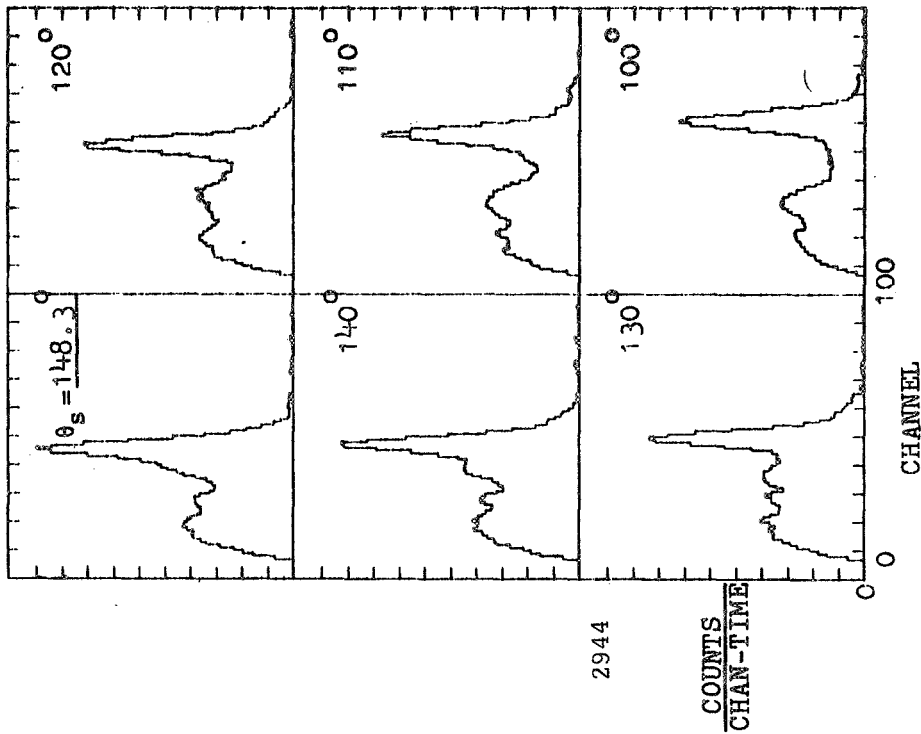


FIGURE VI-3

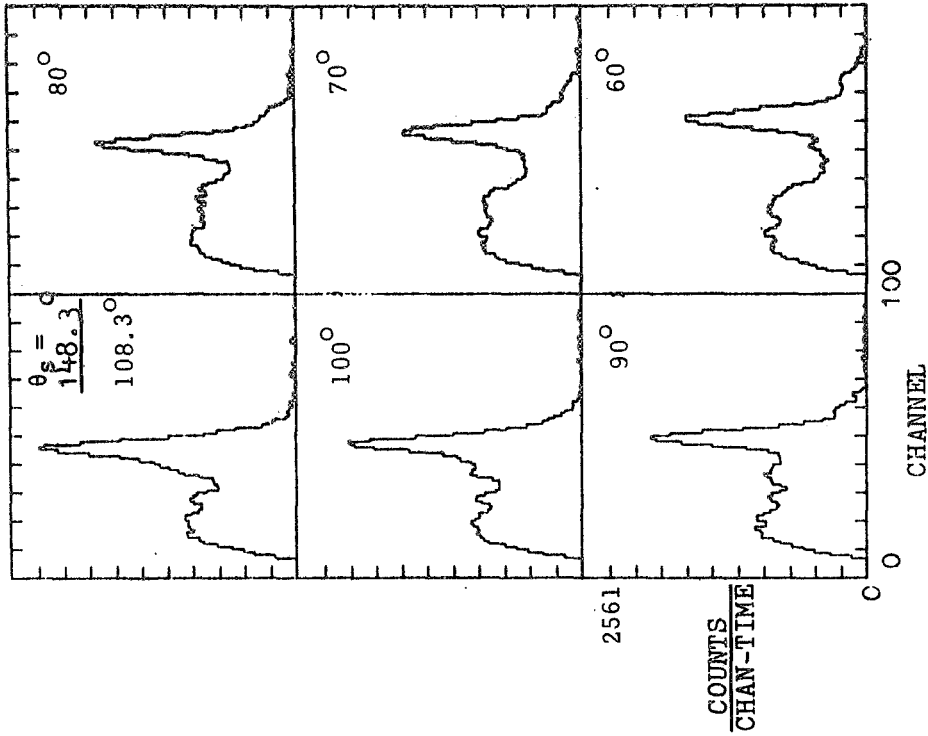
NaI(Tl) Scintillation Spectra Showing
Gamma Photon Backscatter Distribution as a
Function of Scattering Material Thickness

Cs¹³⁷; Graphite
 400 Min; $\theta_s = 80 - (\theta_o + \theta)$



8 (a) Perpendicular Incidence:
 Spectral Distribution as a Function
 of Scatter Angle θ_s for $E_o = 0.662$ MeV
 and $\theta_o = 0$

Cs¹³⁷; Graphite
 400 Min; $\theta_s = 180 - (\theta_o + \theta)$



8 (b) Slant Incidence:
 Spectral Distribution as a Function
 of Scatter Angle θ_s for $E_o = 0.662$ MeV
 and $\theta_o = 40$

FIGURE VI-4

NaI(Tl) Scintillation Spectra Showing
 Gamma Photon Scatter Distribution as a
 Function of Incident-Angle, θ_o

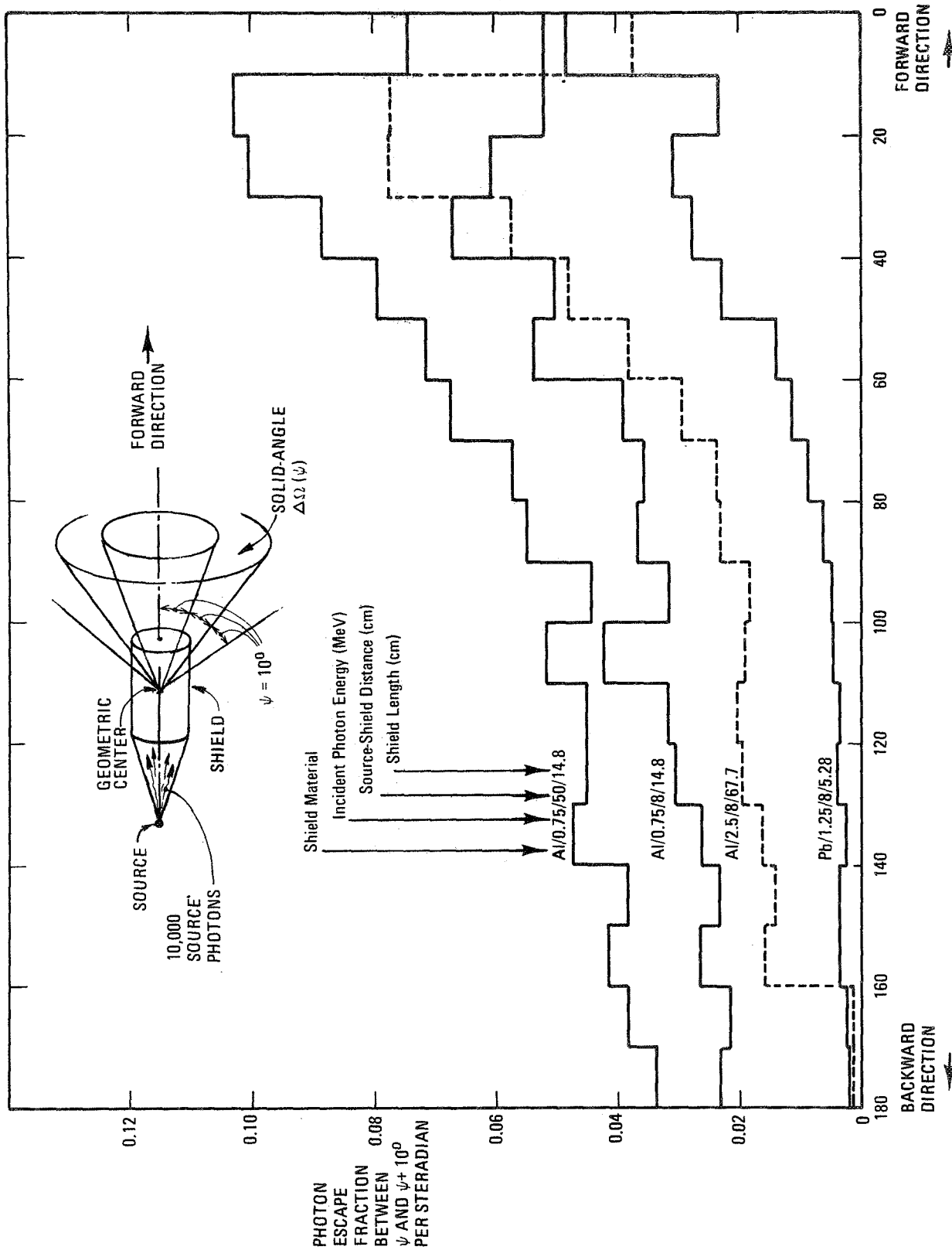


FIGURE VI-5
ENERGY-INTEGRATED ANGULAR DISTRIBUTION
OF SHIELD SCATTERED PHOTONS

TABLE VI-1

Assumed SNAP-27 Gamma Photon Emission Spectrum
Based On Martin Cronus Data⁽³²⁾

Energy Interval (MeV)	Assumed Energy (MeV)	Photon Emission Rate (γ /MeV-sec)
0.044 - 0.2	0.15	6.54×10^7
0.2 - 0.3	0.24	6.87×10^7
0.3 - 0.4	0.311	7.88×10^7
0.4 - 0.5	0.414	7.86×10^7
0.5 - 0.6	0.583	8.03×10^7
0.6 - 0.7	0.650	7.33×10^7
0.7 - 0.8	0.766	2.26×10^8
0.8 - 0.9	0.851	1.40×10^8
0.9 - 1.0	1.00	6.65×10^6
1.0 - 1.2	1.10	1.87×10^7
1.2 - 1.4	1.40	1.73×10^7
1.4 - 1.6	1.59	7.71×10^6
1.6 - 1.8	1.63	1.63×10^7
1.8 - 2.0	1.90	1.54×10^7
2.0 - 3.0	2.61	1.07×10^8
3.0 - 4.0	3.50	3.03×10^5
4.0 - 5.0	4.50	9.10×10^3
5.0 - 6.0	5.50	3.01×10^4

TABLE VI-2

SNAP-27-1 Fast Neutron Emission Spectrum⁽¹⁾

Energy Interval (MeV)	Neutron Emission Rate (n/MeV-sec)
0 - 1.0	5.06×10^7
1.0 - 3.0	4.16×10^7
3.0 - 4.0	1.79×10^7
4.0 - 5.0	3.56×10^6
5.0 - 6.0	1.90×10^6
6.0 - 8.0	4.50×10^5
8.0 - 10.0	1.14×10^5

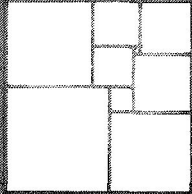
Energy Integrated Emission Rate = 5.7×10^7 n/sec.

TABLE VI-3

Reproduced from Reference⁽³²⁾

Gamma spectra, photons/cm²-sec for RTG at various times
after plutonium separation (Normalized to 1.0 for
energy interval 0.5-1.0 MeV at 18 years)

Energy (MeV)	0 year	1 year	5 year	10 year	18 year
0.04 - 0.5	0.12	0.16	0.56	0.90	1.0
0.5 - 1.0	0.23	0.25	0.30	0.33	0.35
1.0 - 2	0.096	0.096	0.096	0.096	0.096
2 - 3	0.003	0.018	0.18	0.32	0.37
3 - 5	0.0003	0.0003	0.0003	0.0003	0.0003
5 - 7	0.00003	0.00003	0.00003	0.00003	0.00003



NUS CORPORATION